

Zoo of Correlation Inequalities in Holography and Beyond

Kyan Louisia^{a,b} **Takato Mori**^{b,c} **Herbie Warner**^b

^a*King's College London, Strand, London, WC2R 2LS, United Kingdom*

^b*Perimeter Institute for Theoretical Physics, Waterloo, Ontario N2L 2Y5, Canada*

^c*Department of Physics, Rikkyo University, 3-34-1 Nishi-Ikebukuro, Toshima-ku, Tokyo 171-8501, Japan*

E-mail: kyan.louisia@gmail.com, takato.mori@yukawa.kyoto-u.ac.jp,
herbie.warner1@outlook.com

ABSTRACT: Information-theoretic inequalities often impose nontrivial constraints on holographic states. In this work, we study measurement-based classical and quantum correlations in holography, focusing on the proposed duals of classical correlation J_W , quantum discord D_W , and one-shot distillable entanglement E_D , defined in terms of the entanglement wedge cross section (EWCS). We develop a homological framework tailored to inequalities involving multiple EWCSs and Ryu–Takayanagi surfaces, and use it to prove a family of inequalities, including monotonicity and monogamy/polygamy-type relations, as well as one-way strong superadditivity. For strong superadditivity, we additionally confirm its two-way version using Haar random states. We also examine holography-inspired boundary duals in terms of the reflected entropy and provide proofs and counterexamples for their information-theoretic inequalities. Taken together, our results provide further evidence for the duality between the EWCS and its proposed boundary counterparts—measurement-based correlations and one-shot distillable entanglement—while also furnishing a unified, rigorous method for proving multi-EWCS inequalities.

Contents

1	Introduction	2
2	Classical and Quantum Correlations	4
2.1	Classical and Quantum Correlation Measures	5
2.2	Holographic duals	6
2.3	Correlation Inequalities	8
3	Assumptions and Technical Tools	10
3.1	Assumptions for holographic proofs	10
3.2	Conventions and Definitions	11
3.3	Example of a holographic proof	14
3.4	Properties of the Entanglement Wedge Cross Section	16
4	Holographic Monotonicity	18
4.1	Measured Party	19
4.2	Unmeasured Party	20
5	Holographic Monogamy/Polygamy	21
5.1	Polygamy of discord	21
5.2	Monogamy of classical correlations	23
5.2.1	Measured party	24
5.2.2	Unmeasured party	25
6	Holographic Strong Superadditivity	25
6.1	Distillable entanglement and holographic conjecture	26
6.2	Holographic proof of one-way strong superadditivity	27
6.3	Toward holographic proof of two-way strong superadditivity	28
6.4	Haar Random analysis	29
7	Boundary dual to holographic correlations from reflected entropy	30
7.1	Definition and relation to original measures	30
7.2	Monotonicity of reflected measures	32
7.2.1	Measured party	32
7.2.2	Unmeasured party	33
7.3	Monogamy/Polygamy of reflected measures	34
7.3.1	Measured party	34
7.3.2	Unmeasured Party	35
8	Summary and future outlook	36

A	Summary of notation	39
B	Mathematica code for strong superadditivity of Haar random states	41
C	Counterexample to monotonicity of reflected discord in measured party	42
D	Additional tools for proofs	43
E	Proof: Barrier theorem	47
E.1	Proof by reflected entropy	47
E.2	Proof by cycles	49
F	Proof: Monotonicity in unmeasured party	53
G	Proof: Monogamy of classical correlations: Measured party	57
H	Proof: Monogamy of classical correlations: Unmeasured party	62
I	Proof: One-way strong superadditivity of classical correlations	66

1 Introduction

Quantifying correlations between subsystems is a central objective in both quantum information theory (QI) and quantum gravity (QG). Over the past two decades, this intersection has flourished, particularly through the AdS/CFT correspondence and the black hole information paradox [1–7]. A landmark result was the Ryu-Takayanagi (RT) formula [1], which equates the entanglement entropy of a boundary region to the area of a minimal surface in the bulk called the holographic entanglement entropy (HEE). This relationship showed that entanglement entropy is a key aspect of holographic theories for the emergence of bulk geometry.

While entanglement entropy fully characterizes correlations in pure states, its extension to mixed states is more subtle. In holography, a natural extension of the RT formula to mixed states is the entanglement wedge cross section (EWCS) [8]. Defined as the minimal-area surface that splits the entanglement wedge of a bipartite state ρ_{AB} into regions homologous to A and B , the EWCS is expected to capture some mixed-state correlation structure in a geometric way, extending the logic of the RT formula.

The EWCS has several proposed boundary duals; many works have connected it to mixed-state entanglement measures involving optimization, such as the entanglement of purification [8] and the entanglement of formation [9]. Later, quantities without optimization such as reflected entropy S_R [10], odd entropy [11], and balanced partial entanglement [12] have also been identified as possible boundary duals. However, information theoretic aspects of these holography-inspired quantities remain unclear (although there has been some analysis in monotonicity of reflected entropy [13] and some indicative results with tripartite entanglement [14, 15]).

In this work, we extend the program of the duality between entanglement and geometry to more general correlations, following [16]. In particular, we focus on classical and quantum correlations such as quantum discord [17] and investigate their behavior in both holographic and non-holographic systems.

Although entanglement is often identified with quantum correlations, it is only one aspect of “quantumness”. In fact, quantum correlations can exist even in separable states: for instance, the two-qubit state

$$\rho_{AB} = \frac{|00\rangle\langle 00| + |1+\rangle\langle 1+|}{2}, \quad |+\rangle = \frac{|0\rangle + |1\rangle}{\sqrt{2}} \quad (1.1)$$

is separable but exhibits correlations beyond classical ones. By contrast, classically correlated states are separable taking the form

$$\rho_{AB}^{\text{CC}} = \sum_{\alpha} p_{\alpha} |\varphi_{\alpha}\rangle\langle\varphi_{\alpha}|_A \otimes |\chi_{\alpha}\rangle\langle\chi_{\alpha}|_B, \quad (1.2)$$

where $\{|\varphi_\alpha\rangle\}, \{|\chi_\alpha\rangle\}$ form orthonormal bases of the respective Hilbert spaces. These correlations are entirely classical and encoded in a single probability distribution p_α and associated orthogonal bases on A and B .

This type of quantum correlation beyond entanglement is captured by quantum discord [17] as we will review later in this paper. While the primary focus of this paper is information theoretic properties of this quantity in AdS/CFT and its boundary dual, it is worth noting that there is a physical motivation to study discord aside from its entanglement properties. For example in scenarios involving decoherence, including thermalization or the infall of measurement devices into black holes or inflating cosmologies, discord reveals aspects of quantum correlations that entanglement fails to track [16, 18, 19].

Recently, one of the authors proposed bulk duals for classical and quantum correlations [9], where classical correlation is defined by locally accessible information and quantum correlation is defined by discord. Both are conjectured to admit bulk duals in terms of the EWCS and RT formula. Moreover the study indicates that there exists both classical and quantum correlation in holography, with the latter always exceeding entanglement. The difference between holographic discord and entanglement turns out to be related to distillable entanglement and tripartite entanglement. In addition, while the reflected entropy itself is not a correlation measure [13], it was shown that it composes the classical and quantum correlation-like quantities when it is combined with entropies. This motivates us to ask: is there any characteristic behavior of holographic correlation quantities? Do these obey some basic information theoretic inequalities like monotonicity and monogamy?

Monotonicity implies that a correlation measure should not increase under local operations such as partial trace. This property is a defining feature for a resource theory of correlations. It enforces the second law-like structure and governs the convertibility and irreversibility. In holography, monotonicity is also understood geometrically: for example, monotonicity of mutual information and EWCS follows from entanglement wedge nesting [8, 20, 21], stemming from bulk locality and reconstructability [22–26].

Monogamy, by contrast, limits how quantum correlations can be shared. If A is maximally entangled with B , it cannot also be entangled with C . This principle, tied to the no-cloning theorem, highly constrains quantum theory, e.g. it underpins security in quantum cryptography [27, 28] and is also fundamental to the black hole information paradox [7].

Holographic states display distinctive correlation structures. A well-known example is the monogamy of mutual information [29]. Another characteristic feature is that they carry substantial multipartite entanglement while supporting very little classical correlation, which motivates our investigation of further inequalities constraining classical and quantum correlations.

These constraints have geometric roots. Our holographic arguments rely on structures like the homology condition, extremality of HEE, and entanglement wedge nesting, which make inequalities such as subadditivity and strong subadditivity manifest geometrically [30]. Beyond these, monogamy of mutual information has been formalized in the holographic entropy cone program [31], which attempts a systematic classification of all entropy inequalities consistent with the bulk geometry.

However, inequalities involving multiple EWCSs remain less understood. While the EWCS has been linked to quantities such as the entanglement of formation/purification, the reflected entropy, the Markov gap, and the distillable entanglement [32], only a few inequalities have been confirmed. Some, like the non-negativity of the Markov gap [14] and the vanishing of distillable entanglement [9], reinforce the idea that holographic states favor multipartite quantum correlations. But generalizations involving multiple EWCS terms are more involved [33, 34]; it is challenging to prove them rigorously due to lack of systematic mathematical tools. This suggests a more delicate structure than for entropy-based measures.

In this work, we investigate this structure by analyzing a family of inequalities involving classical and quantum correlations in holography and their boundary versions. In Section 2, the definitions of several correlation measures are given both on the boundary and in the bulk. We also give definitions of correlation inequalities here. In Section 3, we list our assumptions, introduce some of the technical tools required for proofs, and discuss some topological properties of the EWCS. In Section 4, we study monotonicity for both correlation types, and in Section 5, we establish their monogamy and polygamy properties. In Section 6, we further examine the strong superadditivity of holographic classical correlation, which is conjectured to be dual to distillable entanglement, using geometric arguments and Haar random analysis. In Section 7, motivated from a holographic duality, we map the bulk quantities to boundary ones again by replacing the EWCS with a half of the reflected entropy, defining so-called reflected measures — analytic and computationally efficient proxies for classical and quantum correlations. We examine their properties like monotonicity and monogamy with various few-qubit counterexamples. See Tables 1 and 2 for a summary of the results. Due to the lengths of proofs, we only provide sketches of each in the main body and relegate the complete proofs to the Appendices B-I. See Appendix A for a summary of notations used throughout.

2 Classical and Quantum Correlations

In this section, we review the correlation measures of interest in this work. These include the classical correlation $J(A|B)$ and quantum discord $D(A|B)$, as well as their conjectured gravity duals $J_W(A|B)$ and $D_W(A|B)$ which are defined in terms of the entanglement wedge cross section (EWCS). We also introduce the boundary duals of these geometric quantities based on the reflected entropy, which provide

computable, optimisation-free entanglement measures. We then summarize the correlation inequalities of interest such as monotonicity, monogamy and strong superadditivity. Our ultimate goal is to study whether these properties are universal across quantities on both sides of the bulk/boundary duality.

2.1 Classical and Quantum Correlation Measures

First we introduce the three key correlation measures relevant to our analysis: total correlation or mutual information $I(A : B)$, classical correlation $J(A|B)$, and quantum discord $D(A|B)$.

Mutual Information. The (quantum) mutual information $I(A : B)$ quantifies the total correlation between two subsystems A and B of a bipartite state ρ_{AB} , defined as

$$I(A : B) := S_A + S_B - S_{AB}, \quad (2.1)$$

where S_X is the von Neumann entropy of the reduced density matrix on subsystem X . In terms of the quantum conditional entropy $S(A|B) = S_{AB} - S_B$, the mutual information becomes

$$I(A : B) = S_A - S(A|B). \quad (2.2)$$

Intuitively, this represents a residual entropy (\sim uncertainty) of A after quantum conditioning on B .

Classical Correlation. A different form of mutual correlation can be defined by measuring a subsystem B . Given a positive operator-valued measure (POVM) $\Pi = \{E_x\}_x$ on B , a conditional state of A after observing outcome x is $\rho_A^x = \frac{1}{p_x} \text{Tr}_B(E_x \rho)$, with probability $p_x = \text{Tr}(E_x \rho)$. The (classical) mutual information $J_\Pi(A|B)$ can be obtained by replacing the quantum conditional entropy in (2.1) with the (classical) conditional entropy, defined as the average residual entropy of A after measuring B with Π :

$$J_\Pi(A|B) = S_A - \sum_x p_x S(\rho_A^x). \quad (2.3)$$

Intuitively, this quantifies the reduction in uncertainty about A due to a measurement on B . In this sense, it is occasionally called as the Groenewold-Ozawa information gain or the locally accessible information [35]. The classical correlation is defined by maximizing J_Π over all possible POVM measurements:

$$J(A|B) = \max_\Pi J_\Pi(A|B). \quad (2.4)$$

It coincides with $I(A : B)$ only when ρ_{AB} is quantum-classical (i.e., classical on B). On the one hand, $J(A|B)$ can be nonzero even in the absence of entanglement and on the other, classical correlation in this definition may include contributions from entanglement. For example, for a maximally entangled Bell pair, one finds

$J(A|B) = \log 2$. For a classically correlated state, whose information can be reduced to a single probability distribution like $\rho_{AB} = \sum_i p_i |i\rangle\langle i|_A \otimes |\varphi_i\rangle\langle\varphi_i|_B$, one finds $J(A|B)$ equals the Shannon entropy, representing the entropy of classically correlated bits.

The Koashi-Winter relation [36] provides an alternative expression for the classical correlation in terms of the entanglement of formation E_F between A and a purification partner C of ρ_{AB} . Namely,

$$J(A|B) = S_A - E_F(A : C), \quad (2.5)$$

where $\rho_{AB} = \text{Tr}_C |\Psi\rangle\langle\Psi|_{ABC}$ for arbitrary purification $|\Psi\rangle_{ABC}$ and the Entanglement of formation is defined as

$$E_F(A : C) = \inf \sum_x p_x S_A(|\psi_x\rangle\langle\psi_x|), \quad (2.6)$$

where the infimum is taken over all purifications of $\rho_{AC} = \sum_x p_x |\psi_x\rangle\langle\psi_x|_{AC}$.

Quantum Discord. We define the quantum correlation between A and B as the difference between the total and classical correlation:

$$D(A|B) = I(A : B) - J(A|B), \quad (2.7)$$

which is known as the Quantum Discord [17]. It captures nonclassical correlations that survive even in separable states, and like the classical correlation it is in general asymmetric with respect to which party is being measured.

We note that, by construction, both $J(A|B)$ and $D(A|B)$ involve an optimization over all POVM measurements. While the optimal POVM is known to be rank-one [37], it is not necessarily orthogonal, and there are examples where projective measurements are suboptimal [38, 39]. Computing discord is NP-complete in general [40], making it infeasible to evaluate for high-dimensional systems.

In this paper, we address this challenge by exploring bulk and boundary duals of these measures. These duals allow for efficient computation of classical and quantum correlation quantities, even in a high-dimensional Hilbert space.

2.2 Holographic duals

In this subsection, we introduce the holographic counterparts of the classical correlation $J(A|B)$ and quantum discord $D(A|B)$ at leading order in G_N and in static (time-independent) spacetimes.

Holographic Entanglement Entropy. In the static (or more generally time reflection symmetric) cases, the entanglement entropy of a subregion A in a boundary

theory is given by the Ryu-Takayanagi formula [1]. The bulk dual is called the holographic entanglement entropy (HEE), which is proportional to the minimal area of a codimension-two¹ surface homologous to A :

$$S_A = \min_{\gamma_A} \frac{\text{Area}(\gamma_A)}{4G_N}. \quad (2.8)$$

Entanglement Wedge Cross Section. The EWCS between A and C is proportional to the minimal area of a codimension-two surface separating the entanglement wedge of AC (denoted by $\mathcal{E}(AC)$) into two bulk subregions homologous to A and C . Namely,

$$E_W(A : C) = \min_{\Gamma_{A:C}} \frac{\text{Area}(\Gamma_{A:C})}{4G_N}, \quad (2.9)$$

where the minimization is over all codimension-two surfaces $\Gamma_{A:C} \subset \mathcal{E}_{AC}$ that bisect the entanglement wedge.

The EWCS is conjectured to be dual to several different boundary quantities related to mixed-state entanglement, including the entanglement of formation E_F , entanglement of purification E_P , and a half of reflected entropy S_R [8, 10, 41].

Bulk duals for classical and quantum correlations. A recent proposal by one of the authors [16] conjectures that the classical and quantum correlations admit bulk duals in holography. Given a purification $|\Psi\rangle_{ABC}$ of a bipartite mixed state $\rho_{AB} = \text{Tr}_C |\Psi\rangle\langle\Psi|$, the bulk duals of classical correlation $J(A|B)$ and quantum discord $D(A|B)$ are proposed as

$$J_W(A|B) \equiv S_A - E_W(A : C), \quad D_W(A|B) \equiv S_B - S_C + E_W(A : C). \quad (2.10)$$

This is supported either by holographic measurements or the $E_F = E_W$ conjecture, utilizing a disentangled basis along the minimal surface for B . We refer the readers to [9] for more details.

Reflected Entropy. The reflected entropy is defined as

$$S_R(A : B) = S_{AA^*}(|\rho^{1/2}\rangle), \quad (2.11)$$

where $|\rho^{1/2}\rangle_{AA^*BB^*}$ is the *canonical purification* of ρ_{AB} , which is found using the following procedure. Let $\{\lambda_n, |n\rangle\}_n$ be the set of eigenvalues and eigenvectors of the density matrix ρ_{AB} . Here we include zero eigenvalues as well. Then, the canonical purification is given by

$$|\rho^{1/2}\rangle_{AA^*BB^*} = \sum_n \sqrt{\lambda_n} |n\rangle_{AB} \otimes |n\rangle_{A^*B^*}, \quad (2.12)$$

where $\mathcal{H}_{AB} \rightarrow \mathcal{H}_{A^*B^*}$ is an endomorphism.

¹We will always use codimension with respect to the full spacetime (not just the Cauchy slice).

In this work, we also aim to propose an alternative measure to classical and quantum correlations without optimizations. Employing a particular boundary dual of the EWCS, we aim to deduce a boundary quantity out of the holographic measures. Since our aim is to circumvent a difficult optimization, we employ the duality between the EWCS and the reflected entropy,

$$S_R(A : B) = 2E_W(A : B), \quad (2.13)$$

which holds at $\mathcal{O}(1/G_N)$ [10]. The subleading correction could be expected depending on the quantum definition of the EWCS.

One-shot distillable entanglement. Holographic classical correlation $J_W(A|B)$ (as well as its analog of Haar random states) is proposed to admit another boundary interpretation — one-shot, one-way distillable entanglement $E_D^{[1\text{WAY}]}(A|B)$ [9]. It is defined as the number of EPR pairs that can be extracted from a bipartite state via one-way local operations and classical communication (LOCC) up to a sufficiently small error (See [9] for a precise definition). Symmetrizing this definition leads to the one-shot distillable entanglement under one-way LOCC in both directions:

$$E_D^{[1\text{WAY}]}(A : B) = \max(J_W(A|B), J_W(B|A)) =: J_W(A : B), \quad (2.14)$$

An important question is whether one-way LOCC outperform two-way LOCC or not. In general, two-way LOCC is a larger set of operations than one-way LOCC in both directions as the latter does not feedforward the measurement outcome to the subsequent LOCC in the other direction. While we do not provide a direct answer to this question, we give supporting evidence by considering the strong superadditivity for both one-way and two-way distillable entanglement.

2.3 Correlation Inequalities

We now define the functional properties we examine in this work. Let $\sigma(A|B)$ be any (potentially asymmetric) bipartite correlation measure between arbitrary subsystems A and B . We denote other subsystems by C, D . Note that ρ_{ABCD} is not necessarily pure.

Definition 2.1 (Monotonicity). A measure $\sigma(A|B)$ is *monotone* under partial trace with respect to the measured party if

$$\sigma(A|BC) \geq \sigma(A|B) \quad (2.15)$$

and monotone under partial trace with respect to the unmeasured party if

$$\sigma(AC|B) \geq \sigma(A|B). \quad (2.16)$$

Definition 2.2 (Monogamy). A measure $\sigma(A|B)$ is *monogamous* with respect to the measured party if

$$\sigma(A|B) + \sigma(A|C) \leq \sigma(A|BC), \quad (2.17)$$

and monogamous with respect to the unmeasured party if

$$\sigma(A|B) + \sigma(C|B) \leq \sigma(AC|B). \quad (2.18)$$

We call σ *polygamous* if the opposite inequality is true.

Definition 2.3 (Strong superadditivity). A measure $\sigma(A|B)$ is *strongly superadditive* if

$$\sigma(AC|BD) \geq \sigma(A|B) + \sigma(C|D). \quad (2.19)$$

The strong superadditivity follows from the inclusion relation of operations for optimized quantities. It implies monogamy by taking $A = C$ or $B = D$.

While entanglement measures are often monogamous and monotone, the same is not true for classical correlation or quantum discord. We illustrate this with an explicit counterexample. Consider a tripartite state

$$\rho_{ABC} = \frac{1}{2} |000\rangle\langle 000| + \frac{1}{2} |+11\rangle\langle +11|, \quad (2.20)$$

where $|+\rangle = (|0\rangle + |1\rangle)/\sqrt{2}$. Its marginals are

$$\rho_{BA} = \rho_{CA} = \frac{1}{2} |00\rangle\langle 00| + \frac{1}{2} |1+\rangle\langle 1+|, \quad \rho_{BC} = \frac{1}{2} |00\rangle\langle 00| + \frac{1}{2} |11\rangle\langle 11|. \quad (2.21)$$

One finds that $D(C|AB) = 0$ but $D(C|A) > 0$, violating monotonicity with respect to the measured (second) party. Furthermore, $D(C|A) = D(B|A) = D(BC|A) > 0$ while $D(C|B) = D(C|AB) = 0$, showing discord is not generally monogamous for either party.

Although quantum discord is known to be monotone with respect to the unmeasured (first) party and classical correlation is monotone in both arguments [42, 43], monogamy is not guaranteed [44]. This means strong superadditivity is neither guaranteed. Holographic duals, however, may obey stronger constraints.² (Note the above counterexample is a classically correlated state; such a state is unlikely holographic [9, 16, 45–47].) Testing these inequalities provides not only a consistency check for the proposed dualities but also additional characteristic features of holographic states.

²For example, mutual information is known to be monogamous for holographic states while it is not necessarily monogamous for non-holographic states [29].

3 Assumptions and Technical Tools

In this section, we summarize the assumptions and definitions we use in our proofs. In particular, we define various notations of AdS/CFT topologically in Section 3.2 and demonstrate a proof of a holographic inequality in Section 3.3 with our notations. In Section 3.4 we provide a topological characterization of the EWCS by providing some key definitions and properties. See Appendix A for a summary of notation and Appendix D for additional notation used in the complete proofs.

3.1 Assumptions for holographic proofs

Before turning to the holographic proofs of the aforementioned functional properties, we briefly summarize the key assumptions in this work.

Assumption 3.1 (Leading-order analysis). In this paper, we always work with the semiclassical limit where Newton's constant $G_N \rightarrow 0$. In this limit, entropic quantities like I , J_W , and D_W are decomposed into the area term proportional to G_N^{-1} and the bulk matter term which is usually $O(1)$. We do not consider any backreaction from the bulk matter or nonperturbative corrections in this paper.

Assumption 3.2 (Time-reflection symmetry). Generally speaking, all the entropic quantities can be defined in a time-dependent setting using the Hubeny-Rangamani-Takayanagi (HRT) formula [48] or the maximin prescription [23]. However, in this paper, we restrict to the time-reflection symmetric setup, where we can rely on the Ryu-Takayanagi (RT) formula. This is because when one considers a linear combination of multiple entropic quantities (HEE and EWCS), they do not necessarily lie on the same HRT/maximin surface and a mere comparison on a single surface may not be justified.

Assumption 3.3 (Minimality and Homology Condition). In the calculation of HEE and EWCS, all relevant surfaces are homologous to the boundary subregions in the entanglement wedge of interest and are chosen to minimize the area functional.

Assumption 3.4 (Entanglement Wedge Nesting (EWN)). For nested boundary regions, their corresponding entanglement wedges also form a nested structure in the bulk. In particular, the monotonicity of the EWCS

$$E_W(A : BC) \geq E_W(A : B) \tag{3.1}$$

follows from EWN [22, 23, 49]. See Figure 7 for an example.

Assumption 3.5 (No multiple intersections of geodesics on an AdS Cauchy slice). This is a standard property of holographic spacetimes under our other assumptions where any two distinct length minimizing geodesics on the slice intersect in the

interior of the slice at most once. If they intersect more than once, say at points x and y , then they coincide between x and y .

This is of course necessary information theoretically. If the extremal surfaces associated to different boundary subregions intersect with each other, the entanglement wedge reconstruction can transmit bulk quantum information inside the intersection of the entanglement wedges to either boundary subregion simultaneously. However, this violates the no-cloning theorem in QI which prohibits cloning unknown quantum information.

Assumption 3.6 (Bulk boundaries). In the definitions and proofs below, we assume that the asymptotic boundaries are the only boundaries of the bulk dual to a pure state. The arguments, however, extend straightforwardly to bulks with additional non-asymptotic boundaries, such as cutoff surfaces or end-of-the-world branes. In the former case, the boundary Hilbert space is defined on both the asymptotic boundaries and any non-asymptotic boundaries. In the latter case, the brane is dynamically constrained and does not introduce independent degrees of freedom beyond those of the asymptotic boundary [50]; accordingly, surfaces that lie along the brane contribute no area term even though they geometrically form part of the bulk boundary. In addition, when a non-asymptotic boundary admits a naive RT surface that would lie outside the physical bulk, the entanglement wedge must be replaced by the generalized entanglement wedge [51].

Assumption 3.7 (Disjoint boundary subsystems). When proving holographic correlation inequalities for some boundary state $ABC\dots$ we will always assume each subsystem is non-overlapping unless otherwise stated. That is $A \cap B$ is empty or codimension two and so on, with this intersect only along the subsystem boundaries on the cut-off surface.

Remark 3.1. Although we use the Poincaré disk picture of $\text{AdS}_3/\text{CFT}_2$ to illustrate the proofs, we emphasize that our methodology is general and is valid regardless of dimensionality.

3.2 Conventions and Definitions

Since our proofs will be based on topological arguments, here we define some necessary terminology.

Definition 3.1 (Bulk). The *bulk slice* is a fixed time-reflection symmetric Cauchy slice, denoted by Σ . All geometric objects (subregions, hypersurfaces) considered in this work are taken to lie in Σ .

Definition 3.2 (Boundary notation). For a codimension-one surface $U \subseteq \Sigma$, we write $\partial_\Sigma U$ for its boundary *within the bulk slice* Σ (i.e. the bulk Cauchy slice excluding the bulk asymptotic boundary). We write $\partial_\infty U$ for the boundary lying on the

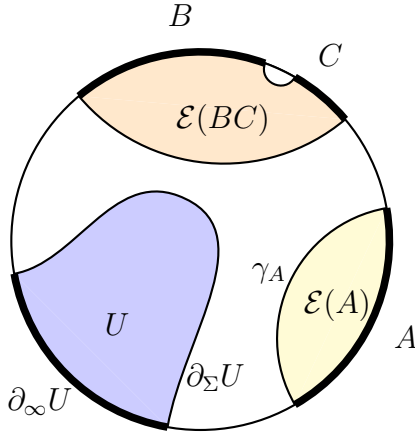


Figure 1. Example of definitions given below on the Poincaré disk.

asymptotic boundary of Σ . Therefore, all the boundary subregions are a subset of $\partial_\infty \Sigma$. By default, we use a shorthand notation, $\partial \equiv \partial_\Sigma$, unless otherwise stated.

Definition 3.3 (Subsystem complement). Given a subsystem A , we write \bar{A} to be its complement such that $A \cup \bar{A}$ is a pure state.

Definition 3.4 (Entanglement wedge). For a boundary subsystem A , the *entanglement wedge* $\mathcal{E}(A) \subseteq \Sigma$ is the bulk region whose asymptotic and bulk boundaries satisfy

$$\partial_\infty \mathcal{E}(A) = A, \quad \partial_\Sigma \mathcal{E}(A) = \gamma_A,$$

where γ_A is the RT surface of A . For two disjoint boundary subsystems A and B , the *joint entanglement wedge* $\mathcal{E}(AB) \subseteq \Sigma$ is defined analogously using the RT surfaces γ_{AB} again with equality iff the state on AB is pure.

Definition 3.5 (Bridged wedges). We can categorize the various types of joint entanglement wedges as follows. For two disjoint boundary subsystems A and B , with

$$A = \bigsqcup_i A_i, \quad B = \bigsqcup_j B_j, \quad A \cap B = \emptyset, \quad A_i \cap A_j = A_i \delta_{ij}, \quad B_i \cap B_j = B_i \delta_{ij},$$

we can decompose $\mathcal{E}(AB)$ into its connected (in the standard topological sense) components

$$\mathcal{E}(AB) = \bigsqcup_\alpha W_\alpha.$$

For each component W_α consider its asymptotic boundary $\partial_\infty W_\alpha \subseteq A \cup B$. We classify components as follows:

- W_α is an *A-only component* iff $\partial_\infty W_\alpha \subseteq A$.
- W_α is a *B-only component* iff $\partial_\infty W_\alpha \subseteq B$.

- W_α is an *A–B bridged component* iff its asymptotic boundary meets both sides,

$$\partial_\infty W_\alpha \cap A \neq \emptyset, \quad \partial_\infty W_\alpha \cap B \neq \emptyset.$$

The union of all *A–B bridged components*,

$$\mathcal{E}_{\text{brid}}(A:B) := \bigsqcup_{\alpha: W_\alpha \text{ bridged}} W_\alpha,$$

is called the *(A:B)-bridged entanglement wedge*. We say that A and B have a *bridged entanglement wedge* if $\mathcal{E}_{\text{brid}}(A:B) \neq \emptyset$.³

Moreover we say for some $A_i \in A$ that A_i is an *A-only component* of AB iff there exists an *A-only component* W_α such that $A_i \subseteq \partial_\infty W_\alpha$. We define B_i as a *B-only component* similarly and say A_i is a *bridged component* of AB iff there exists an *A–B bridged component* W_α such that $A_i \subseteq \partial_\infty W_\alpha$. See Figure 2 for an example.

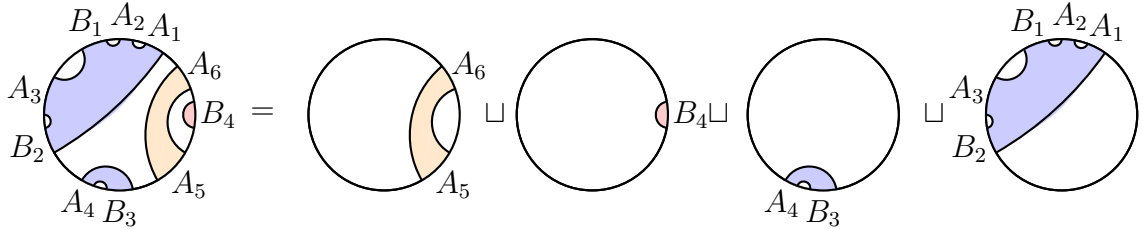


Figure 2. Decomposition of $\mathcal{E}(AB)$ into its *A-only component* in orange, *B-only component* in red and a disjoint bridged entanglement wedge $\mathcal{E}_{\text{brid}}(A : B)$ in blue (disjoint as the last two panels are both bridged but disjoint from each other). We have $\{A_5, A_6\}$ are *A-only components* of AB , B_4 a *B-only component* of AB , and $\{A_1, A_2, A_3, A_4, B_1, B_2, B_3\}$ bridged components of AB .

Remark 3.2 (Bridged wedges and correlation measures). Given some (mixed) state on AB , we generally have $\mathcal{E}(AB) = \bigsqcup_\alpha W_\alpha$, with each W_α some connected codimension-one surface. Identify all *A-only components* within this decomposition and label the subset $\mathcal{A} \subseteq A$ such that \mathcal{A} is the full set of *A-only components* in AB . Define \mathcal{B} similarly. We can then find the AB bridged components $\mathcal{F}_A = A \setminus \mathcal{A}$ and $\mathcal{F}_B = B \setminus \mathcal{B}$ such

³The relation to a connected (entanglement) wedge used in literature is as follows. If the entanglement wedge of two boundary subsystems (composed of multiple boundary subregions) is connected (i.e. non-factorizing), then there is at least one bridged component among the boundary subregions. Thus, a connected entanglement wedge contains a bridged entanglement wedge. However, they are not equivalent as we specifically refer the components connecting a portion of A and a portion of B as *bridged* among various components of the connected entanglement wedge.

that \mathcal{F}_A is the AB bridged components of A , and \mathcal{F}_B is the AB bridged components of B . By defining $\mathcal{F} = \mathcal{F}_A \cup \mathcal{F}_B$, it then follows that

$$\mathcal{E}(AB) = \mathcal{E}(\mathcal{A}) \sqcup \mathcal{E}(\mathcal{B}) \sqcup \mathcal{E}(\mathcal{F}), \quad (3.2)$$

and so entropies split additively to

$$S_{AB} = S_{\mathcal{A}} + S_{\mathcal{B}} + S_{\mathcal{F}}, \quad \text{and} \quad E_W(A : B) = E_W(\mathcal{F}_A : \mathcal{F}_B). \quad (3.3)$$

For example in Figure 2 we have $S_{AB} = S_{A_5A_6} + S_{B_4} + (S_{A_1A_2A_3B_1B_2} + S_{A_4B_3})$. We have two terms from the bridged component as $\mathcal{E}_{\text{brid}}(AB)$ is composed of the corresponding two disjoint components:

$$\mathcal{E}_{\text{brid}}(AB) = \mathcal{E}(\mathcal{F}) = \mathcal{E}(A_1A_2A_3B_1B_2) \sqcup \mathcal{E}(A_4B_3). \quad (3.4)$$

Due to EWN, $\mathcal{E}(A) \subset \mathcal{E}(AB)$ when B is non-empty, thus A -only components in AB disconnect to AB -bridged components.

This leads to

$$S_A = S_{\mathcal{A}} + S_{\mathcal{F}_A}. \quad (3.5)$$

That is, when only considering $\mathcal{E}(A)$, \mathcal{A} and \mathcal{F}_A remain unbridged in A . The same argument holds for B .

Definition 3.6 (Homologous). Let A be a boundary subsystem and let $U \subseteq \Sigma$ be a codimension-one bulk *subregion*.

- (a) We write $U \sim A$ to mean that $\partial_\infty U = A$ and $\partial_\Sigma U$ is homologous to A . That is, U is a codimension-one bulk region whose only asymptotic boundary component is A , and it is otherwise bounded by a closed codimension two bulk surface in Σ .
- (b) We write $U \sim_V A$, with $V \subseteq \Sigma$ a codimension-one bulk subregion, to mean the above definition but the replacement of Σ to V .
- (c) For a state on AB , we write $U \sim_{AB} A$ to mean $U \sim_{\mathcal{E}(AB)} A$, i.e. $\partial_\Sigma U$ bounds A inside the entanglement wedge $\mathcal{E}(AB)$.

Definition 3.7 (Interior). We denote $\text{Int } \mathcal{E}(A)$ as the open bulk interior of the wedge, i.e. $\mathcal{E}(A) \setminus \partial \mathcal{E}(A)$.

3.3 Example of a holographic proof

Let us consider a simple inequality to demonstrate our strategy for proving a holographic inequality using the notations introduced above. We prove the following inequality for a mixed state on AB :

$$S_{AB} + E_W(A : B) \geq \max(S_A, S_B), \quad (3.6)$$

with an example configuration in Figure 3.

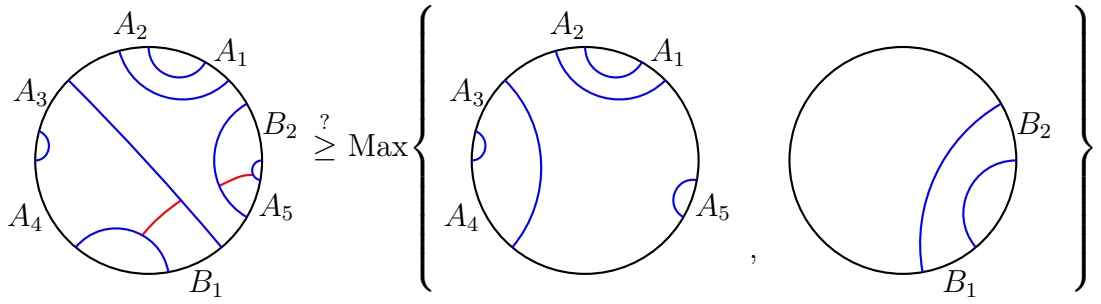


Figure 3. Holographic proof of (3.6). On the LHS, blue curves are γ_{AB} and red curves are $\Gamma_{A:B}^W$. On the RHS, they are γ_A and γ_B respectively.

Proof. The proof is in two steps. First, we decompose the LHS and RHS to cancel the disjoint components between two sides. Then, we simply cut and glue various surfaces from the LHS together to serve as upper bounds for the terms on the RHS.

Step 1: Isolating A -only components. We write $A = \cup A_i$ and $B = \cup B_i$, and denote C as the purifier of AB . Without loss of generality we can assume $S_A \geq S_B$ as the equation is symmetric under $A \leftrightarrow B$. Generally A can consist of multiple disjoint boundary subsystems and so we decompose $A = \mathcal{A} \cup \mathcal{F}$ with \mathcal{F}_A the AB bridged components of A , and \mathcal{A} the A -only components in AB . For example in Figure 3 we have $\mathcal{F}_A = A_3 \cup A_4 \cup A_5$ and $\mathcal{A} = A_1 \cup A_2$. Then, entropies split additively to

$$S_{AB} = S_{\mathcal{A}} + S_{\mathcal{F}_{A \cup B}}, \quad S_A = S_{\mathcal{F}_A} + S_{\mathcal{A}}, \quad (3.7)$$

with the second equality following from the first by EWN (see Remark 3.2). For example, using the shorthand notation $S_{ij\dots} = S_{A_i A_j \dots}$ and similarly for the entanglement wedge $\mathcal{E}_{ij\dots}$, in Figure 3, $S_A = S_{12} + S_{34} + S_5$, as these have disjoint wedges.

Returning to the general case, we can substitute (3.7) into our target inequality, and using that $E_W(A : B) = E_W(\mathcal{F}_A : B)$ as $\mathcal{A} = A \setminus \mathcal{F}_A$ is an A -only component of AB , we obtain the inequality

$$S_{\mathcal{F}_{A \cup B}} + E_W(\mathcal{F}_A : B) \stackrel{?}{\geq} S_{\mathcal{F}_A}. \quad (3.8)$$

This is the same as (3.6) but with the constraint that $\mathcal{F}_A B$ has no \mathcal{F}_A -only components. Note it may consist of multiple disjoint *bridged* wedges, as in the case of Figure 3 where $\mathcal{E}_{\mathcal{F}_A B} = \mathcal{E}_{34 B_1} \sqcup \mathcal{E}_{5 B_2}$. Thus the contribution from \mathcal{A} is exactly canceled between the LHS and RHS. Hence we rewrite $\mathcal{F}_A \rightarrow A$ absorbing the original \mathcal{A} into our purifier C , and can now assume there are no A -only components in AB .

Step 2: Proving (3.8). Let us define the *LHS surface* \mathbf{L} so that

$$\frac{\text{Area}(\mathbf{L})}{4G_N} = \text{LHS}$$

of a given inequality. In the current case, it is given by

$$\mathbf{L} = \gamma_{AB} \cup \Gamma_{A:B}^W, \quad (3.9)$$

where γ_{AB} is the RT surface of AB and $\Gamma_{A:B}^W$ defines the EWCS of $(A : B)$ as γ_{AB} and $\Gamma_{A:B}^W$ have no intersection (except measure zero sets).

Now, consider $\mathcal{E}(AB) \setminus \Gamma_{A:B}^W$. By the definition of EWCS this splits $\mathcal{E}(AB)$ into an A -sided region U_A and a B -sided region U_B . In our notation this is the statement that $\partial_\infty U_A = A$ and $\partial_\infty U_B = B$. As it stands U_A is a codimension-one bulk subregion with a closed boundary along the original arc of γ_{AB} from which it was formed but an open arc along $\Gamma_{A:B}^W$ where it was split from U_B . Thus we can close U_A in Σ by taking

$$U_A^{\text{cl}} = U_A \cup \Gamma_{A:B}^W, \quad (3.10)$$

which is just adjoining the boundary $\Gamma_{A:B}^W$ to U_A along its open edge.

This is illustrated in Figure 4 based on the example (Figure 3), where $U_A = U_{34} \sqcup U_5$.

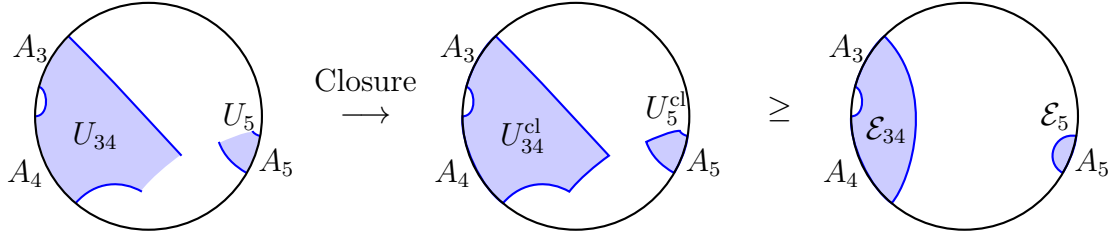


Figure 4. Decomposition of Figure 3 into A -homologous regions. We compute the closure via (3.10) which just glues $\Gamma_{A:B}^W$ to U_A .

Then $\partial U_A^{\text{cl}} \subset \mathbf{L}$ as its boundary is just a subset of γ_{AB} glued to $\Gamma_{A:B}^W$. Moreover as γ_{AB} separates U_A from C , and $\Gamma_{A:B}^W$ separates A from B within $\mathcal{E}(AB)$ it must be that $U_A^{\text{cl}} \sim A$. Thus ∂U_A^{cl} is homologous to A and so by RT minimality and that $\partial U_A^{\text{cl}} \subset \mathbf{L}$ we have

$$S_{AB} + E_W(A : B) = \frac{\text{Area}(\mathbf{L})}{4G_N} \geq \frac{\text{Area}(\partial U_A^{\text{cl}})}{4G_N} \geq S_A,$$

proving the claim. \square

3.4 Properties of the Entanglement Wedge Cross Section

To permit some of our later proofs we must first establish, among the aforementioned qualities (e.g. EWN), some properties of the EWCS. In particular, as evidenced in the

proof of equation (3.6), we need to know when a surgically constructed surface, can be used to upper bound a particular correlation measure; that is whether it satisfies the topological requirements of said measure, but is not necessarily a minimal choice. Hence we define an *RT admissible class* and *EWCS admissible class*.

Definition 3.8 (RT admissible class). Let A be boundary subsystem and let \mathfrak{S}_A be the set of properly embedded, piecewise smooth⁴, codimension-two hypersurfaces $\gamma \subset \Sigma$ such that

$$(i) \quad \Sigma \setminus \gamma = U_A \sqcup U_{\bar{A}}, \text{ with } \partial_\infty U_A = A \text{ and } \partial_\infty U_{\bar{A}} = \bar{A},$$

where \bar{A} purifies A . This is just the statement that γ is homologous to A . We say a surface is RT admissible for A iff it satisfies the above condition. Moreover there exists a member $\gamma_A \in \mathfrak{S}_A$ which is the RT surface of A such that $S_A = \text{Area}(\gamma_A)/4G_N$.

Definition 3.9 (EWCS admissible class). Let A, B be disjoint boundary subsystems. Let $\mathfrak{S}_{A:B}$ be the set of properly embedded, piecewise smooth, codimension-two hypersurfaces $\Gamma \subset \mathcal{E}(AB)$ such that

$$(i) \quad \partial_\Sigma \Gamma \subset \gamma_{AB} \text{ (bulk anchoring of } \Gamma \text{ on } \gamma_{AB} = \partial \mathcal{E}(AB)),$$

$$(ii) \quad \mathcal{E}(AB) \setminus \Gamma = U_A \sqcup U_B \text{ with } \partial_\infty U_A = A \text{ and } \partial_\infty U_B = B.$$

We say a surface is EWCS admissible for $(A : B)$ iff it satisfies the above conditions. Moreover there exists a member $\Gamma_{A:B}^W \in \mathfrak{S}_{A:B}$ which is the *entanglement wedge cross section* (EWCS), with $E_W(A : B) = \text{Area}(\Gamma_{A:B}^W)/(4G_N)$. We will always refer to $\Gamma_{A:B}^W$ as the member of the class that minimizes the area function.

Proving the admissibility of some constructed codimension-two hypersurface can be lengthy. In our proofs we generally achieve this by constructing paths beginning and ending on certain points at the asymptotic boundary and showing in their evolution they intersect the required surface. As we only include proof sketches in the main text this formalism is outlined in Appendix D. We now introduce a fundamental property of the EWCS which will be required for several of our proofs.

Theorem 3.1. The EWCS surface, $\Gamma_{A:B}^W$, with $\text{Area}(\Gamma_{A:B}^W)/4G_N = E_W(A : B)$, never enters the interior of the individual wedges of its two arguments:

$$\Gamma_{A:B}^W \cap \text{Int } \mathcal{E}(A) = \emptyset, \quad \Gamma_{A:B}^W \cap \text{Int } \mathcal{E}(B) = \emptyset. \quad (3.11)$$

⁴We require smoothness only piecewise as we will construct admissible surfaces by gluing various smooth surfaces in a non-smooth way.

From an information theoretic perspective this is of course a necessary condition. In the holographic code picture, $\text{Int } \mathcal{E}(A)$ consists of bulk degrees of freedom that are reconstructible from A alone, i.e. they are “local” to one boundary party. Since $E_W(A : B)$ is intended to quantify correlations that are genuinely *shared* between A and B —those accessible only from the joint region AB —its dual surface $\Gamma_{A:B}^W$ must not “count” any part of the bulk already attributable to a single side. Hence $\Gamma_{A:B}^W$ lives in the joint-only region $\mathcal{E}(AB) \setminus (\mathcal{E}(A) \cup \mathcal{E}(B))$. Equivalently, in the bit-thread formulation, $E_W(A : B)$ is the maximum flux of threads connecting A to B within $\mathcal{E}(AB)$, and the RT surfaces γ_A, γ_B act as capacity bottlenecks for outward flux; any $A \leftrightarrow B$ thread bundle that detours into $\mathcal{E}(A)$ or $\mathcal{E}(B)$ wastes scarce capacity without improving connectivity, so the optimal max flow (and hence the minimal cut $\Gamma_{A:B}^W$) can be pushed to avoid the interiors of the individual wedges.

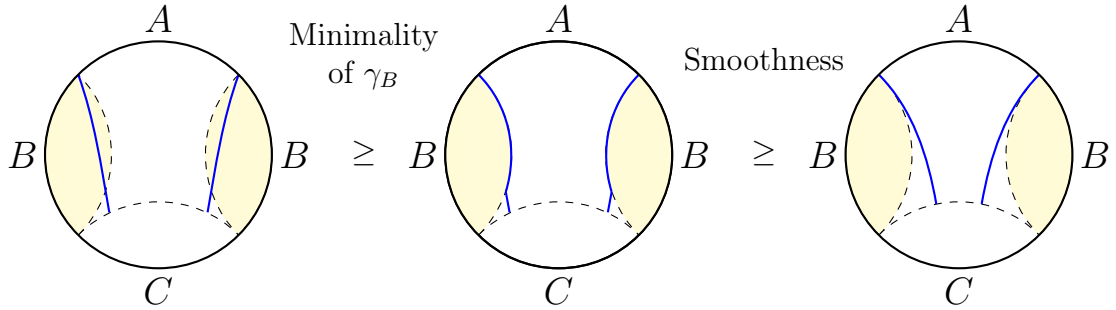


Figure 5. $\mathcal{E}(B)$ shaded in yellow. Crossing of $\Gamma_{A:B}^W$ into $\mathcal{E}(B)$ would require two intersections with γ_B (left). By uniqueness, the left segment must coincide with γ_B between those points, then non-smoothly join the curve anchoring on γ_C . By smoothness of minimizers this is forbidden.

Holographically it is true based on minimality arguments along with EWN. For instance consider in Figure 5 where we initially assume $\Gamma_{A:B}^W$ enters $\text{Int } \mathcal{E}(AB)$. However under Assumption 3.5 this is forbidden as we can always push $\Gamma_{A:B}^W$ out of $\mathcal{E}(B)$ to the assumed minimizing geodesic γ_B . Then by smoothness our original choice of $\Gamma_{A:B}^W$ was incorrect. Of course there is another case with $\mathcal{E}(B)$ a connected wedge as in Figure 6. However even here by considering the addition of S_A we find such a configuration erroneously implies $E_W(A : B) > S_A$, and hence the barrier theorem holds. We give a detailed proof of the theorem in Appendix E in two ways: considering the relation between reflected entropy and the EWCS (equation (2.13)) and imposing EWN, and considering a cycle type argument akin to Figure 6.

4 Holographic Monotonicity

Having presented the necessary dictionary, as well as various proof tools, we can now proceed to study the monotonicity of the holographic correlation measures J_W and

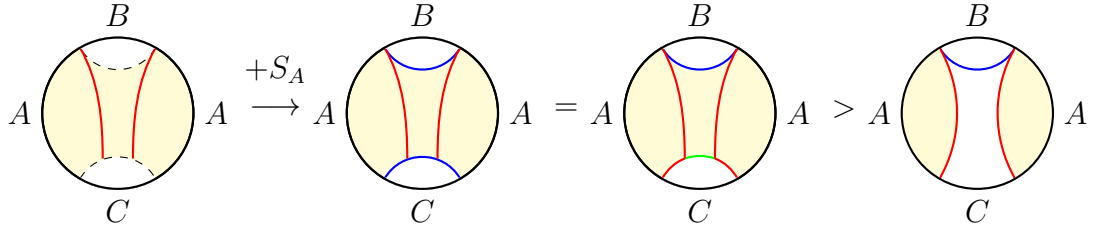


Figure 6. Other case in the barrier theorem. We have the dashed curves are γ_A , the yellow region $\mathcal{E}(A)$ and the red curve $\Gamma_{A:B}^W$ intersects $\text{Int } \mathcal{E}(A)$. This is not a violation however as this configuration implies that $E_W(A : B) > S_B$ which is axiomatically false.

D_W . As a summary of our findings, we prove the following monotonicity relations for a mixed state on ABC :

$$D_W(A|BC) \not\geq D_W(A|B), \quad (4.1)$$

$$J_W(AB|C) \geq J_W(A|B), \quad (4.2)$$

$$D_W(AC|B) \geq D_W(A|B), \quad (4.3)$$

$$J_W(AC|B) \geq J_W(A|B), \quad (4.4)$$

where $\not\geq$ does not imply the opposite inequality, only that neither is generally true.

4.1 Measured Party

In this subsection, we will show that J_W is monotone with respect to the measured party and that D_W is not. Namely,

$$D_W(A|BC) \not\geq D_W(A|B), \quad (4.5)$$

$$J_W(A|BC) \geq J_W(A|B), \quad (4.6)$$

which are consistent with the known properties for D and J [52].

The property for J_W is straightforward: expanding out the inequality reduces to

$$E_W(A : CD) \stackrel{?}{\geq} E_W(A : D), \quad (4.7)$$

where D purifies ABC . This is true by EWN and is visualized in Figure 7.

For D_W , there are counterexamples to the inequality in both directions. Consider a pure ABC , such that the monotonicity of D_W reduces to

$$I(A : C) \stackrel{?}{\geq} E_W(A : C), \quad (4.8)$$

which is not true in general. For example, when A and C are barely connected, $I(A : C) \approx 0$ while $E_W(A : C) = O(1/G_N)$. Thus, holographic discord is not monotone with respect to the measured party.

The opposite inequality can also be violated, that is, monotonicity sometimes holds. For example, if one takes A and C adjacent to each other, counting the UV divergence satisfies equation (4.8).

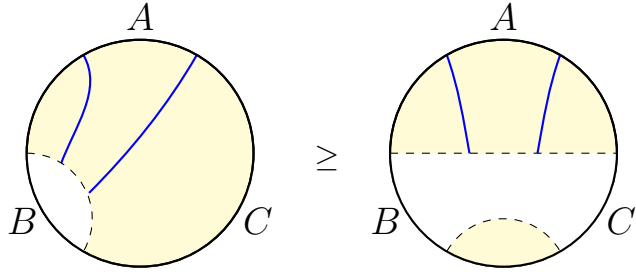


Figure 7. Example for $E_W(A : CD) \geq E_W(A : D)$. The blue curves denote the EWCS. Coloured region on the LHS shows $E(ACD)$ and on the RHS $E(AD)$.

4.2 Unmeasured Party

Here we show that both D_W and J_W are monotone with respect to the unmeasured party. This is consistent with the known monotonicity relations of the original boundary correlation measures $D(AC|B) \geq D(A|B)$ and $J(AC|B) \geq J(A|B)$ [52, 53].

Lemma 4.1 (Monotonicity in the unmeasured party of either J_W or D_W implies the other). For a mixed boundary state ABC we have

$$D_W(AC|B) \geq D_W(A|B) \iff J_W(AC|B) \geq J_W(A|B). \quad (4.9)$$

Proof. Expanding out equations (4.3) and (4.4) we see

$$\begin{aligned} D_W(AC|B) \geq D_W(A|B) &\implies S_{CD} + E_W(AC : D) \geq S_D + E_W(A : CD) \\ J_W(AC|B) \geq J_W(A|B) &\implies S_{AC} + E_W(A : CD) \geq S_A + E_W(AC : D) \end{aligned}$$

where D purifies ABC . Taking $A \leftrightarrow D$ in the second and using the symmetry of EWCS shows they are identical inequalities. \square

We have shown one implies the other and so we only need to prove a single measure is monotone.

Theorem 4.1. D_W is monotone in the unmeasured party. That is D_W satisfies

$$D_W(AC|B) \geq D_W(A|B), \quad (4.10)$$

for any state on ABC (not necessarily pure).

We give a detailed proof of this theorem in Appendix F and here we just illustrate the proof with a particular configuration. After relabeling the subsystems, (4.10) is equivalent to

$$S_{BC} + E_W(AB : C) \geq S_C + E_W(A : BC),$$

again with ABC not necessarily pure. Figure 8 shows one particular configuration of systems in the leftmost diagram. The middle diagram corresponds to the same

curves, but grouped differently such that the blue curve is EWCS admissible for $(A : BC)$ and so upper bounds $E_W(A : BC)$ and the red curve is RT admissible for C and so upper bounds S_C . This implies the inequality showing the theorem is true in this configuration. In the figure, the green piece is a leftover and not needed to upper bound the LHS.

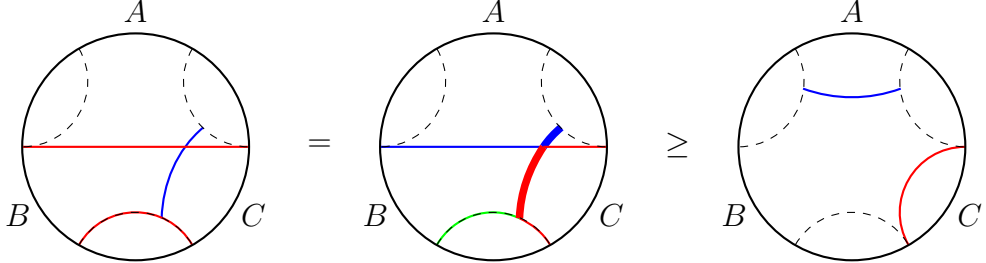


Figure 8. Example configuration showing D_W in monotone in the unmeasured party. On the left, red denotes γ_{BC} and blue denotes $\Gamma_{AB:C}^W$; the dashed curve is γ_{ABC} . In the middle, we reassign pieces of the combined red and blue surfaces into a new decomposition serving as an RT candidate for C in red, and EWCS candidate for $(A : BC)$ in blue. The right-hand panel shows γ_C and $\Gamma_{A:BC}^W$; by smoothness/minimality, our candidate surfaces in the middle panel have strictly larger area than these extremizers on the right.

5 Holographic Monogamy/Polygamy

In this section, we study the monogamy/polygamy properties of our holographic correlation measures, D_W and J_W . As an initial summary, we find that

$$D_W(A|B) + D_W(A|C) \not\leq D_W(A|BC), \quad (5.1)$$

$$D_W(A|B) + D_W(C|B) \not\leq D_W(AC|B), \quad (5.2)$$

$$J_W(A|B) + J_W(C|B) \leq J_W(AC|B), \quad (5.3)$$

$$J_W(A|B) + J_W(A|C) \leq J_W(A|BC), \quad (5.4)$$

where as before $\not\leq$ does not imply the opposite just that neither way is true. However for pure ABC we find discord to be polygamous with respect to the unmeasured party

$$D_W(A|B) + D_W(C|B) \geq D_W(AC|B), \quad \text{pure } ABC. \quad (5.5)$$

5.1 Polygamy of discord

We first begin by showing that holographic discord is polygamous for the unmeasured party when ABC are pure:

$$D_W(A|B) + D_W(C|B) \geq D_W(AC|B). \quad (5.6)$$

For pure ABC , this is equivalent to

$$E_W(A : C) \geq \frac{I(A : C)}{2}, \quad (5.7)$$

which is a known lower bound for the EWCS [8, 54]. Moreover, when dealing with non-holographic states, we can replace E_W with E_P or $S_R/2$, and the inequality remains true. It is not true however for the original quantum discord, in which $E_W \rightarrow E_F$. For example, the polygamy of the original quantum discord is violated for a maximally mixed state, whose purification is the GHZ state on ABC . Given the conjectured duality between D and D_W , such a polygamy-violating state should be prohibited in holography — indicating no GHZ entanglement in holography.

For mixed states however polygamy does not hold. For example consider three contiguous intervals ACB , namely, C is placed between A and B . The rest of the boundary is denoted by D . If C is small enough, we have $S_{AB} = S_{CD} = S_C + S_{ABC}$ and $E_W(A : CD) = E_W(AC : D) + E_W(C : AD) < S_A$, leading to

$$\begin{aligned} & D_W(A|B) + D_W(C|B) - D_W(AC|B) \\ &= S_B - S_{AB} - S_{BC} + S_{ABC} + E_W(A : CD) + E_W(C : AD) - E_W(AC : D) \\ &= S_B - (S_C + S_{ABC}) - S_{BC} + S_{ABC} + E_W(AC : D) + E_W(C : AD) \\ &\quad + E_W(C : AD) - E_W(AC : D) \\ &= S_B + 2E_W(C : AD) - S_C - S_{BC}. \end{aligned} \quad (5.8)$$

This is illustrated in Fig. 9. Due to the minimality condition, (5.8) is non-negative, indicating polygamy of discord in this case.

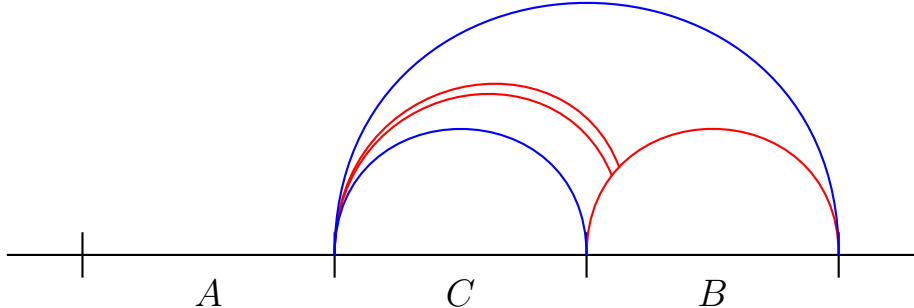


Figure 9. Polygamy of discord for mixed state ABC on the Poincaré patch: $S_B + 2E_W(C : AD) - S_C - S_{BC} \geq 0$. Positive curves colored in red and negative in blue.

Moreover, holographic mixed states allow a range of monogamous examples as well. For example, consider three disjoint intervals on the boundary circle:

$$A = \left(0, \frac{\pi}{3} + \theta\right), \quad B = \left(\frac{2\pi}{3}, \pi + \theta\right), \quad C = \left(\frac{4\pi}{3}, \frac{5\pi}{3} + \theta\right). \quad (5.9)$$

When $\theta = 0$, they are equally spaced and when $\theta = \pi/3$, the state on ABC is pure and the subsystems are mutually adjacent. Then, the remaining purifying subsystem D consists of three segments

$$D_j = \left(\frac{(2j-1)\pi}{3} + \theta, \frac{2j\pi}{3} \right), \quad (5.10)$$

where j runs from 1–3. When $\theta > 0$ is sufficiently small, all regions are disconnected. Moreover, the EWCS are just given by the entropies of the smallest argument, and so the inequality becomes

$$\sin\left(\frac{\frac{\pi}{3} - \theta}{2}\right) \stackrel{?}{\geq} \sin\left(\frac{\frac{\pi}{3} + \theta}{2}\right). \quad (5.11)$$

which is violated for any sufficiently small $\theta > 0$.

Thus, this concludes that holographic discord is neither monogamous or polygamous for mixed states.

Is there a monogamy relation for holographic discord with respect to the measured party? Namely, we ask whether

$$D_W(A|B) + D_W(A|C) \stackrel{?}{\leq} D_W(A|BC). \quad (5.12)$$

Expanding the inequality for pure $ABCD$ yields

$$S_D + I(B : C) + E_W(A : CD) + E_W(A : BD) \stackrel{?}{\leq} S_{CD} + S_{BD} + E_W(A : D). \quad (5.13)$$

An easy counter example is taking $D = \emptyset$ in which this reduces to

$$E_W(A : C) + E_W(A : B) \stackrel{?}{\leq} S_A, \quad (5.14)$$

which has obvious violating configurations. Similarly we can violate the polygamy by taking $C = \emptyset$ in which the inequality reduces to

$$E_W(A : D) \stackrel{?}{\geq} S_A, \quad (5.15)$$

which is axiomatically false. Thus D_W is neither polygamous nor monogamous for the measured party.

Lastly, we briefly remark on strong superadditivity. Since holographic discord D_W is not monogamous, it does not satisfy strong superadditivity (2.19) as well: strong superadditivity implies monogamy so taking its contraposition denies strong superadditivity of D_W for either party.

5.2 Monogamy of classical correlations

We will now prove that J_W is monogamous in both arguments beginning with the measured party.

5.2.1 Measured party

Theorem 5.1. J_W is monogamous in the measured party. That is J_W satisfies

$$J_W(A|B) + J_W(A|C) \leq J_W(A|BC). \quad (5.16)$$

for any state ABC (not necessarily pure).

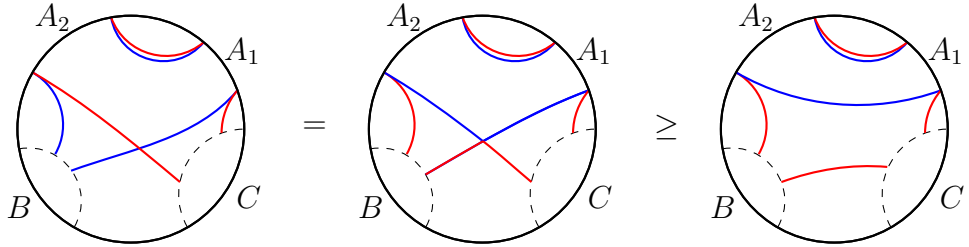


Figure 10. Example for monogamy of J_W for the measured party. On the LHS we have $\Gamma_{A:CD}^W$ in blue, and $\Gamma_{A:BD}^W$ in red. The dashed lines are the RT surfaces of γ_B and γ_C and we slightly displace to top red and blue curves to show they are both present. We decompose this in the middle figure into a blue curve ∂r_A , an RT candidate for A , and a red curve Γ , which is an EWCS candidate for $(A : D)$. This upper bounds the RHS figure via smoothness.

For pure ABC , it immediately follows from the polygamy of D_W . By combining that 1.) quantum mutual information is monogamous in holography [29] and 2.) $I(A : B) = D_W(A|B) + J_W(A|B)$ by definition, J_W must be monogamous to compensate for the polygamy of D_W for pure states on ABC . To summarize,

$$\left\{ \begin{array}{l} D_W(A|B) + D_W(C|B) \geq D_W(AC|B) \\ I_W(A : B) + I_W(C : B) \leq I_W(AC : B) \\ I_W(A : B) = D_W(A|B) + J_W(A|B) \end{array} \right\} \Rightarrow J_W(A|B) + J_W(C|B) \leq J_W(AC|B). \quad (5.17)$$

Beyond pure states, the full proof is presented in Appendix G. For an example case consider Figure 10 which plots the expansion of Theorem 5.1:

$$E_W(A:BD) + E_W(A:CD) \geq S_A + E_W(A:D). \quad (5.18)$$

The proof in this configuration then proceeds similarly to that of Theorem 4.1. We simply consider the LHS surfaces and relabel particular components to serve as admissible surfaces for the quantities on the RHS. One has to be careful about formalizing such a decomposition however due to potential degeneracy of surfaces as seen in Figure 10 where we have two identical curves. This is just due to representing two surfaces on the same copy of the bulk. Hence we need to keep track of the multiplicities involved (see Definition D.3).

5.2.2 Unmeasured party

Theorem 5.2. J_W is monogamous in the unmeasured party. That is J_W satisfies

$$J_W(A|B) + J_W(C|B) \leq J_W(AC|B).$$

for any states on ABC (not necessarily pure).

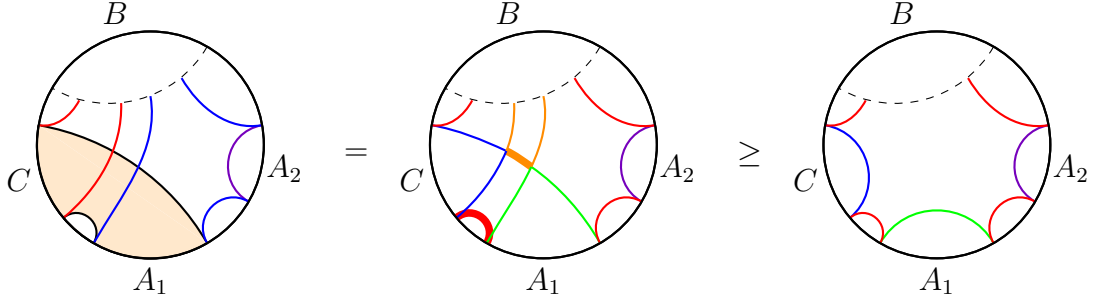


Figure 11. Example for monogamy of J_W for the unmeasured party, for $\mathcal{F} = A_1 \cup C$. On the LHS we have $\gamma_{\mathcal{F}}$ in black, $\mathcal{E}(\mathcal{F})$ shaded in orange, $\Gamma_{C:AD}^W$ in red, $\Gamma_{A:CD}^W$ in blue, and γ_{A_2} in purple. We decompose this in the middle figure into a blue curve $\partial U_{\mathcal{F}_C}^{\text{cl}}$, a green curve $\partial U_{\mathcal{F}_A}^{\text{cl}}$, a red curve Γ , and an extra orange curve. This upper bounds the RHS figure via minimality. S_{A_2} is identical in each panel and hence cancels identically.

Here we will illustrate this with an explicit example as shown in Figure 11. The full proof is given in Appendix H. Expanding out (5.16) in terms of HEE and EWCS is equivalent to

$$S_{AC} + E_W(A:CD) + E_W(C:AD) \geq S_A + S_C + E_W(AC:D), \quad (5.19)$$

for a pure state $ABCD$. In our example A is disjoint with two intervals A_1 and A_2 . First, notice that the unbrided components of A and C when computed in AC will have their entropic contributions to S_{AC} cancel with the corresponding unbrided contributions to S_A and S_C by Remark 3.2. This is seen in Figure 11 where the purple curve, defining S_{A_2} , is present in all panels. We then proceed similarly to the proof of Theorem 4.1. Going from the leftmost to the middle diagram of Figure 11, we have only relabeled surface so that each color upper bounds the corresponding minimal surface on the right-hand side, except the orange curve which is an extra piece. Formalizing this process for a general setting proves Theorem 5.2.

6 Holographic Strong Superadditivity

In this section, we turn to a different type of inequality from those discussed earlier—namely, the strong superadditivity of J_W . This is motivated from the fact that distillable entanglement satisfies strong superadditivity and a previous observation that J_W equals the distillable entanglement E_D , which will be reviewed briefly here.

6.1 Distillable entanglement and holographic conjecture

The distillable entanglement between A and B , denoted by $E_D(A : B)$, quantifies the *maximum* number of EPR pairs that can be extracted via local operations and classical communication (LOCC) between A and B .⁵ In most cases, this procedure requires one party to perform a measurement and send the outcome to the other, thereby necessitating classical communication.

Since E_D is operationally defined, a restricted set of LOCC will lead to smaller E_D . For instance let us consider four parties A, B, C, D and focus on the distillable entanglement between AB and CD . The set of LOCC operations allowed between the joint systems AB and CD is evidently much larger than the set of operations achievable when performing LOCC separately between $A - C$ and $B - D$. This leads to the following inequality called strong superadditivity:

$$E_D(AB : CD) \geq E_D(A : C) + E_D(B : D). \quad (6.1)$$

In [9], it is proposed that a one-way, one-shot distillable entanglement admits a gravity dual as

$$E_D(A \leftarrow B) = J_W(A|B) \quad (6.2)$$

at leading order in G_N for holographic states and in the large-dimension limit for random states. $A \leftarrow B$ means the LOCC considered here is one-way from B to A . Specifically equation (6.2) follows from the following three inequalities:

$$E_D(A \leftarrow B) \lesssim J(A|B) \quad (6.3)$$

$$E_D(A \leftarrow B) \geq J_W(A|B) \quad (6.4)$$

$$J(A|B) = J_W(A|B). \quad (6.5)$$

The first inequality is a general relation that holds whenever high-fidelity EPR pairs are distilled; it is not limited to holographic or random states. It follows from the fact that, once an EPR pair has been successfully distilled, measuring one of its subsystems necessarily reduces the entropy by a corresponding amount.

The second inequality arises from the quantum error-correcting property of holographic or random states. One can explicitly construct a one-way LOCC distillation protocol that makes use of the expansion of the entanglement wedge of A after a partial measurement on B . The resulting distillable entanglement coincides with $J_W(A|B)$. Although this protocol may not be optimal, it constitutes a valid distillation procedure and thus provides a lower bound on E_D .

The third inequality can be shown independently in two settings: holographic or Haar random states. In the former case, the derivation relies on the assumption of holographic measurements and geometric optimization in fixed-area states of

⁵More precisely, it is defined in either the asymptotic iid limit or one-shot scenario with some error. For more details, see [9, 55, 56] for instance.

holography. In the latter case, the inequality is rigorously argued by the measure concentration of Haar random states.

Given this background, [9] conjectures the classical correlation $J_W(A|B)$ is dual to one-way distillable entanglement $E_D(A \leftarrow B)$ and so we expect a one-way version of strong superadditivity:

$$J_W(AB|CD) \stackrel{?}{\geq} J_W(A|C) + J_W(B|D). \quad (6.6)$$

It is worth noting that this one-way strong superadditivity implies the monogamy relation for both unmeasured and measured parties if one takes $C = D$ or $A = B$. However, for holographic states, since our topological proof assumes non-overlapping subsystems, monogamy and strong superadditivity must be proven independently.

Restricting to holographic/random basis measurements (without feedback), one-way LOCC does not outperform two-way LOCC. If it is generically true for holographic/random states, the two-way, one-shot distillable entanglement should be given by

$$E_D(A : B) \stackrel{?}{=} \max(E_D(A \leftarrow B), E_D(B \leftarrow A)). \quad (6.7)$$

This motivates us to think of a symmetrized classical correlation [9, 16]

$$J_W(A : B) \equiv \max(J_W(A|B), J_W(B|A)). \quad (6.8)$$

While answering question (6.7) is hard, here we ask if its consequences hold or not. If the two-way distillable entanglement is dual to the symmetrized correlation, that is, $E_D(A : B) = J_W(A : B)$, then there must be a two-way strong superadditivity

$$J_W(AB : CD) \stackrel{?}{\geq} J_W(A : C) + J_W(B : D). \quad (6.9)$$

This is strictly stronger than (6.6) so it does not follow from the one-way strong superadditivity. Proving this holographically and/or for random states provides partial supporting evidence that one-way LOCC is sufficient in holography and/or random states.

6.2 Holographic proof of one-way strong superadditivity

In this section we show that $J_W(A|B)$ respects strong superadditivity in the one-way direction.

Theorem 6.1. J_W is one-way strongly superadditive. That is J_W satisfies

$$J_W(AB|CD) \geq J_W(A|C) + J_W(B|D). \quad (6.10)$$

for any states on $ABCD$ (not necessarily pure).

The full proof is given in Appendix I. The one-way strong superadditivity (6.10) is equivalently written as

$$S_{AB} + E_W(A : BDE) + E_W(B : ACE) \stackrel{?}{\geq} S_A + S_B + E_W(AB : E). \quad (6.11)$$

The proof proceeds with the same strategy as all our other holographic proofs: consider the LHS surfaces, relabel particular components, show these components are admissible, and hence upper bound, quantities on the RHS. This is seen in Figure 12.

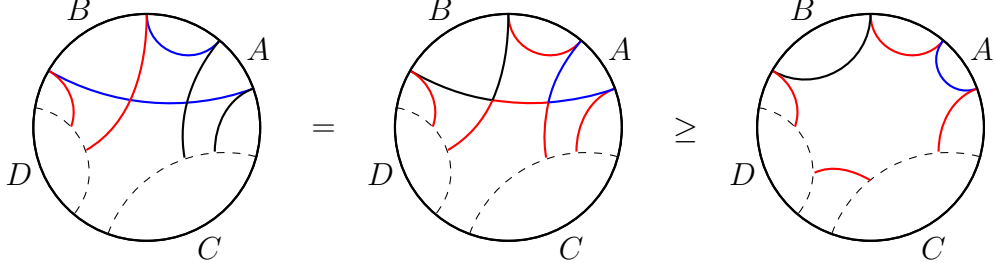


Figure 12. Example for one way classical strong super additivity. On the LHS we have $\Gamma_{A:BDE}^W$ in black, $\Gamma_{B:ACE}^W$ in red, and γ_{AB} in blue. The dashed lines are the RT surfaces of γ_C and γ_D . We decompose this in the middle figure into a black curve ∂r_B , a blue curve ∂r_A , and a red curve Γ . These upper bound S_B , S_A and $E_W(AB : E)$ respectively by minimality.

6.3 Toward holographic proof of two-way strong superadditivity

Although we are not able to present a complete proof here it is worth analyzing why the method employed for all other proofs fails. For convenience, let us introduce the following shorthand notation:

$$\begin{aligned} \alpha_1 &\equiv J_W(AB|CD) = S_{AB} - E_W(AB : E), \\ \alpha_2 &\equiv J_W(CD|AB) = S_{CD} - E_W(CD : E), \\ \beta_1 &\equiv J_W(A|C) = S_A - E_W(A : BDE), \\ \beta_2 &\equiv J_W(C|A) = S_C - E_W(C : BDE), \\ \gamma_1 &\equiv J_W(B|D) = S_B - E_W(B : ACE), \\ \gamma_2 &\equiv J_W(D|B) = S_D - E_W(D : ACE). \end{aligned}$$

Then, the one-way strong superadditivity (6.10) is written as

$$\alpha_1 \stackrel{?}{\geq} \beta_1 + \gamma_1, \quad (6.12)$$

while the two-way version corresponds to

$$\max(\alpha_1, \alpha_2) \stackrel{?}{\geq} \max(\beta_1, \beta_2) + \max(\gamma_1, \gamma_2). \quad (6.13)$$

As we show (6.12) the only remaining case is

$$\alpha_1 \stackrel{?}{\geq} \beta_1 + \gamma_2, \quad (6.14)$$

subject to $\alpha_1 \geq \alpha_2$, $\beta_1 \geq \beta_2$ and $\gamma_2 \geq \gamma_1$. The various other cases are implied by equations (6.12) and (6.14) and the assumed max statements within.

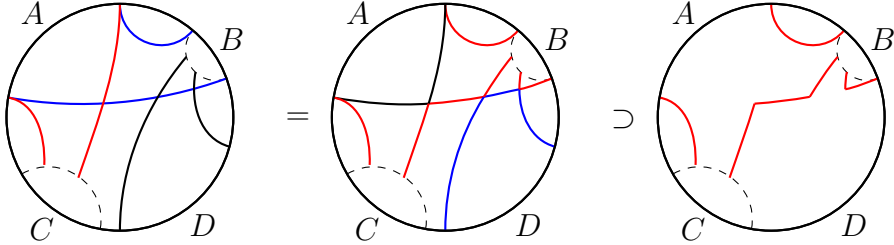


Figure 13. Failure of standard proof methodology for two-way strong superadditivity. On the LHS we have $\Gamma_{A:BDE}^W$ in red, $\Gamma_{D:ACE}^W$ in black, and γ_{AB} in blue. The dashed lines are the RT surfaces of γ_C and γ_B . We attempt the usual decomposition into a black curve upper bounding S_A , a blue curve upper bounding S_D and a remaining red curve to upper bound $E_W(AB : E)$. Evidently the remaining curve is not EWCS admissible for $E_W(AB : E)$ and the standard proof method fails.

For the one-way direction proof we did not need to invoke the additional information provided by the assumed max statements: the one-way inequality in equation (6.11) is true for arbitrary $ABCD$. However for the remaining two-way condition,

$$J_W(AB|CD) \stackrel{?}{\geq} J_W(A|C) + J_W(D|B), \quad (6.15)$$

we find the standard approach insufficient (see Figure 13). The proof thus requires a step beyond considering the basic topology of these surfaces and invoking more exotic properties along with the assumed inequalities between α_1 and α_2 and so on. Nevertheless, we find no counterexample both analytically or numerically. Since most holographic inequalities are proven on topological grounds, it is interesting if there exists some approach that captures more fine-grained details of holographic theories.

6.4 Haar Random analysis

In this subsection, we consider n -qudit Haar random pure states composed of five subsystems A, B, C, D, E . A subsystem X contains n_X qudits and the total number of qudits is denoted by n . In the large- n limit with fixed n_X/n , the Haar random state is the simplest toy model of holography, in a sense that the EE is calculated by the minimal bond cut surface as the RT formula does. Since it is volume-law entangled, it is identified with the infinite-temperature pure black hole state or the coarse-grained random tensor network corresponding to a fixed-area state.

Since the one-way strong superadditivity is generically proven based on topological arguments, which also apply for the large- n asymptotics of Haar random states, the only remaining case we should examine is equation (6.14). In the large- n limit, it simplifies to (up to exponentially suppressed corrections)

$$\begin{aligned} & \min(n_A + n_B, n_C + n_D + n_E) + \min(n_A, n_B + n_D + n_E) + \min(n_D, n_A + n_C + n_E) \\ & \stackrel{?}{\geq} \min(n_A, n_B + n_C + n_D + n_E) + \min(n_D, n_A + n_B + n_C + n_E) + \min(n_A + n_B, n_E) \end{aligned} \quad (6.16)$$

under the assumptions $\alpha_1 \geq \alpha_2$, $\beta_1 \geq \beta_2$, and $\gamma_2 \geq \gamma_1$. This simplification is because there is a measure concentration, which leads to

$$S_X = \min(n_X, n_{\bar{X}}), \quad E_W(X : Y) = \min(n_X, n_Y) \quad (6.17)$$

where \bar{X} represents the complementary subsystem to X . We confirm strong superadditivity (6.16) analytically by case analysis (see Appendix B).

7 Boundary dual to holographic correlations from reflected entropy

In this section, inspired by holographic correlation measures, we map our correlation measures back to boundary quantities by making use of another duality between EWCS and a half of reflected entropy, defined in 2.11. We define reflected correlation measures by making the following replacement:

$$E_W(A : B) \rightarrow \frac{S_R(A : B)}{2}. \quad (7.1)$$

The reflected correlation measures not only match with the original correlation measures for holographic/random states, but also provide well-defined, computable quantities in any quantum systems away from the holographic regime. Notably, they are free of complex optimizations that the original measures have.

In Section 7.1, we define these reflected correlation measures and conjecture a bound on the original measures. We demonstrate this bound with two-qubit states. In Section 7.2 and 7.3, we investigate monotonicity and monogamy/polygamy for the reflected measures. While reflected entropy is not a correlation measure [13], it turns out J_R and D_R obey the same monotonicity and monogamy relations as the original measures except for monotonicity in the measured party.

7.1 Definition and relation to original measures

Let us define the reflected classical correlation J_R and reflected discord D_R by

$$J_R(A|B) \equiv S_A - \frac{S_R(A : C)}{2}, \quad (7.2)$$

$$D_R(A|B) \equiv I(A : B) - J_R(A : B) = S_B - S_{AB} + \frac{S_R(A : C)}{2}, \quad (7.3)$$

where C purifies AB . Unlike the original measures, they no longer have a complex optimization over all possible subsystem POVMs, offering an alternative, computable measure for classical and quantum correlations. Furthermore, they do not depend on the choice of the purification partner C as they are entirely entropic.

It is immediate to see that

$$D_R \geq D \Leftrightarrow J_R \leq J \Leftrightarrow S_R \geq 2E_F, \quad (7.4)$$

if E_f is additive over a canonical purification. This is as additivity implies that

$$S_R(A : B) = E_F(AA^* : BB^*) \geq E_F(A : B) + E_F(A^* : B^*) = 2E_F(A : B), \quad (7.5)$$

showing equation (7.4). While it is known that the additivity of the entanglement of formation can be violated [57], it is not clear whether it is also violated for canonically purified states. Furthermore, whether there exists an extensive⁶ (large) violation remains an open problem [58–60].

It is also interesting to note that there was a conjecture about the relation between the reflected entropy and entanglement of purification $E_P(A : B)$: a quantity closely related to entanglement of formation. Namely, it is generically true that [61]

$$E_P(A : B) \geq E_F(A : B). \quad (7.6)$$

It was conjectured by [62] that $2E_P(A : B) \geq S_R(A : B)$ but later fine-tuned counterexamples were found numerically [63]. For these counterexamples, our conjecture (7.4) is automatically true due to $S_R \geq 2E_P \geq 2E_F$. However, for most states, including two-qubits with no known counterexamples, (7.4) remains nontrivial.

Let us give an explicit, neither holographic nor random example: a family of two-qubit states, called the Bell-diagonal states [64], where we can confirm the conjecture explicitly. These Bell-diagonal take the form

$$\rho_{AB} = p |\Phi^+\rangle\langle\Phi^+| + (1-p) |\Phi^-\rangle\langle\Phi^-|, \quad (7.7)$$

where the Bell pairs are defined as $|\Phi^\pm\rangle = \frac{1}{\sqrt{2}}(|00\rangle \pm |11\rangle)$.

Since it is a two-qubit state, one can calculate E_f analytically using [65]:

$$E_F(A : B) = h\left(\frac{1 + \sqrt{1 - C^2}}{2}\right), \quad h(q) = -q \log q - (1 - q) \log(1 - q), \quad (7.8)$$

with the concurrence C given by [66]

$$C = \max(0, 2 \max(p, 1 - p) - 1) = |2p - 1|. \quad (7.9)$$

⁶By extensive, we mean that it scales as $O(\log d)$ as we increase the dimension d .

With this, one finds that

$$E_F(A : B) = h\left(\frac{1 + 2\sqrt{p(1-p)}}{2}\right). \quad (7.10)$$

Meanwhile, the reflected entropy can be calculated as follows. The canonical purification is

$$|\sqrt{\rho}\rangle_{ABA'B'} = \sqrt{p}|\Psi^+\rangle_{AB} \otimes |\Psi^+\rangle_{A'B'} + \sqrt{1-p}|\Psi^-\rangle_{AB} \otimes |\Psi^-\rangle_{A'B'}. \quad (7.11)$$

After partial trace over BB' , one finds that

$$\rho_{AA'} = \frac{I_{AA'}}{4} + \frac{\sqrt{p(1-p)}}{2}Z_A \otimes Z_{A'}, \quad Z = \begin{pmatrix} 1 & 0 \\ 0 & -1 \end{pmatrix}, \quad (7.12)$$

leading to the reflected entropy

$$S_R(A : B) = S_{AA'} = 2(-\lambda_+ \log \lambda_+ - \lambda_- \log \lambda_-), \quad \lambda_{\pm} = \frac{1}{4} \pm \frac{\sqrt{p(1-p)}}{2}. \quad (7.13)$$

Thus, the question $S_R(A : B) \stackrel{?}{\geq} 2E_F(A : B)$ is equivalent to

$$-\lambda_+ \log \lambda_+ - \lambda_- \log \lambda_- \stackrel{?}{\geq} h\left(\frac{1 + 2\sqrt{p(1-p)}}{2}\right), \quad (7.14)$$

which is satisfied for any valid p ($0 \leq p \leq 1$).

7.2 Monotonicity of reflected measures

Let us turn to examine the monotonicity properties of reflected correlation measures. In summary, we find monotonicity in the measured party for both measures, and no monotonicity in general for the unmeasured party:

$$D_R(AC|B) \geq D_R(A|B), \quad (7.15)$$

$$J_R(AC|B) \geq J_R(A|B), \quad (7.16)$$

$$D_R(A|BC) \not\geq D_R(A|B), \quad (7.17)$$

$$J_R(A|BC) \not\geq J_R(A|B). \quad (7.18)$$

7.2.1 Measured party

Let us start with asking if monotonicity holds for the measured party in J_R (7.18). The inequality in question is equivalent to asking

$$S_R(A : CD) \stackrel{?}{\geq} S_R(A : D), \quad (7.19)$$

with $ABCD$ pure. However, numerous counterexamples have been found for the monotonicity of S_R [13] and so J_R is not monotone in the measured party.

For the reflected discord, the monotonicity (7.17) is equivalent to

$$2S_{AD} - 2S_D + S_R(A : D) \stackrel{?}{\geq} 2S_B - 2S_{CD} + S_R(A : CD). \quad (7.20)$$

Taking $D = \emptyset$, the inequality becomes

$$I(A : C) \stackrel{?}{\geq} \frac{S_R(A : C)}{2}. \quad (7.21)$$

One such counter example is given by the Werner state [67]:

$$\rho_{AC} = p |\Phi^+\rangle\langle\Phi^+|_{AC} + (1-p) \frac{I_{AC}}{4}, \quad (7.22)$$

which violates (7.21) for $0 < p \lesssim 0.42$ (see Appendix C).

7.2.2 Unmeasured party

Theorem 7.1 (Monotonicity of classical and quantum correlations for the unmeasured party). For a mixed state ABC ,

$$J_R(AC|B) \geq J_R(A|B) \quad (7.23)$$

$$D_R(AC|B) \geq D_R(A|B) \quad (7.24)$$

Proof. As per the holographic case (Lemma 4.1) the inequality for both J_R and D_R is identical after appropriate renaming. The monotonicity of these reflected measures for the unmeasured party is equivalent to asking whether

$$2S_{AB} + S_R(A : BC) \stackrel{?}{\geq} 2S_A + S_R(AB : C). \quad (7.25)$$

We first note that for any subsystems X and Y , it follows that

$$S_R(X : Y) \equiv S_{XX'}(|\psi_{XYX'Y'}\rangle) = S_X + S_{X'} - I(X : X') = 2S_X - I(X : X'), \quad (7.26)$$

where in the last equality, we used that canonical purification implies $S_X = S_{X'}$. Applying this identity to the reflected entropies appearing in (7.25), we have

$$S_R(A : BC) = 2S_A - I(A : A'), \quad S_R(AB : C) = 2S_{AB} - I(AB : A'B'). \quad (7.27)$$

We note that in both $S_R(A : BC)$ and $S_R(AB : C)$, the canonically purified state is identical: $|\psi_{ABCA'B'C'}\rangle$. Hence, we can rewrite the desired inequality (7.25) as

$$I(AB : A'B') - I(A : A') \stackrel{?}{\geq} 0, \quad (7.28)$$

which is indeed positive due to the monotonicity of the mutual information. Thus, D_R and J_R are monotone with respect to the unmeasured party. \square

7.3 Monogamy/Polygamy of reflected measures

Here we investigate the monogamy/polygamy properties of J_R and D_R . We find these quantities are neither monogamous nor polygamous for either party. Namely,

$$J_R(A|B) + J_R(A|C) \not\leq J_R(A|BC), \quad (7.29)$$

$$D_R(A|B) + D_R(A|C) \not\leq D_R(A|BC), \quad (7.30)$$

$$J_R(A|B) + J_R(C|B) \not\leq J_R(AC|B), \quad (7.31)$$

$$D_R(A|B) + D_R(C|B) \not\leq D_R(AC|B). \quad (7.32)$$

7.3.1 Measured party

Just as in (5.17), where the holographic classical correlations were monogamous for pure states and there was a form of trade-off with the polygamy of holographic discord, here we see that states violating the monogamy of one of these reflected correlation measures often violate the polygamy of the other. We present two instances where there is this complementary violation of monogamy/polygamy for J_R and D_R .

W states: Let us consider a counterexample to the polygamy of J_R and the monogamy of D_R with respect to the measured party. The monogamy of D_R for the measured party means, for pure $ABCD$,

$$D_R(A|B) + D_R(A|C) \leq D_R(A|BC), \quad (7.33)$$

$$\Leftrightarrow J_R(A|B) + J_R(A|C) - J_R(A|BC) \geq I(A : B : C), \quad (7.34)$$

$$\Leftrightarrow S_A - \frac{1}{2}(S_R(A : CD) + S_R(A : BD) - S_R(A : D)) \geq I(A : B : C), \quad (7.35)$$

where $I(A : B : C) = S_A + S_B + S_C - S_{AB} - S_{BC} - S_{CA} + S_{ABC}$ is the tripartite information [68]. Since this quantity vanishes for pure ABC , showing a violation to the measured-party monogamy of D_R is equivalent to showing a violation to the measured-party polygamy of J_R .

Consider the three-qubit W state (with empty D)

$$|\Psi\rangle_{ABC} = \frac{1}{\sqrt{3}} (|001\rangle + |010\rangle + |100\rangle). \quad (7.36)$$

Since $S_R(A : B) = S_R(A : C)$ and $S_R(A : C) = \log 6 - \frac{1}{\sqrt{3}} \log(2 + \sqrt{3}) > S_A = \log 3 - \frac{2}{3} \log 2$, the W state is neither polygamous for J_R nor monogamous for D_R . Thus, J_R is not necessarily polygamous and D_R is not necessarily monogamous for the measured party.

Four-qubit state violations Let us now consider a four-qubit state that violates the measured-party monogamy of J_R . Consider a four-qubit pure state

$$|\Psi\rangle_{ABCD} = \frac{1}{\sqrt{2}} (|0100\rangle + |1011\rangle)_{ABCD}. \quad (7.37)$$

The measured-party monogamy of J_R is equivalent to

$$2S_A + S_R(A : D) \stackrel{?}{\leq} S_R(A : BD) + S_R(A : CD). \quad (7.38)$$

By symmetry and straightforward computation,

$$S_A = S_R(A : D) = S_R(A : BD) = S_R(A : CD) = \log 2, \quad (7.39)$$

so that the monogamy inequality is violated by $\log 2$.

To show that D_R is neither polygamous, consider

$$|\Psi\rangle_{ABCD} = \frac{1}{2} (|0000\rangle + |0011\rangle + |0110\rangle + |1101\rangle). \quad (7.40)$$

Since

$$S_B = S_C = S_D = \log 2, \quad S_{BC} = S_{BD} = S_{CD} = \frac{3}{2} \log 2, \quad (7.41)$$

$$S_R(A : CD) = S_R(A : BD) = 3 \log 2 - \frac{5}{8} \log 5, \quad (7.42)$$

$$S_R(A : D) = \frac{3}{2} \log 2 + \frac{1}{2\sqrt{2}} \log \frac{2 - \sqrt{2}}{2 + \sqrt{2}}. \quad (7.43)$$

The discord polygamy inequality is

$$D_R(A|B) + D_R(A|C) \stackrel{?}{\leq} D_R(A|BC), \quad (7.44)$$

but substituting the above values violates the inequality. Thus, this state is neither monogamous for reflected classical correlations nor polygamous for reflected discord; this is the same as the original quantities.

7.3.2 Unmeasured Party

Just as in the measured-party case, we find that monogamy and polygamy of boundary correlation measures J_R and D_R tend to fail in complementary pairs. In particular, we again observe that states violating the monogamy of one quantity often violate the polygamy of the other. We present two examples that exhibit this complementary pattern for the unmeasured party.

Tripartite pure state violations We first examine the discord monogamy inequality:

$$S_R(C : AD) + S_R(A : CD) + 2S_B + 2S_D \stackrel{?}{\leq} 2S_{AD} + 2S_{CD} + S_R(AC : D). \quad (7.45)$$

Taking $D = \emptyset$, this reduces to:

$$S_R(A : C) \stackrel{?}{\leq} I(A : C), \quad (7.46)$$

which is the negation of the known upper bound to the reflected entropy [10], and therefore not generally satisfied. This provides a direct counterexample to monogamy of discord.

To show that classical correlations are not polygamous either, we again take $D = \emptyset$, reducing the inequality to (7.46) which is again the negation of the known upper bound and thus not true. Hence, classical correlation is neither monogamous nor polygamous with respect to the unmeasured party. However we note that for pure ABC , classical correlation is monogamous.

Four-qubit state violations For classical correlations, the monogamy inequality is given by:

$$2I(A : C) + S_R(AC : D) \stackrel{?}{\leq} S_R(A : CD) + S_R(C : AD). \quad (7.47)$$

Consider the four-qubit state:

$$|\Psi\rangle_{ABCD} = \frac{1}{\sqrt{2}} (|0001\rangle + |1110\rangle), \quad (7.48)$$

with the ordering of subsystems given by $ABCD$. Then we have, in base-2 logarithms,

$$I(A : C) = S_R(AC : D) = S_R(A : CD) = S_R(C : AD) = 1, \quad (7.49)$$

thus violating the inequality. The values of the reflected entropy follow from tracing out B , yielding:

$$\rho_{ACD} = \frac{1}{2} (|001\rangle\langle 001| + |110\rangle\langle 110|), \quad (7.50)$$

which is symmetric under all system permutations with appropriate qubit flipping. To show that discord is also not polygamous, consider the state:

$$|\Psi\rangle_{ABCD} = \frac{1}{\sqrt{3}} (|0101\rangle + |0110\rangle + |1011\rangle). \quad (7.51)$$

By symmetry and standard reflected entropy properties, we find:

$$S_C = S_A = S_R(A : CD) = S_R(AC : D) = S_R(C : AD) = \log 3 - \frac{2}{3} \log 2 \quad (7.52)$$

$$S_{AC} = \log 3 \quad (7.53)$$

which substituting these into (7.47) shows the LHS exceeds the RHS, violating polygamy of discord as well.

8 Summary and future outlook

In this work, we performed a systematic analysis of the classical and quantum correlation measures on both sides of the holographic duality. In particular, we examined

whether the bulk measures J_W, D_W and the boundary measures J_R, D_R , originally proposed in [16], obey various properties of correlation measures such as monotonicity, monogamy, and strong superadditivity. Our study tests the information theoretic consistency of the holographic proposal through these zoo of correlation inequalities.

	Monotonicity		Monogamy/Polygamy		S. Superaddit.
Party	Unmeasured	Measured	Unmeasured	Measured	
J	Known	Known	No	No	No
J_W	Proved	Proved	Proved	Proved	1WAY No Counter
J_R	Proved	Counterex. [13]	Counterex.	Counterex.	Proved for Haar random

Table 1. Summary of inequalities for classical correlation measures: J (original), J_W (holographic), and J_R (reflected). S. Superaddit. stands for strong superadditivity.

	Monotonicity		Monogamy/Polygamy		S. Superaddit.
Party	Unmeasured	Measured	Unmeasured	Measured	
D	Known	Counterex.	Neither	Neither	No
D_W	Proved	Counterex.	Polygamous (pure)	Counterex.	No
D_R	Proved	Counterex.	Polygamous (pure)	Counterex.	No

Table 2. Summary of inequalities for quantum discord measures: D (original), D_W (holographic), and D_R (reflected).

Based on topological arguments, our results (summarized in Tables 1 and 2) support the holographic proposal $J = J_W$ and $D = D_W$ by proving that J_W is monotone for both parties and D_W is monotone for the unmeasured party in arbitrary dimensions. We also found that D_W is neither monotonic nor monogamous with respect to the measured party. All of these properties are satisfied by the original correlation measures J and D , showing consistency with the proposed duality.

We also found some special features of holographic correlations. We proved the barrier theorem (Theorem (3.1)) which has interesting information theoretic consequences. Moreover, we proved that J_W is monogamous for both unmeasured and measured parties and that D_W is polygamous for the unmeasured party when written over a pure state. These features are special to holographic states; the original correlation measures do not satisfy such properties. Similar to monogamy of holographic mutual information, they provide additional necessary conditions for holographic

states. For example, the polygamous nature of pure-state holographic discord indicates the absence of GHZ entanglement in these states. It also implies a trade-off relation among the monogamy of mutual (total) correlation, the monogamy of classical correlation, and the polygamy of quantum discord in holography.

Another perspective for the monogamy of J_W stems from the one-way strong superadditivity of one-way distillable entanglement. In [9], it has been conjectured that J_W is further dual to the one-way distillable entanglement $E_D^{[1\text{WAY}]}$, which quantifies the number of EPR pairs that can be distilled via one-way LOCC. From operational reasons, if the proposed duality holds, J_W should obey the one-way strong superadditivity, which further implies monogamy. Indeed, we proved the one-way strong superadditivity of J_W , providing a piece of evidence for the conjectured duality $J_W = E_D^{[1\text{WAY}]}$.

On the conjecture between J_W and distillable entanglement, we further ask if J_W could potentially be dual to $E_D \equiv E_D^{[2\text{WAY}]}$, the distillable entanglement under two-way LOCC. While the earlier study indicates a sequence of one-way LOCC with randomized measurements would not improve distillability, whether it can be improved under generic two-way LOCC remains open. One supporting evidence comes from the *two-way* strong superadditivity, which $E_D^{[1\text{WAY}]}$ does *not* necessarily have but $E_D^{[2\text{WAY}]}$ does. We found that *two-way* strong superadditivity holds for Haar random states, which are the simplest toy model of holographic states. Also, in pure AdS_3 , numerically we find no counterexample. Thus, it is tempting to prove the two-way strong superadditivity geometrically in holography. Nevertheless, we also find that while topological proofs succeed in some cases, one remaining case requires a proof beyond a mere topological argument. We leave this conjecture of (two-way) strong superadditivity of J_W as a future problem.

On the technical side, the topological method we employed in this paper works in any dimension and is powerful enough to deal with holographic inequalities involving multiple EWCSs. While there have been numerous such geometric approaches in the past, to our knowledge, only a few papers have developed proofs with such a rigour, especially when multiple EWCSs associated to different subregions are included. Compared to entropies as in the holographic entropic cone program, inequalities involving multiple EWCS are less explored, and the homological tools developed and formalized in this paper would be useful in future systematic exploration.

Going back to the boundary side, we also propose the computable ‘reflected’ measures J_R and D_R based on the duality between the reflected entropy and EWCS. While the duality itself only holds for holographic states, these reflected measures themselves now become computable in any quantum systems without optimizations. We find the reflected measures are similar to the original measures. Namely, both J_R and J are not monogamous with respect to either party; both D_R and D are monotone for the unmeasured party while not for the measured party and not measured-

party monogamous. However, regarding the unmeasured-party polygamy for pure states, D_R is similar to the holographic one. Finally, J_R shows a distinct feature regarding the measured-party monotonicity. It exhibits a counterexample, contrary to the proven monotonicity for J and J_W .

As a future outlook, a natural direction is the systematic exploration of the “EWCS cone”. While the Holographic Entropy Cone program characterizes the constraints on von Neumann entropies in holographic states, our results suggest there may be even more, unexplored inequalities involving both multiple EWCSs and HEEs. A systematic search for such inequalities, perhaps using the techniques developed here, could reveal the broader space of mixed-state correlations in holography. This would be particularly relevant for defining and constraining multipartite generalizations of discord, where the interplay of multiple EWCSs becomes important.

Furthermore, extending our results to time-dependent spacetimes remains a critical task. Our current proofs are based on the RT minimization on a common time slice. Investigating whether properties like monotonicity, monogamy, and strong superadditivity hold in covariant settings using the HRT formula is essential, particularly in the context of black hole evaporation or quenches.

Acknowledgments

Research at Perimeter Institute is supported in part by the Government of Canada through the Department of Innovation, Science and Economic Development and by the Province of Ontario through the Ministry of Colleges, Universities, Research Excellence and Security. KL’s and HW’s work was also supported by Michael Serbinis and Laura Adams through the PSI Start research internship. This work was supported by JSPS KAKENHI Grant Number 23KJ1154, 24K17047.

A Summary of notation

We collect the entropic quantities and topological notations used throughout. Unless stated otherwise, S_X denotes the von-Neumann entropy of ρ_X : $S_X \equiv S(\rho_X) := -\text{Tr}(\rho_X \log \rho_X)$, where $\rho_X = \text{Tr}_{\bar{X}} \rho$.

Information-theoretic quantities

- Classical conditional entropy (2.3): $J_{\Pi}(A|B) = S_A - \sum_x p_x S(\rho_A^x)$
- Classical correlation (2.4): $J(A|B) = \max_{\Pi} J_{\Pi}(A|B)$
- Mutual information: $I(A : B) = S_A + S_B - S_{AB} = S_A - S(A|B)$

- Entanglement of formation (2.6): $E_F(A : C) = \inf \sum_x p_x S_A(|\psi_x\rangle\langle\psi_x|)$
- Quantum discord (2.7): $D(A|B) = I(A : B) - J(A|B)$
- Entanglement wedge cross section (EWCS) (2.9): $E_W(A : C) = \min_{\Gamma_{A:C}} \frac{\text{Area}(\Gamma_{A:C})}{4G_N}$
- Holographic classical correlation (2.10): $J_W(A|B) \equiv S_A - E_W(A : C)$
- Holographic discord (2.10): $D_W(A|B) \equiv S_B - S_C + E_W(A : C)$
- Reflected entropy (2.11): $S_R(A : C) = S_{AA^*}(|\rho^{1/2}\rangle)$
- Canonical purification of ρ (2.12): $|\rho^{1/2}\rangle_{AA^*CC^*}$
- Reflected classical correlation (2.10): $J_R(A|B) \equiv S_A - \frac{1}{2}S_R(A : C)$
- Reflected discord (2.10): $D_R(A|B) \equiv S_B - S_C + \frac{1}{2}S_R(A : C)$
- One-shot distillable entanglement: (See Section 6.1 and [9] for the definition)
 $E_D^{[1\text{WAY}]}(A : B) = \max(E_D^{[1\text{WAY}]}(A \leftarrow B), E_D^{[1\text{WAY}]}(B \leftarrow A))$
- Symmetrized classical correlation (2.14): $J_W(A : B) \equiv \max(J_W(A|B), J_W(B|A))$
- Holographic one-way distillable entanglement conjecture (6.2): $E_D^{[1\text{WAY}]}(A \leftarrow B) = J(A|B)$

Topological quantities. We follow the convention that codimension is counted in the full spacetime; since all objects lie on the Cauchy slice Σ , a spacetime codimension-two surface appears as a codimension-one hypersurface in Σ .

- Σ (Definition 3.1): Cauchy slice (codimension-one spacelike slice)
- For a codimension-one bulk region $U \subseteq \Sigma$:
 - $\partial_\Sigma U \equiv \partial U$ (Definition 3.2): boundary of U within Σ , excluding asymptotic boundary segments.
 - $\partial_\infty U$ (Definition 3.2): boundary of U on the asymptotic boundary of Σ .
- γ_A : the Ryu-Takayanagi (RT) surface for a boundary subsystem A .
- $\mathcal{E}(A)$ (Definition 3.4): entanglement wedge of A (a codimension-one region in Σ), with $\partial_\infty \mathcal{E}(A) = A$ and $\partial_\Sigma \mathcal{E}(A) = \gamma_A$.
- \cup, \cap : union or intersection of subsets.
- \sqcup : disjoint union of subsets. This means each subset is individually put in the set so that the multiplicity is taken into account. We only use disjoint union topologically when the arguments have zero intersect when considered in Σ .

- Wedge decomposition (Definition 3.5, see also Fig. 2). Decompose as

$$\mathcal{E}(AB) = \bigsqcup_{\alpha} W_{\alpha},$$

where each W_{α} is a connected component.

- Component types: W_{α} is *A-only* (resp. *B-only*) if its asymptotic boundary lies entirely in A (resp. B); it is *A–B bridged* if its asymptotic boundary meets both A and B .
- Boundary sets induced by the decomposition:
 - * $\mathcal{A} \subseteq A$ (resp. $\mathcal{B} \subseteq B$): the union of boundary components that are *A-only* (resp. *B-only*) components in $\mathcal{E}(AB)$.
 - * $\mathcal{F}_A := A \setminus \mathcal{A}$ and $\mathcal{F}_B := B \setminus \mathcal{B}$: the bridged boundary portions on each side; $\mathcal{F} := \mathcal{F}_A \cup \mathcal{F}_B$.
- $\mathcal{E}_{\text{brid}}(A : B)$: $(A : B)$ -bridged entanglement wedge, defined as the union of all *A–B bridged* components.
- Homology notation: $U \sim A$ means U is homologous to A (see 3.6); $U \sim_V A$ means homologous to A within a bulk subregion $V \subseteq \Sigma$.
- $\text{Int } \mathcal{E}(A)$: open bulk interior of $\mathcal{E}(A)$ (see 3.7).
- ℓ is a simple path (Definition D.1).
- RT admissible class (Definition 3.8): \mathfrak{S}_A is the class of codimension-2 surfaces homologous to A ; its minimizer is γ_A , whose area computes S_A .
- EWCS admissible class (Definition 3.9): $\mathfrak{S}_{A:B}$ is the class of codimension-2 surfaces in $\mathcal{E}(AB)$ separating A and B ; its minimizer is $\Gamma_{A:B}^W$, whose area computes $E_W(A : B)$.

B Mathematica code for strong superadditivity of Haar random states

```

1 ClearAll[m];
2 m[x_, y_] := (x + y - Abs[x - y])/2;
3
4 ClearAll[a, b, c, d, e];
5 vars = {a, b, c, d, e};
6
7 (*Constraints*)
8 cons = And @@ Thread[vars > 0] && a + b + c + d + e == 1;
9

```

```

10 ab = a + b;
11 cd = c + d;
12 de = d + e;
13 ce = c + e;
14 be = b + e;
15 ae = a + e;
16
17 abe = a + b + e;
18 ace = a + c + e;
19 bde = b + d + e;
20 abce = a + b + c + e;
21 bcde = b + c + d + e;
22 acde = a + c + d + e;
23 abde = a + b + d + e;
24 cde = c + d + e;
25
26 (*J_W assumptions*)
27
28 A1 = m[ab, cde] - m[ab, e] >= m[cd, abe] - m[cd, e];
29 A2 = m[a, bcde] - m[a, bde] >= m[c, abde] - m[c, bde];
30 A3 = m[d, abce] - m[d, ace] >= m[b, acde] - m[b, ace];
31
32 assumptionsAll = cons && A1 && A2 && A3;
33
34 (*Inequality*)
35
36 goal = m[ab, cde] + m[a, bde] + m[d, ace] >=
37     m[a, bcde] + m[d, abce] + m[ab, e];
38
39 (*Formal proof*)
40 proof1 = Resolve[ForAll[vars, Implies[assumptionsAll, goal]], Reals];
41
42 (*Show NO counterexample: if False empty set of counter examples*)
43 noCounterEx = Reduce[assumptionsAll && Not[goal], vars, Reals]

```

C Counterexample to monotonicity of reflected discord in measured party

We consider the Werner state

$$\rho_{AC} = p |\Phi^+\rangle\langle\Phi^+|_{AC} + (1-p) \frac{I_{AC}}{4}, \quad (\text{C.1})$$

and show

$$I(A : C) \stackrel{?}{\geq} \frac{S_R(A : C)}{2}. \quad (\text{C.2})$$

is not true for all $0 \leq p \leq 1$, thus showing the reflected discord is not monotone with respect to its measured party (see Section 7.2.1). The mutual information is given by

$$I(A : C) = \frac{1}{4} (-3(-1 + p) \log(1 - p) + (1 + 3p) \log(1 + 3p)). \quad (\text{C.3})$$

To find $S_R(A : C)$ we first canonically purify to

$$|\rho_{ACA^*C^*}\rangle = \sqrt{\frac{1-p}{4}} \left(|\Phi^-\Phi^-\rangle + |0101\rangle + |1010\rangle \right) + \sqrt{\frac{1+3p}{4}} |\Phi^+\Phi^+\rangle, \quad (\text{C.4})$$

with qubit order ACA^*C^* and $|\Phi^\pm\Phi^\pm\rangle = |\Phi^\pm\rangle \otimes |\Phi^\pm\rangle$. Tracing out CC^* we find

$$\rho_{AA^*} = \frac{3-p+\sqrt{(1-p)(1+3p)}}{8} (|00\rangle\langle 00| + |11\rangle\langle 11|) \quad (\text{C.5})$$

$$+ \frac{1+p-\sqrt{(1-p)(1+3p)}}{8} (|01\rangle\langle 01| + |10\rangle\langle 10|) \quad (\text{C.6})$$

$$+ \frac{1-p+\sqrt{(1-p)(1+3p)}}{4} (|00\rangle\langle 11| + |11\rangle\langle 00|). \quad (\text{C.7})$$

It is block-diagonal with respect to the basis $\{|00\rangle, |11\rangle\} \oplus \{|01\rangle, |10\rangle\}$ and so we find

$$S_R(A : C) = -\lambda_1 \log \lambda_1 - 3 \lambda_2 \log \lambda_2,$$

with

$$\lambda_1 = \frac{5-3p+3\sqrt{(1-p)(1+3p)}}{8}, \quad \lambda_2 = \frac{1+p-\sqrt{(1-p)(1+3p)}}{8}.$$

The original inequality (C.2) is false for $0 \leq p \leq p_{\max}$ with $p_{\max} \approx 0.41598$.

D Additional tools for proofs

For checking EWCS admissibility of a surface, it is more constructive to consider the behavior of paths between the arguments of the EWCS and whether they must cross said surface. We formalize this as follows.

Definition D.1 (Simple path). We define a simple path on Σ as an injective continuous map

$$\ell: [0, 1] \rightarrow \Sigma.$$

This means there are no self-intersections but the path can generally be jagged, have non-smooth corners and the like.

Definition D.2 (Path adjancy to a subsystem). Let Σ be the bulk Cauchy slice with regulated asymptotic boundary $\partial_\infty \Sigma$. Let A be a boundary subsystem ($A \subset \partial_\infty \Sigma$) and set $A^\circ := \text{int}_{\partial_\infty \Sigma}(A) := A \setminus \partial A$. Fix a collar embedding $c : \partial_\infty \Sigma \times [0, \varepsilon_0) \hookrightarrow \Sigma$ with $c(p, 0) = p \in \Sigma$ where $\varepsilon_0 > 0$ is some small number. For $0 < \varepsilon < \varepsilon_0$ define

$$\text{Adj}_\varepsilon(A) := c(A^\circ \times (0, \varepsilon)) \subset \Sigma.$$

We say $x \in \Sigma$ is adjacent to A if $x \in \text{Adj}_\varepsilon(A)$. A simple path $\ell : [0, 1] \rightarrow \Sigma$ starts (ends) adjacent to A if $\ell(0) \in \text{Adj}_\varepsilon(A)$ (resp. $\ell(1) \in \text{Adj}_\varepsilon(A)$).

Remark D.1 (Codimension on Σ). We count codimension with respect to the full spacetime. Since all surfaces considered here lie on the Cauchy slice Σ (see Assumption 3.2), any spacetime codimension-two surface $\gamma \subset \Sigma$ is a codimension-one hypersurface when considered in Σ and may therefore separate Σ and intersect Σ -paths.

Remark D.2 (Path–separation formulation). Condition (ii) in Definition 3.9 can be equivalently phrased as a path–separation property in terms of simple paths. Namely, let $\Gamma \in \mathfrak{S}_{A:B}$ be a properly embedded, piecewise smooth codimension-2 hypersurface with $\partial_\Sigma \Gamma \subset \gamma_{AB}$. Then condition (ii) is equivalent to the requirement that every simple path

$$\ell \subset \mathcal{E}(AB)$$

whose endpoints lie on opposite sides of Γ (for instance, one endpoint in a neighborhood of A and the other in a neighborhood of B on the boundary) must intersect Γ at least once.⁷

Conversely, if a smooth, embedded hypersurface $\Gamma \subset \mathcal{E}(AB)$ with bulk anchoring $\partial_\Sigma \Gamma \subset \gamma_{AB}$ has the property that every such simple path from the A -side to the B -side intersects Γ , then the complement $\mathcal{E}(AB) \setminus \Gamma$ decomposes as

$$\mathcal{E}(AB) \setminus \Gamma = U_A \sqcup U_B \tag{D.1}$$

with $\partial_\infty U_A = A$ and $U_B \partial_\infty = B$. Then Γ is EWCS admissible and in particular

$$\frac{\text{Area}(\Gamma)}{4G_N} \geq E_W(A : B), \tag{D.2}$$

by minimality. Thus checking the intersection properties of specific simple paths are sufficient to prove EWCS admissibility.

Our proofs below rely on comparing various surfaces on the cauchy slice. In particular the proof of equation (3.6), worked well as given the constraint of a bridged wedge when we defined \mathbf{L} in (3.9) we had that $\gamma_{AB} \cap \Gamma_{A:B}^W = 0$ (except points) hence

$$\frac{\text{Area}(\mathbf{L})}{4G_N} = \frac{\text{Area}(\gamma_{AB} \cup \Gamma_{A:B}^W)}{4G_N} = \frac{\text{Area}(\gamma_{AB})}{4G_N} + \frac{\text{Area}(\Gamma_{A:B}^W)}{4G_N} = S_{AB} + E_W(A : B).$$

⁷These paths are similar to bit threads, discussed in a slightly different context [54]. The path-separating surface there is interpreted as a RT surface after optimization.

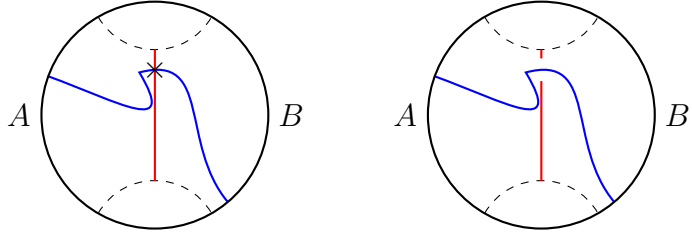


Figure 14. Dashed lines are γ_{AB} , the red line Γ is some surface we are checking for $(A : B)$ EWCS admissibility, and the blue some simple path ℓ . On the left, Γ is EWCS admissible as all choices of ℓ intersect Γ when traveling from A to B within $\mathcal{E}(AB)$. On the right, it is not however as ℓ can start adjacent to A and reach B without crossing Γ .

But in doing this we have naturally embedded both γ_{AB} defining S_{AB} , and $\Gamma_{A:B}^W$ defining $E_W(A : B)$ onto the same Cauchy slice and computed areas from there. Of course if they have non-zero intersect then formally union removes multiplicity. As our proofs are strict numerical inequalities we therefore need to keep track of the multiplicity of surfaces when translating from the numerical measures to their topological description. This motivates the following definition.

Definition D.3 (Sheeted slice, multisurfaces, and multiplicity bookkeeping). Fix the bulk slice Σ . For each $N \in \mathbb{Z}^+$ let

$$\widehat{\Sigma}_N := \bigsqcup_{n=1}^N \Sigma^{(n)}$$

be the disjoint union of N isometric copies (“sheets”) of Σ . Write $\iota_n : \Sigma \hookrightarrow \widehat{\Sigma}_N$ for the canonical inclusion into sheet n and $\pi : \widehat{\Sigma}_N \rightarrow \Sigma$ for the projection forgetting the sheet label.

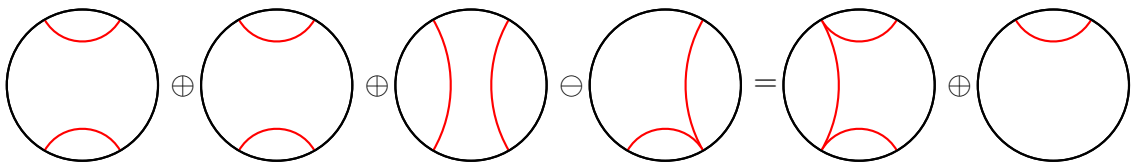


Figure 15. Example of multisurface addition and subtractions for some a representatives of four multisurfaces.

Throughout, “surface” means a *connected* embedded codimension-two hypersurface⁸ in Σ of finite area (we identify surfaces that differ only on sets of codimension-two measure zero). A disconnected surface is always understood as the finite disjoint union of its connected components.

⁸Recall we use codimension in terms of the full spacetime, not the Cauchy slice.

Multisurface (representative). A *representative* of a multisurface is a finite embedded union

$$X = \bigsqcup_{j=1}^k \iota_{s(j)}(\gamma_j) \subset \widehat{\Sigma}_N,$$

where each $\gamma_j \subset \Sigma$ is a connected surface and $s(j) \in \{1, \dots, N\}$. (Thus multiple copies of the same γ are represented by placing them on different sheets, possibly with other surfaces on the same sheet.)

Equivalence. Two representatives $X \subset \widehat{\Sigma}_N$ and $X' \subset \widehat{\Sigma}_{N'}$ are *equivalent* if, after possibly adding empty sheets to either side, one can relabel sheets to match them. Concretely: there exists $L \geq \max\{N, N'\}$ and a permutation $\sigma \in S_L$ such that, viewing both as subsets of $\widehat{\Sigma}_L$ (by adding empty sheets),

$$X' = \widehat{\sigma}(X),$$

where $\widehat{\sigma}$ is the induced isometry of $\widehat{\Sigma}_L$ permuting sheets by σ . A *multisurface* \mathbf{X} is an equivalence class of such representatives.

Support. For any representative $X \subset \widehat{\Sigma}_N$ of \mathbf{X} define the support in the physical slice by

$$|\mathbf{X}| := \pi(X) \subset \Sigma.$$

This is independent of the representative (sheet relabeling does not change π).

Multi-union (stacking). Given multisurfaces \mathbf{X}, \mathbf{Y} with representatives $X \subset \widehat{\Sigma}_N$ and $Y \subset \widehat{\Sigma}_M$, define $\mathbf{X} \oplus \mathbf{Y}$ to be the class of

$$X \sqcup Y \subset \widehat{\Sigma}_{N+M},$$

where X is placed on the first N sheets and Y on the last M sheets. This is well-defined up to equivalence. If γ is some surface on Σ we define $\mathbf{X} \oplus \gamma$ as above taking γ to be a multisurface of multiplicity one.

Difference (removing copies). We say \mathbf{Y} is *removable from* \mathbf{X} , and write $\mathbf{Y} \preceq \mathbf{X}$, if there exist representatives $X, Y \subset \widehat{\Sigma}_L$ on a common sheet number L such that $Y \subset X$ as subsets. In that case define

$$\mathbf{X} \ominus \mathbf{Y}$$

to be the multisurface represented by the set-theoretic difference $X \setminus Y \subset \widehat{\Sigma}_L$. This is well-defined: different choices of representatives with $Y \subset X$ differ only by adding empty sheets and permuting sheets, which preserves the equivalence class of $X \setminus Y$.

Area with multiplicity. For a representative $X \subset \widehat{\Sigma}_N$ define

$$\text{Area}^\oplus(\mathbf{X}) := \text{Area}(X) = \sum_{j=1}^k \text{Area}(\gamma_j),$$

i.e. the ordinary area computed in the disjoint union $\widehat{\Sigma}_N$. Then $\text{Area}^\oplus(\mathbf{X} \oplus \mathbf{Y}) = \text{Area}^\oplus(\mathbf{X}) + \text{Area}^\oplus(\mathbf{Y})$, and if $\mathbf{Y} \preceq \mathbf{X}$ then $\text{Area}^\oplus(\mathbf{X} \ominus \mathbf{Y}) = \text{Area}^\oplus(\mathbf{X}) - \text{Area}^\oplus(\mathbf{Y})$.

E Proof: Barrier theorem

Theorem 3.1. The EWCS surface, $\Gamma_{A:B}^W$, with $\text{Area}(\Gamma_{A:B}^W)/4G_N = E_W(A:B)$, never enters the interior of the individual wedges of its two arguments:

$$\Gamma_{A:B}^W \cap \text{Int } \mathcal{E}(A) = \emptyset, \quad \Gamma_{A:B}^W \cap \text{Int } \mathcal{E}(B) = \emptyset. \quad (3.11)$$

Here we show the barrier theorem via two methods: reflected entropy (in general dimensions), and via cycles on a two-dimensional slice.

E.1 Proof by reflected entropy

Proof of Theorem 3.1 (via reflected entropy). The simplest proof is seen by EWN and the relation in (2.13). We will show that $\Gamma_{A:B}^W \cap \text{Int } \mathcal{E}(A) = \emptyset$ and then the B statement follows by symmetry.

Step 1: Reduction to a single bridged component. If A and B have no $(A:B)$ -bridged entanglement wedge, then $E_W(A:B) = 0$ and we may take $\Gamma_{A:B}^W = \emptyset$, so the claim is trivial. Hence assume A and B have at least one bridged component. Distinct bridged components of $\mathcal{E}(AB)$ are disjoint and the EWCS minimizer decomposes additively across them, so it suffices to work in a single connected bridged wedge, which we continue to denote by $\mathcal{E}(AB)$.

Step 2: Canonical purification and the doubled wedge geometry. Let ρ_{AB} be the boundary state on AB . Consider its canonical purification $|\sqrt{\rho_{AB}}\rangle \in \mathcal{H}_{AB} \otimes \mathcal{H}_{A'B'}$, where A', B' are isomorphic purifying systems. In the holographic, time-reflection-symmetric setup, we model the bulk Cauchy slice dual to $|\sqrt{\rho_{AB}}\rangle$ by the *double* of $\mathcal{E}(AB)$ along its RT surface:

$$\tilde{\Sigma} := \mathcal{E}(AB) \cup_{\gamma_{AB}} \mathcal{E}(AB)', \quad (\text{E.1})$$

where $\mathcal{E}(AB)'$ is an isometric copy of $\mathcal{E}(AB)$, and the two copies are glued along their common codimension-1 boundary

$$\gamma_{AB} = \partial_{\Sigma} \mathcal{E}(AB)$$

(i.e. the RT surface of AB on Σ). The resulting $\tilde{\Sigma}$ carries a \mathbb{Z}_2 involutive isometry \mathcal{R} exchanging the two copies (primed \leftrightarrow unprimed) and fixing γ_{AB} pointwise. We regard the unprimed copy as an isometric embedded submanifold of $\tilde{\Sigma}$, so any subset of $\mathcal{E}(AB)$ is canonically identified with its image in $\tilde{\Sigma}$.

Now let $\Gamma \in \mathfrak{S}_{A:B}$ be any EWCS-admissible surface for $(A:B)$ inside the unprimed copy. Define its \mathbb{Z}_2 -doubling by

$$\tilde{\Gamma} := \Gamma \cup \mathcal{R}(\Gamma) \subset \tilde{\Sigma}. \quad (\text{E.2})$$

Since $\partial_{\Sigma} \Gamma \subset \gamma_{AB}$, the doubled surface $\tilde{\Gamma}$ is a closed embedded codimension-2 hypersurface in $\tilde{\Sigma}$ (any junction along γ_{AB} is a set of codimension-2 measure zero and

does not affect area or admissibility). Moreover, since Γ separates $\mathcal{E}(AB)$ into an A -side and a B -side, the doubled surface $\tilde{\Gamma}$ separates $\tilde{\Sigma}$ into an AA' -side and a BB' -side. Equivalently, $\tilde{\Gamma}$ is RT-admissible (i.e. a valid homology competitor) for both boundary regions AA' and BB' in the doubled geometry.

Step 3: Specialize to the EWCS minimizer and identify an RT surface.
Now take $\Gamma = \Gamma_{A:B}^W$, the area-minimizing member of $\mathfrak{S}_{A:B}$. In the canonical purification, the reflected entropy is defined as

$$S_R(A:B) = S_{\sqrt{\rho_{AB}}}(AA') = S_{\sqrt{\rho_{AB}}}(BB'),$$

which in the static holographic setting gives

$$S_{\sqrt{\rho_{AB}}}(AA') = \frac{\text{Area}(\gamma_{AA'})}{4G_N},$$

where $\gamma_{AA'} \subset \tilde{\Sigma}$ is the RT surface for AA' . By the leading-order holographic relation in (2.13) we have that

$$\text{Area}(\gamma_{AA'}) = 2 \text{Area}(\Gamma_{A:B}^W) = \text{Area}(\widetilde{\Gamma}_{A:B}^W), \quad (\text{E.3})$$

where $\widetilde{\Gamma}_{A:B}^W := \Gamma_{A:B}^W \cup \mathcal{R}(\Gamma_{A:B}^W)$. But Step 2 showed $\widetilde{\Gamma}_{A:B}^W$ is RT-admissible for AA' , hence by RT minimality, $\widetilde{\Gamma}_{A:B}^W$ is itself an RT minimizer for AA' (possibly among several, if the RT surface is non-unique), and so we can identify

$$\gamma_{AA'} = \widetilde{\Gamma}_{A:B}^W. \quad (\text{E.4})$$

This is seen in the central panel of Figure 16.

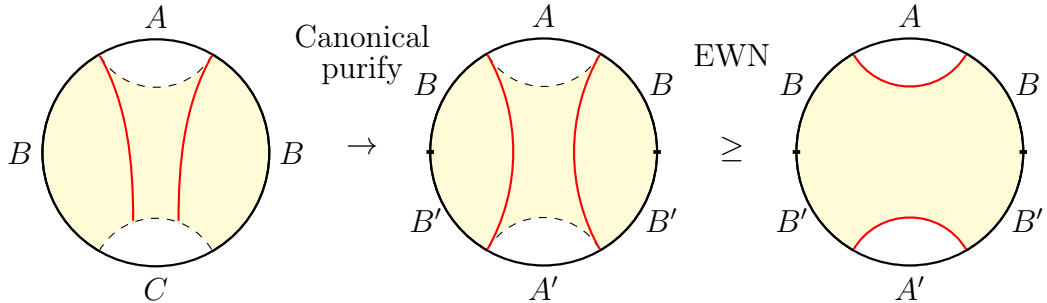


Figure 16. Demonstration of barrier theorem by reflected entropy and EWN. In the first figure we have $\Gamma_{A:B}^W$ naively traverses the yellow region $\mathcal{E}(B)$. Canonically purifying to $\rho_{ABA'B'}$ this becomes the reflected slice in central figure. This new red curve has length $2E_W(A:B) = S_R(A:B) = S_{BB'}$, by equation (2.13). However this violates EWN on this slice and so the original choice of $\Gamma_{A:B}^W$ was non-extremal.

Step 4: Apply EWN in the doubled geometry. Since $\gamma_{AA'}$ is an RT surface for AA' on $\tilde{\Sigma}$, it lies on the boundary of the entanglement wedge $\mathcal{E}_{\tilde{\Sigma}}(AA')$ and therefore does not intersect its interior:

$$\gamma_{AA'} \cap \text{Int } \mathcal{E}_{\tilde{\Sigma}}(AA') = \emptyset. \quad (\text{E.5})$$

However by EWN and our embedding

$$\mathcal{E}_{\Sigma}(A) = \mathcal{E}_{\tilde{\Sigma}}(A) \subseteq \mathcal{E}_{\tilde{\Sigma}}(AA'), \quad (\text{E.6})$$

with equality iff the state on A is pure, and so

$$\widetilde{\Gamma_{A:B}^W} \cap \text{Int } \mathcal{E}_{\tilde{\Sigma}}(A) = \emptyset, \quad \Leftrightarrow \quad \Gamma_{A:B}^W \cap \text{Int } \mathcal{E}_{\Sigma}(A) = \emptyset, \quad (\text{E.7})$$

proving the claim. The B statement holds by symmetry and this concludes the proof. \square

E.2 Proof by cycles

Throughout this subsection we work on a two-dimensional Cauchy slice Σ and assume (as in the main text) that $\mathcal{E}(AB)$ is a single connected bridged wedge. Namely, we decompose the EWCS minimizer into a disjoint union of its connected components

$$\Gamma_{A:B}^W = \bigsqcup_k \sigma_k, \quad (\text{E.8})$$

where each σ_k is a smooth embedded geodesic segment in Σ . Moreover if A is disjoint on the boundary then its RT surface decomposes as

$$\gamma_A = \bigsqcup_i \gamma_i^A, \quad (\text{E.9})$$

with each γ_i^A a geodesic.

Moreover, we define an *excursion* into A as follows. Fix a component σ and parameterize it as an injective continuous map $\sigma : [0, 1] \rightarrow \Sigma$ with $\sigma((0, 1))$ in the bulk. Set

$$T := \{t \in (0, 1) : \sigma(t) \in \text{Int } \mathcal{E}(A)\},$$

such that if $T \neq \emptyset$, pick a connected component $(\tau_1, \tau_2) \subset T$ and set

$$\alpha := \sigma([\tau_1, \tau_2]) \subset \mathcal{E}(A), \quad \alpha^\circ := \sigma((\tau_1, \tau_2)) \subset \text{Int } \mathcal{E}(A).$$

By maximality of (τ_1, τ_2) , the endpoints lie on $\partial \mathcal{E}(A) \cap \Sigma = \gamma_A$:

$$x := \sigma(\tau_1) \in \gamma_i^A, \quad y := \sigma(\tau_2) \in \gamma_j^A, \quad (\text{E.10})$$

for some indices i, j (possibly $i = j$). We term α° the excursion into A .

We will prove that no component of $\Gamma_{A:B}^W$ enters $\text{Int } \mathcal{E}(A)$. The only nontrivial case is when a component enters $\text{Int } \mathcal{E}(A)$ and exits through *different* components of γ_A ; this will be ruled out by a cycle-and-surgery argument which is summarized in Figure 6. By symmetry of $A \leftrightarrow B$ we hence show Theorem 3.1.

Some important notations defined in this subsection are summarized and visualized in Figure 17.

Lemma E.1 (Even-intersection lemma). Fix a connected component γ_i^A of γ_A . Then the number of bulk intersection points $\gamma_i^A \cap \Gamma_{A:B}^W$ is even.

Proof. Because $\Gamma_{A:B}^W$ is EWCS-admissible for $(A:B)$, it separates $\mathcal{E}(AB)$ into two regions U_A and U_B with $\partial_\infty U_A = A$ and $\partial_\infty U_B = B$. Along γ_i^A , define a “side label” by declaring a nearby point to lie on the A -side or B -side according to whether it lies in U_A or U_B . This label can change only when γ_i^A crosses $\Gamma_{A:B}^W$. At both UV ends of γ_i^A the label is the same (namely the A -side), so the label must flip an even number of times. Hence $\#(\gamma_i^A \cap \Gamma_{A:B}^W)$ is even. \square

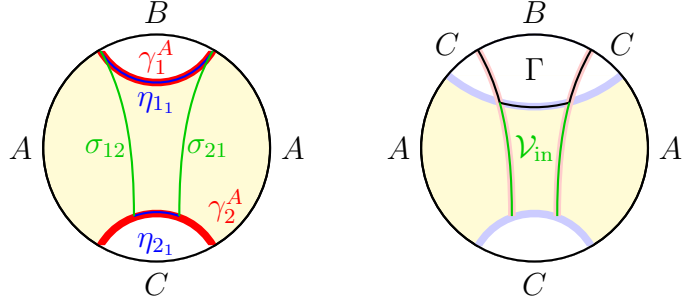


Figure 17. Notation used in proof of the barrier theorem by cycles. In both panels we have $\mathcal{E}(A)$ shaded in yellow. In the first panel the green curves are the conjectured $\Gamma_{A:B}^W$ and the blue curves are the resulting EWCS Γ by (E.14). By Lemma E.5 the area of the blue curves is strictly less than the area of the green curves. In the second panel, unlike the first, we have $\mathcal{V}_{in} \neq \Gamma_{A:B}^W$. The resulting EWCS by (E.14) is in black and has strictly less area than the original EWCS surface in salmon.

Lemma E.2 (Cycle extraction from a cross-component excursion). Assume there exists an excursion $\alpha^\circ \subset \text{Int } \mathcal{E}(A)$ with endpoints $x \in \gamma_i^A$ and $y \in \gamma_j^A$ for $i \neq j$. Then there exists a finite cyclic chain of EWCS components

$$\mathcal{V} := \{\sigma_{i_1 i_2}, \sigma_{i_2 i_3}, \dots, \sigma_{i_n i_1}\} \subset \Gamma_{A:B}^W, \quad n \geq 2, \quad (\text{E.11})$$

such that each $\sigma_{i_k i_{k+1}}$ has a nontrivial excursion into $\text{Int } \mathcal{E}(A)$ with endpoints on $\gamma_{i_k}^A$ and $\gamma_{i_{k+1}}^A$ (and $i_k \neq i_{k+1}$ for all k). Let $\mathcal{V}_{in} := \mathcal{V} \cap \text{Int } \mathcal{E}(A)$ denote the portions of these components lying in $\text{Int } \mathcal{E}(A)$; then $\mathcal{V}_{in} \neq \emptyset$.

Proof. Build a finite multigraph G whose vertices are the indices i labeling components γ_i^A , and whose edges are the EWCS components σ_k that admit an excursion into $\text{Int } \mathcal{E}(A)$: an edge connects i to j if some excursion on σ_k has endpoints on γ_i^A and γ_j^A .

By assumption G contains at least one edge between distinct vertices $i \neq j$. Moreover, by Lemma E.1, every vertex in G has even degree (indeed, excursions contribute bulk intersections on γ_i^A , and the parity constraint forces them to pair). Hence, starting from the edge $i-j$ and walking along adjacent edges, one can never get stuck at a vertex, and since G is finite the walk must eventually repeat a vertex, producing a cycle of edges. Translating back to EWCS components gives (E.11). At least one edge of the cycle exists by assumption, so $\mathcal{V}_{\text{in}} \neq \emptyset$. \square

Lemma E.3 (Closing the cycle on γ_A). Let \mathcal{V} be a cycle as in (E.11), and let \mathcal{V}_{in} be its portions in $\text{Int } \mathcal{E}(A)$. For each vertex i_k in the cycle, let

$$p_{k,-} := \gamma_{i_k}^A \cap \sigma_{i_{k-1}i_k}, \quad p_{k,+} := \gamma_{i_k}^A \cap \sigma_{i_ki_{k+1}}$$

be the two bulk intersection points contributed by the cycle. Let $\eta_{i_k} \subset \gamma_{i_k}^A$ be the (unique) sub-arc connecting $p_{k,-}$ to $p_{k,+}$, and set

$$\mathcal{P} := \bigcup_{k=1}^n \eta_{i_k}. \quad (\text{E.12})$$

Then

$$\mathcal{C} := \mathcal{V}_{\text{in}} \cup \mathcal{P} \quad (\text{E.13})$$

is a simple closed curve contained in $\mathcal{E}(A)$, and hence bounds an open region $U \subset \text{Int } \mathcal{E}(A)$ with $\partial_\infty U = \emptyset$ (except points) and $\partial_\Sigma U = \mathcal{C}$.

Proof. By construction, \mathcal{C} is closed: each geodesic segment in \mathcal{V}_{in} has endpoints on γ_A , and the arcs η_{i_k} join precisely the endpoints of adjacent segments in the cyclic order.

To see \mathcal{C} is simple, note that distinct EWCS components are disjoint in the bulk (otherwise one can cut-and-reglue to reduce total length, contradicting minimality of $\Gamma_{A:B}^W$), and the arcs η_{i_k} lie on distinct components of γ_A . Hence the only intersections occur at the shared endpoints $p_{k,\pm}$.

Since $\mathcal{C} \subset \mathcal{E}(A)$ and does not reach $\partial_\infty \Sigma$, the Jordan curve theorem on the regulated slice implies \mathcal{C} bounds an open region U with $\partial_\infty U = \emptyset$. Moreover $U \subset \text{Int } \mathcal{E}(A)$ because \mathcal{C} meets $\partial \mathcal{E}(A)$ only along γ_A . \square

Lemma E.4 (Surgery and EWCS-admissibility). Let \mathcal{C} and U be as in Lemma E.3. Define the surgically modified surface

$$\Gamma := (\Gamma_{A:B}^W \setminus \mathcal{V}_{\text{in}}) \cup \mathcal{P}. \quad (\text{E.14})$$

Then Γ is EWCS-admissible for $(A:B)$, i.e. $\widehat{\Gamma} \in \mathfrak{S}_{A:B}$.

Proof. Let U_A, U_B be the complementary regions for $\Gamma_{A:B}^W$:

$$\mathcal{E}(AB) \setminus \Gamma_{A:B}^W = U_A \sqcup U_B, \quad \partial_\infty U_A = A, \quad \partial_\infty U_B = B.$$

By Lemma E.3, the loop \mathcal{C} bounds a bubble $U \subset \text{Int } \mathcal{E}(A)$ with $\partial_\infty U = \emptyset$. Replacing \mathcal{V}_{in} by $\mathcal{P} \subset \partial U$ shifts the separating surface across the bubble. Define

$$\widehat{U}_A := U_A \cup U, \quad \widehat{U}_B := U_B \setminus U.$$

Since $\partial_\infty U = \emptyset$, we still have $\partial_\infty \widehat{U}_A = A$ and $\partial_\infty \widehat{U}_B = B$. By construction, the common bulk boundary between \widehat{U}_A and \widehat{U}_B inside $\mathcal{E}(AB)$ is exactly Γ , hence Γ separates $\mathcal{E}(AB)$ into an A -side and a B -side with the correct asymptotic boundaries. Therefore Γ is EWCS-admissible. \square

Lemma E.5 (Strict area improvement). With Γ as in (E.14), one has

$$\text{Area}(\Gamma) < \text{Area}(\Gamma_{A:B}^W).$$

Proof. Define the surfaces

$$X := \Gamma_{A:B}^W \cup \mathcal{P}, \quad Y := \Gamma \cup \mathcal{V}_{\text{in}}.$$

By construction, X and Y have the same support as sets (we have swapped \mathcal{V}_{in} and \mathcal{P}), so

$$X = Y.$$

Taking areas and using that overlaps occur only at finitely many junction points (measure zero), we obtain

$$\text{Area}(\Gamma_{A:B}^W) + \text{Area}(\mathcal{P}) = \text{Area}(\Gamma) + \text{Area}(\mathcal{V}_{\text{in}}). \quad (\text{E.15})$$

Thus, it suffices to show

$$\text{Area}(\mathcal{P}) < \text{Area}(\mathcal{V}_{\text{in}}). \quad (\text{E.16})$$

To prove (E.16), use RT minimality of γ_A via a cut-and-reglue argument. The loop $\mathcal{C} = \mathcal{V}_{\text{in}} \cup \mathcal{P}$ bounds a bubble $U \subset \text{Int } \mathcal{E}(A)$ with $\partial_\infty U = \emptyset$ (Lemma E.3). Excising U from $\mathcal{E}(A)$ produces a new region $\mathcal{E}(A)' = \mathcal{E}(A) \setminus U$ with the same asymptotic boundary A but with bulk boundary

$$\partial_\Sigma \mathcal{E}(A)' = (\gamma_A \setminus \mathcal{P}) \cup \mathcal{V}_{\text{in}}.$$

Hence $(\gamma_A \setminus \mathcal{P}) \cup \mathcal{V}_{\text{in}}$ is a valid RT competitor for A , so

$$\begin{aligned} \text{Area}(\gamma_A) &\leq \text{Area}\left((\gamma_A \setminus \mathcal{P}) \cup \mathcal{V}_{\text{in}}\right) \\ &= \text{Area}(\gamma_A) - \text{Area}(\mathcal{P}) + \text{Area}(\mathcal{V}_{\text{in}}), \end{aligned} \quad (\text{E.17})$$

which implies $\text{Area}(\mathcal{P}) \leq \text{Area}(\mathcal{V}_{\text{in}})$.

The inequality is strict: if $\text{Area}(\mathcal{P}) = \text{Area}(\mathcal{V}_{\text{in}})$ then the competitor would also be RT-minimizing for A . Under the assumed uniqueness/no-multiple-intersections of minimizing geodesics on the slice (see Assumption 3.5), this forces $\mathcal{V}_{\text{in}} \subset \gamma_A$, contradicting $\mathcal{V}_{\text{in}} \subset \text{Int } \mathcal{E}(A)$. Thus, (E.16) holds. Substituting (E.16) into (E.15) gives $\text{Area}(\Gamma) < \text{Area}(\Gamma_{A:B}^W)$ as claimed. \square

Corollary E.1 (No cross-component excursions). There is no excursion $\alpha^\circ \subset \text{Int } \mathcal{E}(A)$ with endpoints on two distinct components γ_i^A and γ_j^A with $i \neq j$.

Proof. Assume such an excursion exists. Then Lemma E.2 produces a cycle \mathcal{V} , Lemma E.3 produces a bubble U bounded by \mathcal{C} , Lemma E.4 produces an EWCS-admissible Γ by surgery, and Lemma E.5 gives $\text{Area}(\Gamma) < \text{Area}(\Gamma_{A:B}^W)$, contradicting the minimality of $\Gamma_{A:B}^W$. \square

Proof of Theorem 3.1 by cycles (2D). We show $\Gamma_{A:B}^W \cap \text{Int } \mathcal{E}(A) = \emptyset$. Suppose not. Then some component $\sigma \subset \Gamma_{A:B}^W$ admits a nontrivial excursion $\alpha^\circ \subset \text{Int } \mathcal{E}(A)$ with endpoints as in (E.10).

Case 1: $i = j$. Then α and γ_i^A are length-minimizing geodesics intersecting at two distinct bulk points. By Assumption 3.5, they must coincide between those points. But $\gamma_i^A \subset \partial \mathcal{E}(A)$ contains no point of $\text{Int } \mathcal{E}(A)$, contradicting $\alpha^\circ \subset \text{Int } \mathcal{E}(A)$.

Case 2: $i \neq j$. This is excluded by Corollary E.1.

Hence no component of $\Gamma_{A:B}^W$ enters $\text{Int } \mathcal{E}(A)$. By symmetry under $A \leftrightarrow B$, the same holds with A and B exchanged, and the barrier theorem follows. \square

F Proof: Monotonicity in unmeasured party

Theorem 4.1. D_W is monotone in the unmeasured party. That is D_W satisfies

$$D_W(AC|B) \geq D_W(A|B), \quad (4.10)$$

for any state on ABC (not necessarily pure).

For a pure state on $ABCD$ after purification, by expanding the target inequality in Theorem 4.1 in terms of HEE and EWCS (and relabeling subsystems), it is equivalent to

$$S_{BC} + E_W(AB:C) \geq S_C + E_W(A:BC). \quad (F.1)$$

Lemma F.1 (Discarding A -only components). Decompose A (with respect to the state on ABC) into A -only components \mathcal{F} and A -bridged components \mathcal{A} , so that $A = \mathcal{F} \cup \mathcal{A}$ and $\mathcal{F} \cap \mathcal{A} = \emptyset$. Then, as in Remark 3.2,

$$E_W(AB:C) = E_W(\mathcal{A}B:C), \quad E_W(A:BC) = E_W(\mathcal{A}:BC). \quad (F.2)$$

In particular, if $\mathcal{A} = \emptyset$ then (F.1) reduces to (3.6). Otherwise, one may replace A by \mathcal{A} and absorb \mathcal{F} into the purifier D without changing (F.1).

Proof. If $\mathcal{A} = \emptyset$, both EWCS terms in (F.1) are unchanged upon removing A , and the inequality reduces to (3.6). If $\mathcal{A} \neq \emptyset$, then (F.2) shows that the EWCS terms depend only on \mathcal{A} ; thus \mathcal{F} decouples and can be absorbed into the purifier D . \square

Hereafter we implicitly use Lemma F.1 assuming A has no A –only components in ABC .

Lemma F.2 (Existence of an RT admissible surface for C from γ_{BC} and $\Gamma_{AB:C}^W$). Let $\Gamma_{AB:C}^W$ be the EWCS minimizer for $(AB:C)$, and let γ_{BC} be the RT surface for BC . Define the restriction of the EWCS to the BC wedge by

$$\Gamma_1 := \Gamma_{AB:C}^W \cap \mathcal{E}(BC), \quad \Gamma_2 := \Gamma_{AB:C}^W \setminus \Gamma_1. \quad (\text{F.3})$$

Then Γ_1 separates $\mathcal{E}(BC)$ into two regions

$$\mathcal{E}(BC) \setminus \Gamma_1 = U_B \sqcup U_C, \quad \partial_\infty U_B = B, \quad \partial_\infty U_C = C.$$

Let $U_C^{\text{cl}} := U_C \cup \Gamma_1$ be the closure obtained by adjoining the open face along Γ_1 . Then U_C^{cl} is C -homologous in $\mathcal{E}(ABC)$, and its boundary

$$\mathbf{E} := \partial U_C^{\text{cl}} \quad (\text{F.4})$$

is a valid RT competitor for C . In particular,

$$\frac{\text{Area}(\mathbf{E})}{4G_N} \geq S_C. \quad (\text{F.5})$$

Proof. Since $\Gamma_{AB:C}^W$ is EWCS-admissible for $(AB:C)$, its restriction Γ_1 to $\mathcal{E}(BC)$ separates $\mathcal{E}(BC)$ into a B -side and a C -side region, giving U_B, U_C as stated. The set $U_C^{\text{cl}} = U_C \cup \Gamma_1$ is C -homologous because it is bounded away from AD by the inherited portion of γ_{BC} and bounded away from B inside $\mathcal{E}(BC)$ by Γ_1 . Thus $\mathbf{E} = \partial U_C^{\text{cl}}$ is a closed codimension-2 surface in Σ homologous to C , so is RT admissible. \square

In the middle of Figure 8 we have U_C^{cl} is the region bounded by the red curves.

Lemma F.3 (Bookkeeping decomposition of the LHS multisurface). Let γ_{BC} be the RT surface for BC and $\Gamma_{AB:C}^W$ the EWCS minimizer for $(AB:C)$. Define the LHS multisurface

$$\mathbf{L} := \gamma_{BC} \oplus \Gamma_{AB:C}^W, \quad (\text{F.6})$$

so that

$$\frac{\text{Area}^\oplus(\mathbf{L})}{4G_N} = S_{BC} + E_W(AB:C).$$

Let $\mathbf{E} = \partial U_C^{\text{cl}}$ be as in Lemma F.2 and set

$$\Gamma := |\mathbf{L} \ominus \mathbf{E}|. \quad (\text{F.7})$$

Then \mathbf{E} is supported on \mathbf{L} and the areas split as

$$\text{Area}^\oplus(\mathbf{L}) = \text{Area}(\Gamma) + \text{Area}(\mathbf{E}). \quad (\text{F.8})$$

Moreover, if γ_{ABC} denotes the RT surface for ABC , the surface

$$\tilde{\Gamma} := \text{cl}\{\Gamma \cap \text{Int } \mathcal{E}(ABC)\}, \quad (\text{F.9})$$

where cl is the standard topological closure, is a codimension-2 surface in $\mathcal{E}(ABC)$ with $\partial\tilde{\Gamma} \subset \gamma_{ABC}$ and

$$\text{Area}(\Gamma) \geq \text{Area}(\tilde{\Gamma}). \quad (\text{F.10})$$

Proof. By construction, \mathbf{E} consists of a sub-arc of γ_{BC} together with $\Gamma_1 \subset \Gamma_{AB:C}^W$, hence \mathbf{E} lies in the support of $\mathbf{L} = \gamma_{BC} \oplus \Gamma_{AB:C}^W$ and the multiset difference $\mathbf{L} \ominus \mathbf{E}$ is well-defined. Since overlaps occur only along codimension-2 junction sets (measure zero), areas satisfy (F.8). Finally, $\tilde{\Gamma}$ is obtained by restricting Γ to $\text{Int } \mathcal{E}(ABC)$ and taking the closure in $\mathcal{E}(ABC)$, which is just reattaching the codimension three boundaries of Γ which we remove by taking the intersect with $\text{Int } \mathcal{E}(ABC)$. This intersect can only decrease area, giving (F.10). \square

In the central panel of Figure 8 we had Γ as the union of the green and blue curves; $\tilde{\Gamma}$ is now just the blue curve as the green lies along $\partial\mathcal{E}(ABC) = \gamma_{ABC}$. The purpose of taking the closure here is to enforce $\partial\tilde{\Gamma} \subset \gamma_{ABC}$ instead of \emptyset .

Lemma F.4 ($\tilde{\Gamma}$ is EWCS admissible for $(A : BC)$). Assume A has no A -only components in ABC . Let $\tilde{\Gamma}$ be defined by (F.9). Then, every simple path in $\mathcal{E}(ABC)$ joining a point adjacent to A to a point adjacent to BC intersects $\tilde{\Gamma}$. Consequently, by Remark D.2, $\tilde{\Gamma}$ is EWCS-admissible for $(A:BC)$.

Proof. Decompose $\tilde{\Gamma}$ into its portion lying on γ_{BC} and its complement:

$$\Gamma_{\text{in}} := \tilde{\Gamma} \cap \gamma_{BC}, \quad \Gamma_{\text{out}} := \tilde{\Gamma} \setminus \Gamma_{\text{in}}.$$

In the middle panel of Figure 8 we have Γ_{in} the thin blue curve and Γ_{out} the thick blue curve. By construction of $\mathbf{E} = \partial U_C^{\text{cl}}$, the excised surface \mathbf{E} consists of (i) an arc $\eta_C \subset \gamma_{BC}$ and (ii) the segment $\Gamma_1 = \Gamma_{AB:C}^W \cap \mathcal{E}(BC)$. Hence the remaining part of $\Gamma_{AB:C}^W = \Gamma_1 \cup \Gamma_2$ inside $\mathcal{E}(ABC)$ but outside $\mathcal{E}(BC)$ is precisely

$$\Gamma_2 = \Gamma_{AB:C}^W \setminus \Gamma_1 = \Gamma_{\text{out}}. \quad (\text{F.11})$$

This is clearly seen for the case in Figure 8 with $\Gamma_{\text{out}} = \Gamma_2$ the thick blue curve.

Now let ℓ be any simple path in $\mathcal{E}(ABC)$ from a point adjacent to A to a point adjacent to BC . Because A has no A -only components in ABC , ℓ must cross γ_{BC} in order to enter the BC -side. Let x be the *first* intersection of ℓ with γ_{BC} along the parameterization of ℓ .

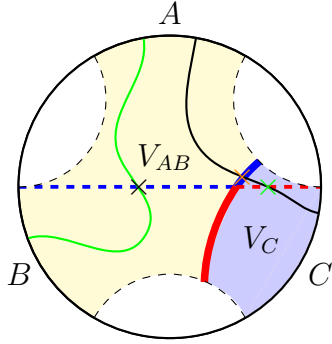


Figure 18. Continuation of case in Figure 8. Taking $\mathcal{E}(ABC) \setminus \Gamma_{AB:C}^W$ yields two regions: V_{AB} in yellow, and V_C in blue. We have $U_C \subset V_C$ as the region bounded by the red curves. *Case 1* shown by green path, and *Case 2* by the black curve with their intersections point x with γ_{BC} marked by black and green \times . Intersection of black path and $\Gamma_{AB:C}^W$ as the orange \times . In either case the path crosses the blue curve $\tilde{\Gamma}$.

Case 1: $x \in \Gamma_{\text{in}}$. Then $x \in \tilde{\Gamma}$ and this concludes the proof.

Case 2: $x \notin \Gamma_{\text{in}}$. Then x lies on the arc $\eta_C \subset \gamma_{BC}$ that was excised as part of \mathbf{E} , i.e. on the γ_{BC} -portion of ∂U_C^{cl} . Therefore immediately after crossing x , the path ℓ enters the region U_C inside $\mathcal{E}(BC)$.

On the other hand, since $\Gamma_{AB:C}^W$ is EWCS-admissible for $(AB:C)$, it partitions $\mathcal{E}(ABC)$ into two regions V_{AB} and V_C with $\partial_\infty V_{AB} = AB$ and $\partial_\infty V_C = C$. By construction $U_C \subset V_C$ (it is the part of V_C lying inside $\mathcal{E}(BC)$), while a neighborhood of A lies in V_{AB} . Thus, as ℓ runs from A towards BC , it must leave V_{AB} and enter V_C at some first parameter value. Let t_* be the first such parameter and set $y = \ell(t_*)$. Then $y \in \Gamma_{AB:C}^W$.

We claim $y \notin \Gamma_1$. Indeed, if $y \in \Gamma_1 \subset \mathcal{E}(BC)$, then y lies in $\mathcal{E}(BC)$. But we already noted that immediately after the *earlier* point x (the first intersection with γ_{BC}), the path lies in $U_C \subset V_C$. Hence ℓ must have entered V_C no later than the parameter of x , contradicting the choice of t_* as the *first* entry into V_C . Therefore $y \in \Gamma_{AB:C}^W \setminus \Gamma_1 = \Gamma_2$. Using (F.11), we conclude $y \in \Gamma_{\text{out}} \subset \tilde{\Gamma}$, so ℓ intersects $\tilde{\Gamma}$ also in Case 2. In all cases ℓ intersects $\tilde{\Gamma}$. The admissibility statement then follows from Remark D.2. \square

Proof of equation (F.1). By Lemma F.1 we may assume A has no A -only components in ABC . Let \mathbf{L} be the LHS multisurface (F.6). Then

$$\frac{\text{Area}^\oplus(\mathbf{L})}{4G_N} = S_{BC} + E_W(AB:C).$$

Let $\mathbf{E} = \partial U_C^{\text{cl}}$ be the C -competitor from Lemma F.2, and define Γ and $\tilde{\Gamma}$ as in

Lemma F.3. Using the bookkeeping identities (F.8) and (F.10), we obtain

$$S_{BC} + E_W(AB:C) = \frac{\text{Area}^\oplus(\mathbf{L})}{4G_N} = \frac{\text{Area}(\Gamma)}{4G_N} + \frac{\text{Area}(\mathbf{E})}{4G_N} \geq \frac{\text{Area}(\tilde{\Gamma})}{4G_N} + \frac{\text{Area}(\mathbf{E})}{4G_N}. \quad (\text{F.12})$$

By Lemma F.2, $\text{Area}(\mathbf{E})/(4G_N) \geq S_C$. By Lemma F.4, $\tilde{\Gamma}$ is EWCS-admissible for $(A:BC)$, hence by EWCS minimality

$$\frac{\text{Area}(\tilde{\Gamma})}{4G_N} \geq E_W(A:BC). \quad (\text{F.13})$$

Substituting these bounds into (F.12) yields

$$S_{BC} + E_W(AB:C) \geq E_W(A:BC) + S_C,$$

which is exactly (F.1) hence proving Theorem 4.1. \square

G Proof: Monogamy of classical correlations: Measured party

Theorem 5.1. J_W is monogamous in the measured party. That is J_W satisfies

$$J_W(A|B) + J_W(A|C) \leq J_W(A|BC). \quad (5.16)$$

for any state ABC (not necessarily pure).

Proof. Using the holographic expressions for J_W in terms of HEE and EWCS and purifying ABC by D , the claim is equivalent to asking

$$E_W(A:BD) + E_W(A:CD) \geq S_A + E_W(A:D). \quad (\text{G.1})$$

Let $\Gamma_{A:BD}^W$ and $\Gamma_{A:CD}^W$ denote EWCS minimizers for $(A : BD)$ and $(A : CD)$. Then introduce the *LHS multisurface*

$$\mathbf{L} := \Gamma_{A:BD}^W \oplus \Gamma_{A:CD}^W, \quad \frac{\text{Area}^\oplus(\mathbf{L})}{4G_N} = E_W(A:BD) + E_W(A:CD).$$

Step 1: Carving an A-homologous region \mathbf{r}_A . By EWCS admissibility, each cross section splits its wedge into an A -side and a complementary side:

$$\begin{aligned} \text{Int}(\mathcal{E}(ABD)) \setminus \Gamma_{A:BD}^W &= U_A^{(BD)} \sqcup U_{BD}^{(A)}, & \partial_\infty U_A^{(BD)} &= A, & \partial_\infty U_{BD}^{(A)} &= BD, \\ \text{Int}(\mathcal{E}(ACD)) \setminus \Gamma_{A:CD}^W &= U_A^{(CD)} \sqcup U_{CD}^{(A)}, & \partial_\infty U_A^{(CD)} &= A, & \partial_\infty U_{CD}^{(A)} &= CD. \end{aligned}$$

We work with the open interiors so that $U_A^{(BD)}$ and $U_A^{(CD)}$ carry no boundary arcs along γ_{ABD} and γ_{ACD} :

$$\partial_\Sigma U_A^{(BD)} = \partial_\Sigma U_A^{(CD)} = \emptyset. \quad (\text{G.2})$$

We then *close* both A -sides in their respective wedges by adjoining the corresponding EWCS surfaces:

$$\widehat{U}_A^{(BD)} := U_A^{(BD)} \cup \Gamma_{A:BD}^W, \quad \widehat{U}_A^{(CD)} := U_A^{(CD)} \cup \Gamma_{A:CD}^W. \quad (\text{G.3})$$

They are of course not generally closed in Σ but by construction satisfy $\widehat{U}_A^{(BD)} \sim_{ABD} A$ and $\widehat{U}_A^{(CD)} \sim_{ACD} A$.

Now define

$$r_A := \widehat{U}_A^{(BD)} \cap \widehat{U}_A^{(CD)}, \quad U_A := \widehat{U}_A^{(BD)} \cup \widehat{U}_A^{(CD)}. \quad (\text{G.4})$$

Thus $r_A \subseteq U_A$, and by the barrier property of the EWCS (Theorem 3.1) we have

$$\Gamma_{A:BD}^W \cap \text{Int } \mathcal{E}(A) = \emptyset, \quad \Gamma_{A:CD}^W \cap \text{Int } \mathcal{E}(A) = \emptyset, \quad (\text{G.5})$$

so that the A -wedge lies on the A -side of both cross sections. In particular,

$$\mathcal{E}(A) \subseteq r_A \subseteq U_A, \quad (\text{G.6})$$

with equality in the first inclusion only if one of the EWCS surfaces coincides with γ_A , and equality in the second one only if both do.

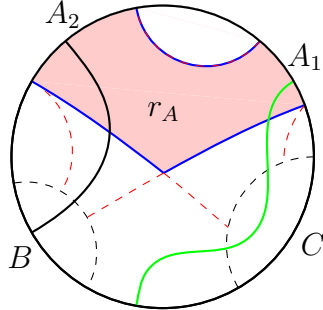


Figure 19. Continuation of case in Figure 10 to show $r_A \sim A$, with ∂r_A in blue. Green path shows ℓ intersects ∂r_A when traveling from $A \rightarrow D$, and black path shows ℓ intersects ∂r_A when traveling to B .

Step 2: Showing $r_A \sim A$. As we know $\partial_\infty r_A = A$, all that remains to show is that ∂r_A is homologous to A . Equivalently any simple path

$$\ell: [0, 1] \rightarrow \Sigma$$

with $\ell(0) \in \text{Int } \mathcal{E}(A)$ and $\ell(1)$ in $\text{Int } \mathcal{E}(B) \cup \text{Int } \mathcal{E}(C) \cup \text{Int } \mathcal{E}(D)$ must intersect ∂r_A .

Define

$$\mathcal{L} := |\mathbf{L}| = \Gamma_{A:BD}^W \cup \Gamma_{A:CD}^W. \quad (\text{G.7})$$

Let us first assume for contradiction that there exists a simple path ℓ with

$$\ell(0) \in \text{Int } \mathcal{E}(A) \subset r_A, \quad \ell(1) \in \text{Int } \mathcal{E}(X), \quad (\text{G.8})$$

for some $X \in \{B, C, D\}$, such that ℓ does *not* intersect \mathcal{L} . We will show this is a contradiction and so all such simple paths satisfying (G.8) must intersect \mathcal{L} ; we will then demonstrate that all first intersection points of ℓ and \mathcal{L} lie on ∂r_A hence showing $r_A \sim A$.

Paths from A to D. First consider $\ell(1) \in \text{Int } \mathcal{E}(D)$. Assume for contradiction ℓ misses $\Gamma_{A:BD}^W$. Then ℓ stays in $U_A^{(BD)}$ and can only exit this region along its open boundary on γ_C into $\text{Int } \mathcal{E}(C)$. This is the green path in Figure 19. If it does not have an open boundary on γ_C then $\Gamma_{A:BD}^W$ coincides with γ_A , and we are done; thus we can assume it is open along this arc. As $\text{Int } \mathcal{E}(C) \cap U_A^{(CD)} = \emptyset$ via the barrier theorem, in evolving from $\ell(0) \in \text{Int } r_A$, it remains in $U_A^{(BD)}$ but must exit $U_A^{(CD)}$ such that it may reach $\text{Int } \mathcal{E}(C)$. However, to exit $U_A^{(CD)}$ without crossing $\Gamma_{A:CD}^W$, ℓ can only achieve this by exiting through $U_A^{(CD)}$'s open arc along γ_B into $\text{Int } \mathcal{E}(B)$. Likewise if this region has no open arc along γ_B then $\Gamma_{A:CD}^W$ coincides with γ_A , and we are also done; we thus continue assuming it has this open surface. However the barrier theorem tells us that $\text{Int } \mathcal{E}(B) \cap U_A^{(BD)} = \emptyset$ so ℓ cannot remain in $U_A^{(BD)}$ whilst exiting $U_A^{(CD)}$ and so this is a contradiction. We argue identically for if ℓ misses $\Gamma_{A:CD}^W$ thus $\ell \cap \mathcal{L} \neq \emptyset$.

Paths from A to B. The argument for $\ell(1) \in \text{Int } \mathcal{E}(B)$ is analogous and is seen by the black path in Figure 19. Assume ℓ misses $\Gamma_{A:CD}^W$, and so remains in $U_A^{(CD)}$ until it crosses its open boundary on γ_B directly into $\text{Int } \mathcal{E}(B)$. However by assumption, it does not cross $\Gamma_{A:BD}^W$ either, and as $\text{Int } \mathcal{E}(B) \cap U_A^{(BD)} = \emptyset$, it cannot reach $\text{Int } \mathcal{E}(B)$ without first exiting $U_A^{(BD)}$ which it can only do along the open arc γ_C . But by assumption it cannot do this whilst remaining in $U_A^{(CD)}$, and hence not missing $\Gamma_{A:CD}^W$, and so we are done in this case. Assuming instead ℓ misses $\Gamma_{A:BD}^W$ we apply similar logic and find a likewise contradiction.

Paths from A to C. This is identical to the previous case with appropriate relabeling of $B \leftrightarrow C$.

We have shown any simple path ℓ with $\ell(0) \in \text{Int } \mathcal{E}(A)$ and $\ell(1) \in \text{Int } \mathcal{E}(X)$, with $X \in \{B, C, D\}$ intersects \mathcal{L} . We will now show the first intersection point lies on ∂r_A . Let t_1 be the first parameter in $[0, 1]$ such that $\ell(t_1) \in \mathcal{L}$. Without loss of generality, assume $\ell(t_1) \in \Gamma_{A:BD}^W$ (the case of $\Gamma_{A:CD}^W$ is identical). There are two possibilities:

- If $\ell(t_1) \in \Gamma_{A:BD}^W \cap \widehat{U}_A^{(CD)}$, as this is a component of ∂r_A , we are done.
- If $\ell(t_1)$ lies on the remainder of $\Gamma_{A:BD}^W \setminus (\Gamma_{A:BD}^W \cap \widehat{U}_A^{(CD)})$, then ℓ must have exited $U_A^{(CD)}$. But this implies ℓ must have already crossed $\Gamma_{A:CD}^W$: if it had not

then $\ell(t_1 - \epsilon) \in U_A^{(BD)}$ (with ϵ a small positive parameter), has not yet crossed $\Gamma_{A:BD}^W$ and so we could deform the path to instead travel to $\text{Int } \mathcal{E}(C)$. However this is impossible without having crossed $\Gamma_{A:CD}^W$ by our previous proof. Thus ℓ crosses $\Gamma_{A:CD}^W$ before crossing $\Gamma_{A:BD}^W \setminus (\Gamma_{A:BD}^W \cap \widehat{U}_A^{(CD)})$ which is a contradiction to t_1 being the first such time that ℓ intersects \mathcal{L} .

We apply the same argument to assuming $\ell(t_1) \in \Gamma_{A:CD}^W$ and have thus shown $\ell(t_1) \in \partial r_A$. Consequently no simple path from $\text{Int } \mathcal{E}(A)$ to $\text{Int } \mathcal{E}(X)$ can avoid ∂r_A and so $r_A \sim_{\Sigma} A$. Hence by RT minimality we must have that

$$\frac{\text{Area}(\partial r_A)}{4G_N} \geq S_A. \quad (\text{G.9})$$

Step 3: Defining a candidate for $\mathbf{E}_W(\mathbf{A} : \mathbf{D})$. Define the *restricted remainder surface*⁹

$$\Gamma := |(\mathbf{L} \ominus \partial r_A)| \cap \mathcal{E}(AD), \quad (\text{G.10})$$

and the *restricted excised surface*

$$\mathbf{E} = \partial r_A \cap \mathcal{E}(AD). \quad (\text{G.11})$$

As Γ is a restriction of the remainder multisurface we must have that

$$\frac{\text{Area}(\Gamma)}{4G_N} + \frac{\text{Area}(\partial r_A)}{4G_N} \leq E_W(A:BD) + E_W(A:CD). \quad (\text{G.12})$$

We now verify that Γ is EWCS admissible for $(A : D)$.

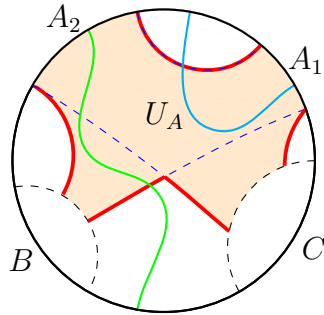


Figure 20. Continuation of case in Figure 10 to show Γ in red is EWCS admissible for $(A : D)$. Blue dashed curves show excise surface ∂r_A , and the union of red and blue dashed curves is \mathcal{L}_{AD} . Any simple path ℓ in $\mathcal{E}(AD)$ starting adjacent to A and ending on D intersects Γ .

⁹In fact, taking the support in the definition of Γ is unnecessary since the resulting surface has multiplicity one everywhere; however, we will not use this fact in the proof. Hence, we will just take the support to ensure multiplicity one.

Step 4: Showing Γ is EWCS admissible for $(A : D)$. To be admissible we need to show the following three properties:

- (a) (*Localization*) $\Gamma \subset \mathcal{E}(AD)$,
- (b) (*Bulk anchoring*) $\partial\Gamma \subset \gamma_{AD}$,
- (c) (*Separation*) $\mathcal{E}(AD) \setminus \Gamma = U_A \sqcup U_D$ with $\partial_\infty U_A = A$, $\partial_\infty U_D = D$.

Generally, the localization condition is not required for admissibility (in the separation sense). However, a surface that satisfies the two latter conditions is never the global minimal surface: we could always amputate the said surface within $\mathcal{E}(AD)$ to produce a smaller surface still satisfying the other conditions. We do exactly this by taking the intersection in equation (G.11).

(a) (*Localization*) Trivial.

(b) (*Bulk anchoring*) Inside $\mathcal{E}(AD)$, each connected component of $\Gamma_{A:CD}^W \cap \mathcal{E}(AD)$ and $\Gamma_{A:BD}^W \cap \mathcal{E}(AD)$ is a smooth codimension-two surface whose bulk endpoints lie on γ_{AD} . They of course cannot have a boundary in $\text{Int } \mathcal{E}(AD)$ as they either anchor on γ_B or γ_C , which both have zero intersect with $\text{Int } \mathcal{E}(AD)$. Moreover, the set $\mathbf{E} \cap \mathcal{E}(AD)$ is a union of sub-arcs of these components; each such sub-arc has endpoints either on γ_{AD} or at an intersection point of $\Gamma_{A:CD}^W$ and $\Gamma_{A:BD}^W$. These are the dashed blue curves in Figure 20. Excising \mathbf{E} from $\mathbf{L} \cap \mathcal{E}(AD)$ thus removes only these sub-arcs, and any remaining endpoints lie on γ_{AD} . Thus $\partial\Gamma \subset \gamma_{AD}$.

(c) (*Separation*) Now set

$$\mathcal{L}_{AD} := \mathcal{L} \cap \mathcal{E}(AD), \quad (\text{G.13})$$

with \mathcal{L} defined in equation (G.7). This just gives the original \mathcal{L} if BC is unbridged, as in Figure 20, but will generally be different if they are bridged.

We show that every simple path

$$\ell : [0, 1] \rightarrow \text{Int } \mathcal{E}(AD), \quad \ell(0) \in \text{Int } \mathcal{E}(A), \quad \ell(1) \in \text{Int } \mathcal{E}(D), \quad (\text{G.14})$$

intersects \mathcal{L}_{AD} . We then show that any such ℓ intersects $\Gamma \subset \mathcal{L}_{AD}$ too.

Claim 1. Any such ℓ intersects \mathcal{L}_{AD} . Indeed, if ℓ missed $\Gamma_{A:BD}^W$ it would lie entirely in $U_A^{(BD)} \supseteq \text{Int } \mathcal{E}(A)$; if it missed $\Gamma_{A:CD}^W$ it would lie entirely in $U_A^{(CD)}$. Missing both forces $\ell \subset U_A^{(BD)} \cap U_A^{(CD)} \subset r_A$. This cannot reach a point in $\text{Int } \mathcal{E}(D)$ as $r_A \sim A$ by Step 2. Hence $\ell \cap \mathcal{L}_{AD} \neq \emptyset$.

Claim 2 (first-hit upgrade). Let t_1 be the first time ℓ meets \mathcal{L}_{AD} . If $\ell(t_1) \notin \mathbf{E}$, then $\ell(t_1) \in \mathcal{L}_{AD} \setminus \mathbf{E} \subset \Gamma$ and we are done. Moreover, if \mathbf{E} and \mathcal{L}_{AD} coincide then it is possible that $\ell(t_1) \in \mathbf{E} \cap \mathcal{L}_{AD}$. Regardless it intersects Γ and we are done. This is the case of the cyan curve in Figure 20. If instead $\ell(t_1) \in \mathbf{E}$ let us assume without loss of generality $\ell(t_1) \in \Gamma_{A:BD}^W$ and $\ell(t_1) \notin \Gamma_{A:CD}^W$. This is the statement that the green path in Figure 20 intersects \mathcal{L}_{AD} first on the blue dashed line which

is a segment of $\Gamma_{A:BD}^W$. Immediately after t_1 , ℓ lies on the BD -side of $\Gamma_{A:BD}^W$ but still on the A -side of $\Gamma_{A:CD}^W$ (since t_1 was the first contact with \mathcal{L}_{AD}). To reach a point adjacent to D , ℓ must cross $\Gamma_{A:CD}^W$ at some later time $t_2 > t_1$. At t_2 it cannot be on ∂r_A (crossing ∂r_A would return into r_A , contradicting that we remain on the BD -side of $\Gamma_{A:BD}^W$). Therefore $\ell(t_2) \in \Gamma_{A:CD}^W \setminus \mathbf{E} \subset \Gamma$. The same argument applies if instead $\ell(t_1) \in \Gamma_{A:CD}^W$ and $\ell(t_1) \notin \Gamma_{A:BD}^W$. If instead $\ell(t_1) \in \Gamma_{A:CD}^W \cap \Gamma_{A:BD}^W \in \partial r_A$, then due to multiplicity, this intersect is also in Γ and we are done. Thus every simple path satisfying equation (G.14) meets Γ and hence separation follows.

As we have shown Γ is EWCS-admissible for $(A:D)$, we can now state

$$\frac{\text{Area}(\Gamma)}{4G_N} \geq E_W(A:D). \quad (\text{G.15})$$

Step 5: Area bookkeeping. From (G.12), (G.9), and (G.15),

$$\frac{\text{Area}^\oplus(\mathbf{L})}{4G_N} \geq \frac{\text{Area}(\Gamma)}{4G_N} + \frac{\text{Area}(\partial r_A)}{4G_N} \geq E_W(A:D) + S_A,$$

which is precisely our original inequality. \square

H Proof: Monogamy of classical correlations: Unmeasured party

Theorem 5.2. J_W is monogamous in the unmeasured party. That is J_W satisfies

$$J_W(A|B) + J_W(C|B) \leq J_W(AC|B).$$

for any states on ABC (not necessarily pure).

Proof of Theorem 5.2. Using the holographic expressions for J_W in terms of HEE and EWCS and purifying ABC by D , Theorem 5.2 is equivalent to

$$S_{AC} + E_W(A:CD) + E_W(C:AD) \geq S_A + S_C + E_W(AC:D). \quad (\text{H.1})$$

Throughout this proof we define γ_{AC} as the RT surface for AC and let $\Gamma_{A:CD}^W$ and $\Gamma_{C:AD}^W$ be the EWCS minimizers for $(A:CD)$ and $(C:AD)$.

Step 1: Bridged and unbridged components. Let us first split A and C into A -only and C -only components in AC , along with their bridged components. Write $A = \mathcal{A} \cup \mathcal{F}_A$, where \mathcal{A} are A -only components in AC and \mathcal{F}_A are A -bridged components in AC . Define $C = \mathcal{C} \cup \mathcal{F}_C$ similarly, and denote the union of the bridged components by

$$\mathcal{F} = \mathcal{F}_A \cup \mathcal{F}_C.$$

Then the HEE splits additively

$$S_{AC} = S_{\mathcal{A}} + S_{\mathcal{C}} + S_{\mathcal{F}}, \quad S_A = S_{\mathcal{A}} + S_{\mathcal{F}_A}, \quad S_C = S_{\mathcal{C}} + S_{\mathcal{F}_C}. \quad (\text{H.2})$$

Hence we can cancel unbridged contributions leading to

$$S_{\mathcal{F}} + E_W(A : CD) + E_W(C : AD) \stackrel{?}{\geq} S_{\mathcal{F}_A} + S_{\mathcal{F}_C} + E_W(AC : D). \quad (\text{H.3})$$

Note that we cannot replace A and C by \mathcal{F}_A and \mathcal{F}_C in E_W terms as we know nothing about A - and C -only components in ACD . Now our goal is to prove (H.3) and hence the theorem.

Step 2: Carving out \mathcal{F}_A and \mathcal{F}_C homologous regions. Let us first introduce the *LHS multisurface*

$$\mathbf{L} := \gamma_{\mathcal{F}} \oplus \Gamma_{A:CD}^W \oplus \Gamma_{C:AD}^W, \quad (\text{H.4})$$

such that

$$\frac{\text{Area}^{\oplus}(\mathbf{L})}{4G_N} = S_{\mathcal{F}} + E_W(A : CD) + E_W(C : AD), \quad (\text{H.5})$$

and consider the restriction

$$\Gamma_{\mathcal{F}} := (\Gamma_{A:CD}^W \cup \Gamma_{C:AD}^W) \cap \mathcal{E}(\mathcal{F}). \quad (\text{H.6})$$

We then have

$$\mathcal{E}(\mathcal{F}) \setminus \Gamma_{\mathcal{F}} = U_{\mathcal{F}_A} \sqcup U_{\mathcal{F}_C} \sqcup U_{\text{extra}}, \quad \partial_{\infty} U_{\mathcal{F}_A} = \mathcal{F}_A, \quad \text{and} \quad \partial_{\infty} U_{\mathcal{F}_C} = \mathcal{F}_C, \quad (\text{H.7})$$

as the restriction converts the homology data on A and C to \mathcal{F}_A and \mathcal{F}_C . U_{extra} is the left over component of $\mathcal{E}(\mathcal{F})$ after this operation; this is the region bounded on four sides by the red, green, orange and blue curves in Figure 11.

We can define their bulk closures as

$$U_{\mathcal{F}_A}^{\text{cl}} = U_{\mathcal{F}_A} \cup (\Gamma_{A:CD}^W \cap \mathcal{E}(\mathcal{F})), \quad \text{and} \quad U_{\mathcal{F}_C}^{\text{cl}} = U_{\mathcal{F}_C} \cup (\Gamma_{C:AD}^W \cap \mathcal{E}(\mathcal{F})). \quad (\text{H.8})$$

This is well defined and produces codimension-one closed bulk subregions as by the barrier theorem $U_{\mathcal{F}_A}$ is only open along $\Gamma_{A:CD}^W \cap \mathcal{E}(\mathcal{F})$ and $U_{\mathcal{F}_C}$ is only open along $\Gamma_{C:AD}^W \cap \mathcal{E}(\mathcal{F})$; in particular $U_{\mathcal{F}_A}$ has no open arc¹⁰ along $\Gamma_{C:AD}^W \cap \mathcal{E}(\mathcal{F})$ and so the gluing in equation (H.8) does generate bounded regions.

Then as $U_{\mathcal{F}_A}^{\text{cl}}$ is separated from $ABCD \setminus \mathcal{F}$ by $\gamma_{\mathcal{F}}$ and further separated from \mathcal{F}_C by $\Gamma_{A:CD}^W \cap \mathcal{E}(\mathcal{F})$ then $U_{\mathcal{F}_A}^{\text{cl}} \sim \mathcal{F}_A$. The same argument applies to $U_{\mathcal{F}_C}^{\text{cl}}$ and so by RT minimality,

$$\frac{\text{Area}(\partial U_{\mathcal{F}_A}^{\text{cl}})}{4G_N} \geq S_{\mathcal{F}_A}, \quad \frac{\text{Area}(\partial U_{\mathcal{F}_C}^{\text{cl}})}{4G_N} \geq S_{\mathcal{F}_C}. \quad (\text{H.9})$$

This is seen in Figure 11 for example.

¹⁰If however $\Gamma_{A:CD}^W \cap \Gamma_{C:AD}^W \neq \emptyset$ then the gluing is still well defined and still only uses a subset of \mathbf{L} by multiplicity.

Step 3: Building an admissible competitor Γ for $E_w(AC:D)$. Set the *excised multisurface*

$$\mathbf{E} := \partial U_{\mathcal{F}_A}^{\text{cl}} \oplus \partial U_{\mathcal{F}_C}^{\text{cl}},$$

which is just the portion of \mathbf{L} we have used to define \mathcal{F}_A and \mathcal{F}_C homologous regions. Then decompose the remainder of \mathbf{L} into an “outer” and an “inner” part:

$$\Gamma_{\text{out}} := |(\Gamma_{A:CD}^W \oplus \Gamma_{C:AD}^W) \cap (\mathcal{E}(ACD) \setminus \mathcal{E}(\mathcal{F}))|, \quad (\text{H.10})$$

$$\Gamma_{\text{in}} := |(\mathbf{L} \ominus \mathbf{E}) \cap \gamma_{\mathcal{F}}|, \quad (\text{H.11})$$

and define the candidate

$$\Gamma := \Gamma_{\text{out}} \cup \Gamma_{\text{in}}. \quad (\text{H.12})$$

In the central panel of Figure 11 we have Γ_{in} as the thick curves and Γ_{out} the non-thick red and orange curves.

By construction,

$$\Gamma \subset \mathcal{E}(ACD), \quad \Gamma_{\text{out}} \cap \Gamma_{\text{in}} = \emptyset, \quad \text{and} \quad \partial_{\Sigma} \Gamma \subset \gamma_{ACD} = \gamma_B. \quad (\text{H.13})$$

The latter holds because the pieces on $\gamma_{\mathcal{F}}$ are glued to the outer legs at their endpoints, so $\gamma_{\mathcal{F}}$ -contacts are *interior* contacts of Γ , not part of $\partial \Gamma$. Such gluing points exist due to the multiplicity: for example if $\Gamma_{A:CD}^W$ intersects $\gamma_{\mathcal{F}}$ at point x then, generally, one copy of x is included for $\partial U_{\mathcal{F}_A}^{\text{cl}}$ and the other in Γ , and so smooth gluing is permitted and no extra (albeit zero measure) sets are introduced in the measured surfaces. Hence the only bulk anchoring of Γ lies on γ_B . We also have $\Gamma \oplus \mathbf{E} = \mathbf{L}$: $\partial U_{\mathcal{F}_A}^{\text{cl}} \oplus \partial U_{\mathcal{F}_C}^{\text{cl}} \subset \mathcal{E}(\mathcal{F})$ and so Γ_{out} has zero intersect with \mathbf{E} , and Γ_{in} also has zero intersect by definition. Thus we have

$$\frac{\text{Area}^{\oplus}(\mathbf{L})}{4G_N} = \frac{\text{Area}(\Gamma)}{4G_N} + \frac{\text{Area}^{\oplus}(\mathbf{E})}{4G_N} = S_{\mathcal{F}} + E_w(A:CD) + E_w(C:AD). \quad (\text{H.14})$$

We claim Γ is EWCS admissible for $(AC : D)$. Condition (i) of Definition 3.9 is satisfied by equation (H.13) and so it remains to check condition (ii).

Step 4: Showing Γ is an admissible competitor for $(AC:D)$. We proceed using the standard path argument: every simple path in $\mathcal{E}(ACD)$ that joins a point adjacent to AC to a point adjacent to D intersects Γ . Consequently,

$$\mathcal{E}(ACD) \setminus \Gamma = U_{AC} \sqcup U_D, \quad \partial_{\infty} U_{AC} = AC, \quad \partial_{\infty} U_D = D. \quad (\text{H.15})$$

Let ℓ be such a simple path with $\ell(0)$ adjacent to AC and $\ell(1)$ adjacent to D . We consider three cases according to where ℓ starts on the boundary.

Case 1: $\ell(0)$ is adjacent to \mathcal{F} . If ℓ begins at some point on \mathcal{F} then it must exit the bridged wedge $\mathcal{E}(\mathcal{F})$ through $\gamma_{\mathcal{F}}$ to reach D . Let x be this first contact point.

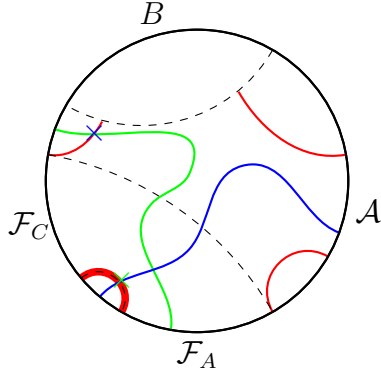


Figure 21. Continuation of case in Figure 11. *Case 1* shown by green path, and *Case 2* by the blue curve with their intersections with Γ marked by \times . In either case the path crosses the red curve Γ rendering Γ EWCS admissible for $(AC : D)$.

If $x \in \Gamma_{\text{in}}$, then $x \in \Gamma$ and we are done. Otherwise $x \notin \Gamma_{\text{in}}$, so x lies on an open arc

$$I \subset \gamma_{\mathcal{F}} \setminus \Gamma_{\text{in}},$$

whose endpoints lie on $\Gamma_{A:CD}^W$ or $\Gamma_{C:AD}^W$. This follows from the definition of **E**: we have excised precisely those arcs of $\gamma_{\mathcal{F}}$ that bound $U_{\mathcal{F}_A}^{\text{cl}}$ and $U_{\mathcal{F}_C}^{\text{cl}}$, so each remaining arc I is bounded by gluing points where outer legs of $\Gamma_{A:CD}^W$ or $\Gamma_{C:AD}^W$ attach (see the green path Figure 21). But since ℓ starts on the \mathcal{F} -side and must reach the D -side, it must cross one of these outer legs. However these legs are precisely $\Gamma_{\text{out}} \subset \Gamma$, so ℓ intersects Γ in either case.

Case 2: $\ell(0)$ is adjacent to \mathcal{A} . If instead ℓ begins on \mathcal{A} , then there are two cases. If the components of $\Gamma_{A:CD}^W$ that generates an EWCS admissible component for \mathcal{A} has zero intersect with $\mathcal{E}(\mathcal{F})$ then necessarily this surface is unaffected by the excision above and so remains in tact in Γ (specifically it is contained within Γ_{out}): thus ℓ must intersect this to reach D by definition of EWCS. If instead this adjacent portion of $\Gamma_{A:CD}^W$ intersects $\gamma_{\mathcal{F}}$ then there is a path from x to a point in \mathcal{F} that nowhere crosses Γ . But we have proved above all ℓ beginning on \mathcal{F} and ending on D must cross Γ and so paths beginning on \mathcal{A} must also intersect Γ to reach D .

Case 3: $\ell(0)$ is adjacent to \mathcal{C} . Identical to case 2 with $\Gamma_{A:CD}^W \rightarrow \Gamma_{C:AD}^W$ and $\mathcal{A} \rightarrow \mathcal{C}$. In all cases we have shown the intersection of such an ℓ proving the lemma.

From (H.13) and (H.15), Γ satisfies the EWCS admissibility for $(AC:D)$ (bulk anchoring on γ_B and separation into regions homologous to AC and D). Therefore

$$\frac{\text{Area}(\Gamma)}{4G_N} \geq E_W(AC : D). \quad (\text{H.16})$$

Step 5: Area bookkeeping and conclusion. By (H.14), (H.9), and (H.16),

$$\frac{\text{Area}^{\oplus}(\mathbf{E})}{4G_N} = \frac{\text{Area}(\partial r_A)}{4G_N} + \frac{\text{Area}(\partial r_C)}{4G_N} \geq S_{\mathcal{F}_A} + S_{\mathcal{F}_C}, \quad \frac{\text{Area}(\Gamma)}{4G_N} \geq E_W(AC : D),$$

whence (H.1) and the theorem follows. \square

I Proof: One-way strong superadditivity of classical correlations

Theorem 6.1. J_W is one-way strongly superadditive. That is J_W satisfies

$$J_W(AB|CD) \geq J_W(A|C) + J_W(B|D). \quad (6.10)$$

for any states on $ABCD$ (not necessarily pure).

This proof is brief in explanation as it is very similar to the proof of Theorem 5.2 (see Appendix H).

Proof. For a mixed state on $ABCD$, we expand (6.10) in terms of HEE and EWCS to obtain

$$S_{AB} + E_W(A : BDE) + E_W(B : ACE) \stackrel{?}{\geq} S_A + S_B + E_W(AB : E).$$

Let γ_{AB} be the RT surface for AB and let $\Gamma_{A:BDE}^W$ and $\Gamma_{B:ACE}^W$ be the EWCS minimizers for $(A : BDE)$ and $(B : ACE)$.

Step 1: Bridged and Unbridged Components. Let \mathcal{A} and \mathcal{B} be the components of A and B that are not bridged in AB , and let $\mathcal{F}_A = A \setminus \mathcal{A}$ and $\mathcal{F}_B = B \setminus \mathcal{B}$ be the bridged components with $\mathcal{F} = \mathcal{F}_A \cup \mathcal{F}_B$. Consequently, the entropy splits additively: $S_{AB} = S_{\mathcal{A}} + S_{\mathcal{B}} + S_{\mathcal{F}}$. Moreover this implies we have $S_A = S_{\mathcal{A}} + S_{\mathcal{F}_A}$ and similarly for B and so we can cancel unbridged entropic terms leading to

$$S_{\mathcal{F}} + E_W(A : BDE) + E_W(B : ACE) \stackrel{?}{\geq} S_{\mathcal{F}_A} + S_{\mathcal{F}_B} + E_W(AB : E), \quad (I.1)$$

whose proof implies our theorem.

Step 2: Carving out \mathcal{F}_A and \mathcal{F}_B homologous regions. Restrict $\Gamma_{A:BDE}^W \cup \Gamma_{B:ACE}^W$ to $\mathcal{E}(\mathcal{F})$. Its complement in $\mathcal{E}(\mathcal{F})$ has (at least two) components whose bulk boundaries are homologous (within $\mathcal{E}(\mathcal{F})$) to \mathcal{F}_A and to \mathcal{F}_B ; denote the bulk closure of these regions by adjoining the relevant EWCS by r_A and r_B .¹¹ Then $r_A \sim \mathcal{F}_A$ and $r_B \sim \mathcal{F}_B$ and so by RT minimality,

$$\frac{\text{Area}(\partial r_A)}{4G_N} \geq S_{\mathcal{F}_A}, \quad \frac{\text{Area}(\partial r_B)}{4G_N} \geq S_{\mathcal{F}_B}. \quad (I.2)$$

¹¹If $\Gamma_{A:BDE}^W$ and $\Gamma_{B:ACE}^W$ overlap tangentially along an arc, use the two copies with their natural multiplicities to contribute one to ∂r_A and the other to ∂r_B .

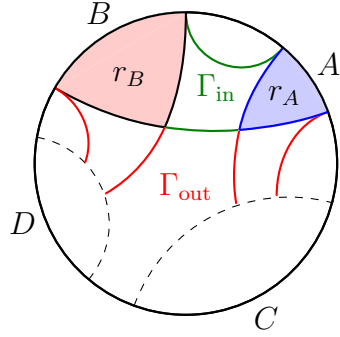


Figure 22. Continuation of case in Figure 12 showing regions and surfaces defined in the proof. We have Γ_{in} as the green curves, and Γ_{out} as the red curves. Homologous regions to A and B shaded in blue and red respectively.

Step 3: Building an admissible competitor Γ for $E_W(AB : D)$. Introduce the *LHS multisurface*

$$\mathbf{L} := \gamma_{\mathcal{F}} \oplus \Gamma_{A:BDE}^W \oplus \Gamma_{B:ACE}^W,$$

and set the *excised multisurface*

$$\mathbf{E} := \partial r_A \oplus \partial r_B,$$

Decompose the remainder of \mathbf{L} into an “outer” and an “inner” part:

$$\Gamma_{\text{out}} := |(\Gamma_{A:BDE}^W \oplus \Gamma_{B:ACE}^W)| \cap (\mathcal{E}(ABE) \setminus \mathcal{E}(\mathcal{F})), \quad (\text{I.3})$$

$$\Gamma_{\text{in}} := |(\mathbf{L} \ominus \mathbf{E})| \cap \gamma_{\mathcal{F}}, \quad (\text{I.4})$$

and define the candidate

$$\Gamma := \Gamma_{\text{out}} \cup \Gamma_{\text{in}}. \quad (\text{I.5})$$

which by construction satisfies,

$$\Gamma \subset \mathcal{E}(ABE), \quad \Gamma_{\text{out}} \cap \Gamma_{\text{in}} = \emptyset, \quad \text{and} \quad \partial_{\Sigma} \Gamma \subset \gamma_C \cup \gamma_D. \quad (\text{I.6})$$

Identically to Theorem 5.2 it follows that $\Gamma \oplus \mathbf{E} = \mathbf{L}$. Moreover, by invoking the same separation lemma in the proof of the said theorem with appropriate replacements of system definitions it follows that Γ satisfies the EWCS admissibility for $(AB : E)$. Therefore

$$\frac{\text{Area}(\Gamma)}{4G_N} \geq E_W(AB : E), \quad (\text{I.7})$$

and the theorem follows. \square

References

- [1] S. Ryu and T. Takayanagi, *Holographic derivation of entanglement entropy from AdS/CFT*, *Phys. Rev. Lett.* **96** (2006) 181602, [[hep-th/0603001](#)].
- [2] J. Maldacena and L. Susskind, *Cool horizons for entangled black holes*, *Fortsch. Phys.* **61** (2013) 781–811, [[arXiv:1306.0533](#)].
- [3] J. Maldacena, *Gravity, particle physics and their unification*, *International Journal of Modern Physics A* **15** (July, 2000) 840–852.
- [4] F. Pastawski, B. Yoshida, D. Harlow, and J. Preskill, *Holographic quantum error-correcting codes: Toy models for the bulk/boundary correspondence*, *JHEP* **06** (2015) 149, [[arXiv:1503.06237](#)].
- [5] P. Hayden, S. Nezami, X.-L. Qi, N. Thomas, M. Walter, and Z. Yang, *Holographic duality from random tensor networks*, *JHEP* **11** (2016) 009, [[arXiv:1601.01694](#)].
- [6] J. Cotler, P. Hayden, G. Penington, G. Salton, B. Swingle, and M. Walter, *Entanglement Wedge Reconstruction via Universal Recovery Channels*, *Phys. Rev. X* **9** (2019), no. 3 031011, [[arXiv:1704.05839](#)].
- [7] P. Hayden and J. Preskill, *Black holes as mirrors: Quantum information in random subsystems*, *JHEP* **09** (2007) 120, [[arXiv:0708.4025](#)].
- [8] T. Takayanagi and K. Umemoto, *Entanglement of purification through holographic duality*, *Nature Phys.* **14** (2018), no. 6 573–577, [[arXiv:1708.09393](#)].
- [9] T. Mori and B. Yoshida, *Does connected wedge imply distillable entanglement?*, [arXiv:2411.03426](#).
- [10] S. Dutta and T. Faulkner, *A canonical purification for the entanglement wedge cross-section*, *JHEP* **03** (2021) 178, [[arXiv:1905.00577](#)].
- [11] K. Tamaoka, *Entanglement Wedge Cross Section from the Dual Density Matrix*, *Phys. Rev. Lett.* **122** (2019), no. 14 141601, [[arXiv:1809.09109](#)].
- [12] Q. Wen, *Balanced Partial Entanglement and the Entanglement Wedge Cross Section*, *JHEP* **04** (2021) 301, [[arXiv:2103.00415](#)].
- [13] P. Hayden, M. Lemm, and J. Sorce, *Reflected entropy: Not a correlation measure*, *Phys. Rev. A* **107** (2023), no. 5 L050401, [[arXiv:2302.10208](#)].
- [14] P. Hayden, O. Parrikar, and J. Sorce, *The Markov gap for geometric reflected entropy*, *JHEP* **10** (2021) 047, [[arXiv:2107.00009](#)].
- [15] Y. Zou, K. Siva, T. Soejima, R. S. K. Mong, and M. P. Zaletel, *Universal tripartite entanglement in one-dimensional many-body systems*, *Phys. Rev. Lett.* **126** (2021), no. 12 120501, [[arXiv:2011.11864](#)].
- [16] T. Mori, *Quantum correlation beyond entanglement: Holographic discord and multipartite generalizations*, [arXiv:2506.02131](#).

[17] H. Ollivier and W. H. Zurek, *Quantum discord: A measure of the quantumness of correlations*, *Phys. Rev. Lett.* **88** (Dec, 2001) 017901.

[18] Y. Nambu and Y. Ohsumi, *Classical and Quantum Correlations of Scalar Field in the Inflationary Universe*, *Phys. Rev. D* **84** (2011) 044028, [[arXiv:1105.5212](https://arxiv.org/abs/1105.5212)].

[19] A. Matsumura and Y. Nambu, *Squeezing of primordial gravitational waves as quantum discord*, *Universe* **6** (2020), no. 2 33, [[arXiv:2001.02474](https://arxiv.org/abs/2001.02474)].

[20] M. Headrick, *General properties of holographic entanglement entropy*, *JHEP* **03** (2014) 085, [[arXiv:1312.6717](https://arxiv.org/abs/1312.6717)].

[21] C. Akers, V. Chandrasekaran, S. Leichenauer, A. Levine, and A. Shahbazi Moghaddam, *Quantum null energy condition, entanglement wedge nesting, and quantum focusing*, *Phys. Rev. D* **101** (2020), no. 2 025011, [[arXiv:1706.04183](https://arxiv.org/abs/1706.04183)].

[22] B. Czech, J. L. Karczmarek, F. Nogueira, and M. Van Raamsdonk, *The Gravity Dual of a Density Matrix*, *Class. Quant. Grav.* **29** (2012) 155009, [[arXiv:1204.1330](https://arxiv.org/abs/1204.1330)].

[23] A. C. Wall, *Maximin Surfaces, and the Strong Subadditivity of the Covariant Holographic Entanglement Entropy*, *Class. Quant. Grav.* **31** (2014), no. 22 225007, [[arXiv:1211.3494](https://arxiv.org/abs/1211.3494)].

[24] A. Almheiri, X. Dong, and D. Harlow, *Bulk Locality and Quantum Error Correction in AdS/CFT*, *JHEP* **04** (2015) 163, [[arXiv:1411.7041](https://arxiv.org/abs/1411.7041)].

[25] D. L. Jafferis, A. Lewkowycz, J. Maldacena, and S. J. Suh, *Relative entropy equals bulk relative entropy*, *JHEP* **06** (2016) 004, [[arXiv:1512.06431](https://arxiv.org/abs/1512.06431)].

[26] X. Dong, D. Harlow, and A. C. Wall, *Reconstruction of Bulk Operators within the Entanglement Wedge in Gauge-Gravity Duality*, *Phys. Rev. Lett.* **117** (2016), no. 2 021601, [[arXiv:1601.05416](https://arxiv.org/abs/1601.05416)].

[27] M. Tomamichel, S. Fehr, J. Kaniewski, and S. Wehner, *A monogamy-of-entanglement game with applications to device-independent quantum cryptography*, *New Journal of Physics* **15** (Oct., 2013) 103002, [[arXiv:1210.4359](https://arxiv.org/abs/1210.4359)].

[28] Z. Khanian, D. Lee, D. Leung, Z. Li, A. May, T. Mori, S. Miao, F. Salek, J. Yi, and B. Yoshida, *Entanglement sharing schemes*, [arXiv:2509.21462](https://arxiv.org/abs/2509.21462).

[29] P. Hayden, M. Headrick, and A. Maloney, *Holographic Mutual Information is Monogamous*, *Phys. Rev. D* **87** (2013), no. 4 046003, [[arXiv:1107.2940](https://arxiv.org/abs/1107.2940)].

[30] M. Headrick and T. Takayanagi, *A Holographic proof of the strong subadditivity of entanglement entropy*, *Phys. Rev. D* **76** (2007) 106013, [[arXiv:0704.3719](https://arxiv.org/abs/0704.3719)].

[31] N. Bao, S. Nezami, H. Ooguri, B. Stoica, J. Sully, and M. Walter, *The Holographic Entropy Cone*, *JHEP* **09** (2015) 130, [[arXiv:1505.07839](https://arxiv.org/abs/1505.07839)].

[32] E. M. Rains, *A Rigorous treatment of distillable entanglement*, *Phys. Rev. A* **60** (1999) 173, [[quant-ph/9809078](https://arxiv.org/abs/quant-ph/9809078)].

[33] N. Bao, A. Chatwin-Davies, and G. N. Remmen, *Entanglement wedge cross section inequalities from replicated geometries*, *JHEP* **07** (2021) 113, [[arXiv:2106.02640](https://arxiv.org/abs/2106.02640)].

[34] P. Jain, N. Jokela, M. Jarvinen, and S. Mahapatra, *Bounding entanglement wedge cross sections*, *JHEP* **03** (2023) 102, [[arXiv:2211.07671](https://arxiv.org/abs/2211.07671)].

[35] M. Ozawa, *On information gain by quantum measurements of continuous observables*, *Journal of Mathematical Physics* **27** (Mar., 1986) 759–763.

[36] M. Koashi and A. Winter, *Monogamy of quantum entanglement and other correlations*, *Phys. Rev. A* **69** (2004), no. 2 022309, [[quant-ph/0310037](https://arxiv.org/abs/quant-ph/0310037)].

[37] A. Datta, *Studies on the role of entanglement in mixed-state quantum computation*, [arXiv:0807.4490](https://arxiv.org/abs/0807.4490).

[38] Q. Chen, C. Zhang, S. Yu, X. X. Yi, and C. H. Oh, *Quantum discord of two-qubit x -states*, *Physical Review A* **84** (Oct., 2011) [[arXiv:1102.0181](https://arxiv.org/abs/1102.0181)].

[39] F. Galve, G. L. Giorgi, and R. Zambrini, *Orthogonal measurements are almost sufficient for quantum discord of two qubits*, *EPL (Europhysics Letters)* **96** (Nov., 2011) 40005, [[arXiv:1107.2005](https://arxiv.org/abs/1107.2005)].

[40] Y. Huang, *Computing quantum discord is np-complete*, *New Journal of Physics* **16** (Mar., 2014) 033027.

[41] N. Bao and I. F. Halpern, *Holographic Inequalities and Entanglement of Purification*, *JHEP* **03** (2018) 006, [[arXiv:1710.07643](https://arxiv.org/abs/1710.07643)].

[42] V. Vedral, *Classical correlations and entanglement in quantum measurements*, *Physical Review Letters* **90** (Feb., 2003) [[quant-ph/0207116](https://arxiv.org/abs/quant-ph/0207116)].

[43] A. Streltsov, H. Kampermann, and D. Bruß, *Linking quantum discord to entanglement in a measurement*, *Physical Review Letters* **106** (Apr., 2011).

[44] R. Prabhu, A. K. Pati, A. Sen(De), and U. Sen, *Conditions for monogamy of quantum correlations: Greenberger-horne-zeilinger versus w states*, *Phys. Rev. A* **85** (Apr, 2012) 040102.

[45] L. Susskind, *ER=EPR, GHZ, and the consistency of quantum measurements*, *Fortsch. Phys.* **64** (2016) 72, [[arXiv:1412.8483](https://arxiv.org/abs/1412.8483)].

[46] S. Nezami and M. Walter, *Multipartite Entanglement in Stabilizer Tensor Networks*, *Phys. Rev. Lett.* **125** (2020) 241602, [[arXiv:1608.02595](https://arxiv.org/abs/1608.02595)].

[47] X. Dong, X.-L. Qi, and M. Walter, *Holographic entanglement negativity and replica symmetry breaking*, *JHEP* **06** (2021) 024, [[arXiv:2101.11029](https://arxiv.org/abs/2101.11029)].

[48] V. E. Hubeny, M. Rangamani, and T. Takayanagi, *A Covariant holographic entanglement entropy proposal*, *JHEP* **07** (2007) 062, [[arXiv:0705.0016](https://arxiv.org/abs/0705.0016)].

[49] C. Akers, J. Koeller, S. Leichenauer, and A. Levine, *Geometric Constraints from Subregion Duality Beyond the Classical Regime*, [arXiv:1610.08968](https://arxiv.org/abs/1610.08968).

[50] T. Takayanagi, *Holographic Dual of BCFT*, *Phys. Rev. Lett.* **107** (2011) 101602, [[arXiv:1105.5165](https://arxiv.org/abs/1105.5165)].

[51] R. Bousso and G. Penington, *Entanglement wedges for gravitating regions*, *Phys. Rev. D* **107** (2023), no. 8 086002, [[arXiv:2208.04993](https://arxiv.org/abs/2208.04993)].

[52] L. Henderson and V. Vedral, *Classical, quantum and total correlations*, *J. Phys. A* **34** (2001), no. 35 6899, [[quant-ph/0105028](https://arxiv.org/abs/quant-ph/0105028)].

[53] K. Modi, A. Brodutch, H. Cable, T. Paterek, and V. Vedral, *The classical-quantum boundary for correlations: Discord and related measures*, *Reviews of Modern Physics* **84** (Nov., 2012) 1655–1707, [[arXiv:1112.6238](https://arxiv.org/abs/1112.6238)].

[54] M. Freedman and M. Headrick, *Bit threads and holographic entanglement*, *Commun. Math. Phys.* **352** (2017), no. 1 407–438, [[arXiv:1604.00354](https://arxiv.org/abs/1604.00354)].

[55] E. M. Rains, *Bound on distillable entanglement*, *Phys. Rev. A* **60** (Jul, 1999) 179–184.

[56] Z. Li, T. Mori, and B. Yoshida, *Tripartite Haar random state has no bipartite entanglement*, [arXiv:2502.04437](https://arxiv.org/abs/2502.04437).

[57] M. B. Hastings, *Superadditivity of communication capacity using entangled inputs*, *Nature Phys.* **5** (2009), no. 4 255–257, [[arXiv:0809.3972](https://arxiv.org/abs/0809.3972)].

[58] P. Hayden and G. Penington, *Black hole microstates vs. the additivity conjecture*, [arXiv:2012.07861](https://arxiv.org/abs/2012.07861).

[59] S.-G. Youn and B. Collins, *Additivity violation of the regularized minimum output entropy*, *Documenta Mathematica* **27** (2022) 1299–1320.

[60] M. Kalantar and H. Shobeiri, *More examples of additivity violation of the regularized minimum output entropy in the commuting-operator setup*, [arXiv:2501.15462](https://arxiv.org/abs/2501.15462).

[61] B. M. Terhal, M. Horodecki, D. W. Leung, and D. P. DiVincenzo, *The entanglement of purification*, *J. Math. Phys.* **43** (2002), no. 9 4286–4298, [[quant-ph/0202044](https://arxiv.org/abs/quant-ph/0202044)].

[62] C. Akers, T. Faulkner, S. Lin, and P. Rath, *Entanglement of purification in random tensor networks*, *Phys. Rev. D* **109** (2024), no. 10 L101902, [[arXiv:2306.06163](https://arxiv.org/abs/2306.06163)].

[63] J. Couch, P. Nguyen, S. Racz, G. Stratis, and Y. Zhang, *Possibility of entanglement of purification to be less than half of the reflected entropy*, *Phys. Rev. A* **109** (2024), no. 2 022426, [[arXiv:2309.02506](https://arxiv.org/abs/2309.02506)].

[64] R. Horodecki, P. Horodecki, M. Horodecki, and K. Horodecki, *Quantum entanglement*, *Rev. Mod. Phys.* **81** (2009) 865–942, [[quant-ph/0702225](https://arxiv.org/abs/quant-ph/0702225)].

[65] W. K. Wootters, *Entanglement of formation of an arbitrary state of two qubits*, *Phys. Rev. Lett.* **80** (1998) 2245–2248, [[quant-ph/9709029](https://arxiv.org/abs/quant-ph/9709029)].

[66] M. D. Lang and C. M. Caves, *Quantum Discord and the Geometry of Bell-Diagonal States*, *Phys. Rev. Lett.* **105** (2010), no. 15 150501, [[arXiv:1006.2775](https://arxiv.org/abs/1006.2775)].

[67] R. F. Werner, *Quantum states with Einstein-Podolsky-Rosen correlations admitting a hidden-variable model*, *Phys. Rev. A* **40** (1989) 4277–4281.

[68] H. Casini and M. Huerta, *Remarks on the entanglement entropy for disconnected regions*, *JHEP* **03** (2009) 048, [[arXiv:0812.1773](https://arxiv.org/abs/0812.1773)].